THE PURSUIT OF SUBCHEMICAL ACCURACY IN QUANTUM CHEMISTRY VIA BASIS SET EXTRAPOLATION TECHNIQUES

By

Michael S. Schuurman

(Under the Direction of Henry F. Schaefer III)

ABSTRACT

Techniques that employ the extrapolation of atomic basis sets, in concert with sophisticated *ab initio* treatments of electron correlation, are now capable of generating precise molecular properties and reaction energies of subchemical ($\leq$ 0.1 kcal mol^{-1}) accuracy. In this dissertation, these techniques are applied to a range of chemical systems. Computational thermochemistry is the focus of the first investigation, in which the enthalpies of formation of NCO and the isomers of [H, N, C, O] are determined using formation reactions explicitly designed to minimize errors in the computed reaction energies. The mean computed enthalpies of formation (from two independent NCO formation reactions and seven HNCO reactions) are given by $\Delta_f H_0^\circ$(NCO) = +30.5 ± 0.2, and $\Delta_f H_0^\circ$(HNCO) = –27.6 ± 0.2 kcal mol^{-1}. To achieve such precision, additive corrections for core correlation, spin-orbit coupling, special relativity, anharmonic zero-point vibrational energies, and non-Born-Oppenheimer effects, must be considered.

In the second study, extrapolated gradient techniques are employed to obtain complete basis set (CBS) limit CCSD(T) geometries of BH_3 and BH_5, the structure of the latter species exhibiting a prodigious basis set dependence. Focal-point extrapolations yield a C_s-symmetry global minimum comprised of BH_3 and H_2 subunits and featuring interfragment B – H distances of (1.401, 1.414) Å, an H_2 bond length elongated to 0.803 Å, and a $BH_3 + H_2$ dissociation energy D_e (D_0) = 6.6 (1.2) kcal mol^{-1}. The vibrationless barriers for H_2 internal rotation and hydrogen scrambling are 0.07 and 5.81 kcal mol^{-1}, respectively. As a first step in investigating the extremely anharmonic 12-dimensional vibrational dynamics of BH_5, a complete quartic force field has been computed at the all-electron cc-pCVQZ CCSD(T) level of theory.

The final application combines extrapolated gradient and energy techniques to construct a CBS limit CCSD(T) quartic force field for BH_3. The reference structure (r_e = 1.18642 Å) for this force field was optimized employing extrapolated CCSD(T) gradients. The resulting vibrational frequencies, given by ν_1 = 2502.5 cm^{-1}, ν_2 = 1147.4 cm^{-1}, ν_3 = 2602.7 cm^{-1}, and ν_4 = 1196.3 cm^{-1}, display a mean absolute error of only 0.5 cm^{-1} with infrared gas-phase fundamental frequencies.

INDEX WORDS: basis set, extrapolation, thermochemistry, focal point analysis, HNCO, NCO, *ab initio*, BH_5, BH_3, vibrational perturbation theory, quartic force field, computational spectroscopy

THE PURSUIT OF SUBCHEMICAL ACCURACY IN QUANTUM CHEMISTRY VIA BASIS SET EXTRAPOLATION TECHNIQUES

by

MICHAEL S. SCHUURMAN

B. S., The King's University College, Canada, 1999

A Dissertation Submitted to the Graduate Faculty of The University of Georgia in Partial Fulfillment of the Requirements of the Degree

DOCTOR OF PHILOSOPHY

ATHENS, GEORGIA

2004

THE PURSUIT OF SUBCHEMICAL ACCURACY IN QUANTUM CHEMISTRY VIA BASIS SET EXTRAPOLATION TECHNIQUES

by

MICHAEL S. SCHUURMAN

Major Professor: Henry F. Schaefer III

Committee: Nigel G. Adams
Lucia M. Babcock
Charles Kutal
Henning H. Meyer

Electronic Version Approved:

Maureen Grasso
Dean of the Graduate School
The University of Georgia
December 2004

ACKNOWLEDGEMENTS

At each stage in my life I've somehow been able to find my way into a community of like minded people. First and foremost, the community most central to my life is that of my family. My Mom and Dad have both had a profound impact on my intellectual development. While *they* say I was primarily "self-motivated", they always proof-read my papers, helped me with my homework and questioned me about my current academic interests. I particularly remember dinner times, which my sisters, Anne and Caroline, and I would use as occasion to harass and question my parents on topics of politics, religion, philosophy, or whatever else came to mind. As I recall, even at young age, my parents rarely spoke down to us and engaged our questions honestly, creating an environment that fostered intellectual curiosity. These experiences, more than any others, were the foundations of whatever academic aspirations that would follow. Also, Matt, Tisa, and Quin have provided me with a home away from home, for which I have been very grateful.

I have always viewed my close friends as members of my extended family, particularly those that have lasted through my childhood and up until today. Travis Boonstra, Joel VanderSchaaf, Jon Bosch, Sean VanEerden, Matthew Manning, Shauna Johannesen, and others too numerous to mention here made leaving Edmonton incredibly difficult, but have also kept me coming back on a regular basis.

During my undergraduate studies, my chemistry and physics professors were uniformly first rate. I thank Drs. Peter Mahaffy, Brian Martin, and Ken Newman at King's University College and Dr. Mariusz Klobukowski at the University of Alberta, not only for the scientific knowledge they imparted, but also for the example they set in the classroom and lab. Theirs is the model that I will emulate in my future teaching experiences.

Upon my arrival in Athens, it immediately became apparent that Professor Schaefer has succeeded in creating a real community at the Center for Computational Quantum Chemistry (CCQC). For most people, a research institute so-named likely produces mental images of a cold, impersonal, and antiseptic work environment. However, those impressions couldn't be further from reality. Professor Schaefer has created an ideal research atmosphere, where students are able to get as much out of their graduate experience as they put in. This, I think, is the most any graduate advisor can offer. For this, as well as lively discussions and valuable advice, I owe Professor Schaefer my deepest thanks. Additionally, the staff scientists here at the CCQC, Drs. Yukio Yamaguchi and Wesley Allen, have taught me most of what I know about quantum chemistry, whether it be in the classroom, or in their almost always open offices. I owe particular thanks to Dr. Wesley Allen. He has been an ideal mentor, patiently answering my innumerable questions, and always pushing me to learn more than I need to finish the task at hand. The administrative staff of Linda Rowe, Amy Peterson, Karen Branch do an excellent job of insulating us from the bureaucratic inanities that so many other graduate students are forced to deal with.

My fellow students at the CCQC, past and present, have been an important support network. In particular, Drs. Joe Kenny, Edward Valeev, and Shawn Brown were mentors to me from those first intimidating months at the CCQC. My classmates, Drs. Luboš Horný and Kurt Sattelmeyer, as well as Micah Abrams, have been good friends and invaluable confidants.

Finally, I need to thank Betsy Burtner. I cannot express my gratitude for her in these few lines, so I will try to do it more often in person.

TABLE OF CONTENTS

Page

APPENDICES

CHAPTER 1

INTRODUCTION AND BACKGROUND MATERIAL

1.1 INTRODUCTION

The complementary evolution of accurate techniques to measure physical systems and the corresponding concepts to explain them has been vital to the development of the chemical sciences. Given these origins, it is not surprising that modern quantum chemistry is employed to both quantitatively determine molecular properties as well as explain experimental results. While these applications are not necessarily disparate, they are representative of two distinct paradigms currently at work in computational chemistry.

The primary goal of explanative theoretical chemistry is the development of a set of general computational tools that may be used to gain qualitative insights into the behavior of molecular systems. Under this paradigm, the theoretical chemical sciences are concerned primarily with *model* construction, where the success or failure of a proposed model is determined by its ability to reproduce experimental observations. However, if agreement with empirical results is the fundamental criterion, a chemical model need not demonstrate a strict adherence to first principles quantum mechanics. The most marked advantage of removing such constraints on a theoretical method lies in the reduction of the potentially steep computational cost required to describe most molecular systems. A current exemplar of this approach is Kohn-Sham density functional theory (DFT).[1] The mathematical foundation upon which DFT is constructed, the Hohenberg-Kohn theorem,[2] states that all observable properties of a molecular system are uniquely determined by the electron density. While this formulation of electronic structure theory is formally rigorous, the lack of an analytic form of the exchange-correlation functional has resulted in countless empirically fit expressions for this term. Thus, since there does not exist a systematic method to improve *a priori* the accuracy of DFT for a given molecule

(a characteristic shared by all semi-empirical techniques), the ability to converge the measurable properties of the system to an arbitrary precision is lost.

More foundational approaches in electronic structure theory are characterized by an emphasis on attaining systematically converged *ab initio* results. Currently, the most general quantum chemical techniques that reflect this paradigm are based upon algebraic wave function expansion methods. These *ab initio* schemes derive exclusively from first principles quantum mechanics in the solution of the electronic Schrödinger equation and are formally characterized by the simultaneous expansion of the *n*-particle wave function in the one- and *n*-particle spaces.

In conventional electronic structure methods, the first approximation to the exact wave function is given by an anti-symmetrized product of spin-orbitals called a Slater determinant. Most commonly, the delocalized molecular spin-orbitals are expanded in a linear combination of localized atomic orbitals. Using Gaussian or Slater type functions, the coefficients and exponents defining the atomic orbitals are determined in advance for each atom, and thus identify the specific atomic basis set. The optimal set of expansion coefficients that define the molecular spin-orbitals are determined self-consistently via the Hartree-Fock-Roothan equations.[3,4] Upon generation of the molecular orbital basis, the set may be divided into an *occupied* space consisting of the *n*-lowest energy orbitals, and the remaining orbitals which are denoted as unoccupied or *virtual*. It is the electronic configuration implied by the Slater determinant of occupied orbitals that defines the Hartree-Fock (HF) reference wave function.

While the HF energy is a good first approximation to the exact result, it fails to account for the instantaneous coulombic repulsion experienced by pairs of electrons. These interactions define the dynamical correlation energy, whose determination requires an expansion in the *n*-particle space of Slater determinants. From the Hartree-Fock wave function, new determinants

are generated by the successive substitution of virtual orbitals into the reference function. A natural partition of correlated wave functions arises by grouping determinants that differ from the HF reference by the same number of orbitals. Since in most cases it is not computationally feasible to include all possible substitutions, this *n*-particle expansion is truncated at some low-level excitation order.

Thus, modern electronic structure methods require the resolution of two distinct expansions in order to yield results sufficiently accurate to describe the energy differences relevant to chemical systems. Attaining subchemical ($\leq$ 0.1 kcal mol^{-1}) and spectroscopic ($\leq$ 1 cm^{-1}) accuracy in quantum chemical applications requires a particularly rigorous convergence of the one-particle basis as well as a sufficiently high-order truncation of the *n*-particle expansion.

1.2 Extrapolation Of The One-Particle Basis

The pioneering investigations[5-7] into the convergence properties of the correlation energy were performed by Schwartz,[5,6] who employed Legendre polynomials as a basis for perturbation series expansions. Termed a partial-wave expansion, the contributions to the correlation energy were partitioned in terms of successively saturated angular momentum shells, l. For the ground state of He, Schwartz found that the decay of the correlation energy in a partial wave expansion went roughly as l^{-4}, with the exact functional form given by

$$\frac{45}{256}\left(l+\frac{1}{2}\right)^{-4}\left[1-\frac{19}{8}\left(l+\frac{1}{2}\right)^{-2}+O\left(l^{-4}\right)\right]. \tag{1.1}$$

Kutzelnigg and Morgan demonstrated that this decay profile was also exhibited by expansions based on a Hartree-Fock reference function.[8,9] Subsequent numerical computations[10] on the configuration interaction expansion displayed the same $\left(l+\frac{1}{2}\right)^{-4}$ convergence profile. The

implication of these studies was clear: conventional wave function expansions exhibited an extremely protracted convergence of the correlation energy. In order to achieve μE_h accuracy in the correlation energy, basis sets incorporating prohibitively high angular momentum functions would be required. The origin of the slow convergence of conventional wave function expansions stems from a formally incorrect description of coulombic interactions at small interelectronic distances. Specifically, conventional Slater determinant wave function expansions must have a non-physical zero derivative at the electron coalescence point and therefore may only approximate the electronic coulomb cusp. A modified wave function ansatz, which explicitly includes the inter-electron distance r_{12}, has been shown to qualitatively reproduce the proper cusp conditions and thus produces significantly accelerated convergence (in principle going as $\left(l+\frac{1}{2}\right)^{-8}$)[11,12] to the one-particle limit. However, these methods are a relatively recent development and the reader is directed to other sources for a more extensive review.[11-14] The undeniable import of these initial investigations lies in the elucidation of the physical basis for the convergence properties of the one-particle basis. However, development and application of *general* basis sets for molecular computations based on partial-wave expansions would be difficult given the large number of basis functions required for molecular calculations as well the inherent dependence on the physics of the system under study.

An approach more practical for molecular systems was developed by Dunning and co-workers[15-19] beginning the late 1980's. The objective was to construct a series of basis sets which allowed for the smooth convergence of the correlation energy to the basis set limit. Rather than successively saturate angular momentum shells of a given l, a sequence of basis sets is generated by adding sets of functions which lower the correlation energy by a similar amount. For example, the cc-pVDZ (correlation-consistent polarized valence double zeta) basis set for

first row atoms is given by the contraction 3*s*2*p*1*d* – one correlating orbital for each occupied atomic orbital as well as a *d* polarization function. The next basis set in the hierarchy is generated by adding an additional set of correlating functions as well as additional polarization functions, designated 4*s*3*p*2*d*1*f* (i.e. cc-pVTZ). Thus, the generation of the correlation-consistent series of basis sets should be considered a *principal expansion*, as angular momentum functions are added in shells designated by the principal quantum number *n*. Feller[20] investigated the convergence of both the Hartree-Fock and correlation energies using this sequence of basis sets and proposed an exponential functional form for their extrapolation. The three-parameter function is given by,

$$E_{HF}(X) = E_{\infty} + be^{-cX}, \tag{1.2}$$

where X is the cardinality of the correlation-consistent basis set, E_{∞} is the complete basis set (CBS) limit Hartree-Fock energy and (b, c) are adjustable parameters. His proposal of these functional forms for extrapolation were empirically motivated, based on fits of computed data points for water.

Helgaker and co-workers[21] later proposed a different functional form of the correlation energy, given by

$$E_{corr}(X) = E_{\infty} + bX^{-3}, \tag{1.3}$$

where E_{∞} is the CBS limit correlation energy. Upon inspection it becomes clear that (1.3) is a much simpler functional form. The CBS limit correlation energy is given by a linear combination of cc-pV*X*Z energies:

$$E_{\infty} = \frac{X^3 E(X) - (X-1)^3 E(X-1)}{X^3 - (X-1)^3} \tag{1.4}$$

Furthermore, the X^{-3} extrapolation function has the added benefit of being physically motivated, displaying the same asymptotic behavior as the integrated Schwartz expression,

$$\int_{L+\frac{1}{2}}^{\infty} \left(l+\tfrac{1}{2}\right)^{-4} dl = \frac{1}{3}(L+1)^{-3}. \tag{1.5}$$

While some caution is required in identifying the term L+1 with the cardinal number, X, of a correlation-consistent basis set, the relationship between the two expressions makes a compelling argument for its adoption. Most importantly, whereas the exponential extrapolation formula consistently underestimated correlation energies, benchmark computations demonstrated the X^{-3} functional form to be the appropriate fit to the energy. Subsequent investigations by Helgaker and co-workers[22] confirmed the utility of (1.2) as an appropriate extrapolation formula for the Hartree-Fock energy, although the expressions lack a compelling physical justification. In the intervening years, expressions (1.2) and (1.3) have come to be the standard extrapolation formulas of the Hartree-Fock and correlation energies.

1.3 Hierarchies Of Correlated Methods

The n-particle expansion methods most commonly employed in *ab initio* electronic structure theory are naturally partitioned based on an excitation level relative to the HF reference. The most straightforward illustration of this is seen in the configuration interaction wave function which is decomposed into contributions based on excitations out of the HF reference

$$\Psi_{\mathrm{CI}} = \Phi_0 + \sum_{ia} c_i^a \Phi_i^a + \sum_{i<j,a<b} c_{ij}^{ab} \Phi_{ij}^{ab} + \ldots, \tag{1.6}$$

where Φ_0 is the HF wave function, Φ_i^a is a Slater determinant in which orbital i has been replaced with orbital a, and the indices (i, j) and (a, b) represent occupied and virtual orbitals,

respectively. Truncation of this series to include all singly and doubly excitations yields the CISD (configuration interaction including single and double excitations) wave function, inclusion of all triply excited determinants is termed CISDT, and consideration of all excitations up to order N, where N is the number of orbitals in the reference determinant, is termed full configuration interaction (FCI). The coupled-cluster (CC) series may be analogously partitioned, although the excitation operator takes a slightly more complicated exponential form.

Perturbation expansion methods, including Møller-Plesset (MP) theory, are qualitatively different in that the Hamiltonian is separated into an easily solvable zero-order component (in the case Møller-Plesset theory this is the Fock operator) and a perturbation (instantaneous electron correlation). Corrections to the zero-order wave function, and thus the energy, are computed in the basis of solutions for the zero-order Hamiltonian. Thus, the limit of this series is not the FCI wave function, as is the case for CI and CC formalisms, but MP∞. Extrapolation of the perturbation series may be facilitated by employing the fact that the even- and odd-order terms of the MPn series are a geometrically progressive series. An expression derived by Pople and co-workers,[23]

$$\Delta\varepsilon_{corr} = \frac{\varepsilon_2 + \varepsilon_3}{1 - \frac{\varepsilon_4}{\varepsilon_5}}, \tag{1.7}$$

yields an approximate total correlation energy based on the energies of the MP series through fourth order. This approximation assumes the same geometric relationship between ε_5 and ε_3 as is observed for ε_2 and ε_4. A second, more rigorous approach, is to employ Padé approximants.[24,25] This mathematical technique recasts a series expansion through order N as a ratio of polynomials of order n and m (denoted as the [n, m] approximant), where $n + m = N$. The advantage of this approach lies in the fact that Padé approximants have been shown to be

much more rapidly convergent than simple Taylor series expansions.[26,27] For example, the shifted [2,1] approximant for the MP energy expansion requires energy terms through fifth-order:

$$\varepsilon_{corr} = \frac{\varepsilon_2^2(\varepsilon_4 - \varepsilon_5) + 2\varepsilon_2\varepsilon_3(\varepsilon_4 - \varepsilon_3) + \varepsilon_3^2(\varepsilon_2 - \varepsilon_3)}{(\varepsilon_2 - \varepsilon_3)(\varepsilon_4 - \varepsilon_5) - (\varepsilon_4 - \varepsilon_3)^2}. \tag{1.8}$$

While at first glance these techniques look ideal for high accuracy studies, any enthusiasm is quickly dampened upon application of such methods to actual molecular systems. Specifically, the MP*n* series has been shown to display erratic convergence behavior,[24,28-30] and in fact may be even be divergent in certain cases.[31,32] Thus, while the computation of high-order members of the MPn series are not recommend for the pursuit of highly accurate *ab initio* results, the lower-order members, in particular MP2, remain a good first approximation to the correlation energy, as well as being computationally inexpensive.

It is difficult to apply CI and CC methods that include higher than double excitations to all but the smallest molecular systems. However, this does not present an overly restrictive constraint since not all excited determinants contribute equally to the wave function, and thus the molecular energy. Rather, for systems that may be described using a single reference function, truncation of the *n*-particle expansion at doubly excited determinants is often sufficient for chemical accuracy. The evaluation of these methods from a pragmatic perspective is based on how well the energies approximate full CI results at low truncation order. The efficacy with which low excitation order coupled-cluster wave functions approximate FCI results is superior to that of either conventional CI or MP expansions, as has been documented in benchmark studies.[33] Furthermore, the advent string-based arbitrary order coupled-cluster algorithms has led to numerous investigations into the convergence of the coupled-cluster series.[33-35] While still

prohibitively expensive for the majority of chemical systems, these techniques hold promise for moving beyond the low-order coupled-cluster methods currently available for practical molecular computations.

1.4 Focal point Analysis

As *ab initio* quantum chemistry matures, the push into ever higher accuracy regimes continues unabated. This impetus is felt most strongly in the area of computational thermochemistry, where large quantities of accurate experimental data allow for easy comparison and calibration of new methods. The current state of this research area is the widening of subchemical (≤ 0.1 kcal mol^{-1}) accuracy to larger and larger molecular systems.

One the earliest forays into this area came in the form of the CBS (complete basis set) method, and its numerous extensions, developed by Petersson and co-workers.[36,37] This technique involves the extrapolation of the natural orbital energies to obtain approximate CBS limit Hartree-Fock and configuration interaction correlation energies. The target accuracy of 1 – 2 kcal mol^{-1} is attainable for a wide range of molecular systems since largest basis sets employed [*spf*/*sp*] are relatively small. Differing fundamentally from the CBS method, the Gaussian-*n* family of methods (denoted G2, G3, G3X) developed by Pople and co-workers[38-40] were specifically designed for high accuracy thermochemical studies. A so-called *model chemistry*, each aspect of the technique is defined, including the optimized *ab initio* geometries employed for harmonic frequency analyses required to obtain ZPVEs, the standard Gaussian basis sets used to estimate the CBS limit HF energy, and the electronic structure methods employed to determine the correlation energy. However, this method is not free of empirical corrections, as higher-order correlation effects are accounted for using two parameters fit to a dataset containing

a representative sample (55 [302] for G2 [G3]) of small molecules. The more recent (W1, W2, W3)[41,42] methods of Martin and co-workers are similar in spirit to the G*n* methods. The primary difference is that coupled-cluster (CC) treatments rather than quadratic configuration interaction (QCI) are employed to obtain CBS limit correlation energies. However, like the G3 methods, higher-order correlation energies are scaled by an optimized parameter.

What these approaches share is a design philosophy that emphasizes the algorithmic computation of thermochemical parameters, regardless of the particulars of the system under consideration. While this paradigm is not without its value, particularly in its accessibility to non-experts, its strength may also be a weakness in that the algorithmic structure limits the amount of flexibility that is often required in molecular systems.

The focal point approach differs fundamentally from these previous methods in that it is not a "black box" procedure. Developed by Allen and co-workers,[43-47] Focal-point analyses entail the layout of a two-dimensional extrapolation grid for the basis set dependence of the correlation energy in order to carefully track increments to the reaction energy toward the CBS FCI limit (see schematic focal point table given by Figure 1.1). Along the horizontal access, the *n*-particle expansion is divided into contributions from a hierarchy of methods, starting with the Hartree-Fock reference energy. The total energy for any given basis set is obtained via the horizontal summation of the energy increments across the table. Along the vertical axis, the one-particle basis is systematically increased employing basis sets that allow for extrapolation to the CBS limit. If, due to computational intractability, there are an insufficient number of basis set "points" to allow for extrapolation of an individual energy increment, the largest explicitly computed increment is assumed to be additive. The final focal point energy is attained via the

FIGURE 1.1: Focal point table schematic.[a]

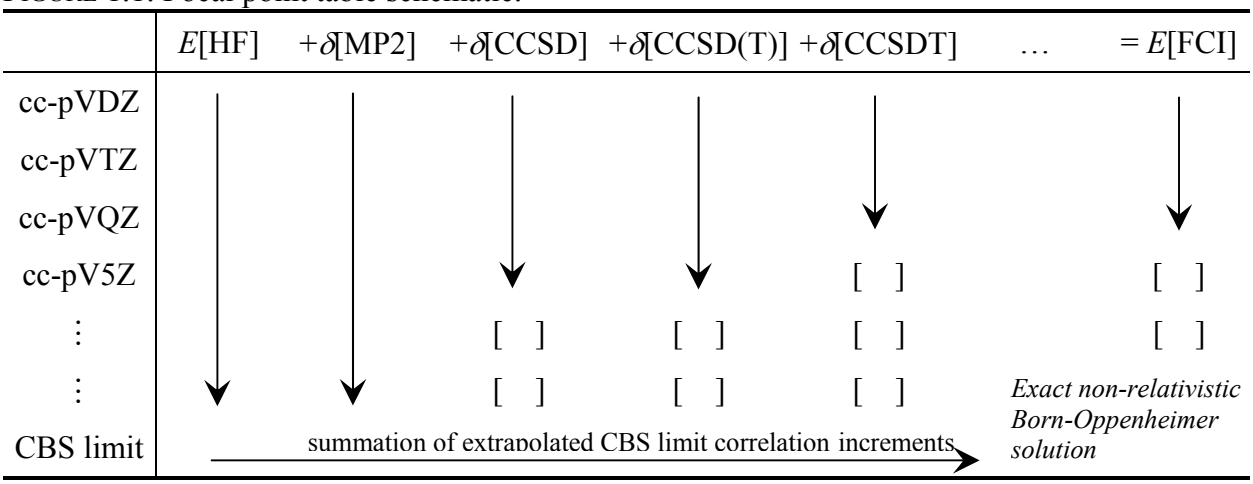

[a] The arrows represent explicitly computed energy increments in successively larger basis sets, whereas the square brackets are extrapolated values, obtained using Eqs. (1.2) and (1.3). In this idealized schematic, the full configuration interaction result is given as the highest-order increment, although in most practical cases the hierarchy of correlated methods is truncated at much lower order. Relativistic, non-Born-Oppenheimer, and other auxiliary effects are considered additively and thus not incorporated into the focal point scheme.

summation of the CBS limit increments, thus yielding an approximate CBS limit energy for the highest-order correlation method present on the horizontal axis.

The efficacy of this approach is best understood by examining the convergence properties of the individual increments. As implied by Eq. (1.2), the most rapidly convergent increment is the Hartree-Fock energy, which converges exponentially when correlation-consistent basis sets are employed. The lower-order correlated increments are determined using prodigious basis sets to ensure an accurate extrapolation to the CBS limit. In practice, the MP2 method serves this purpose well. For many reactions, these two increments comprise the vast majority of the energy. In general, increments past the relatively crude MP2 results may be seen as refinements of this energy. Assuming a hierarchy of coupled-cluster methods, increments past CCSDT are almost exclusively additive, if accessible at all due to their high computational cost. However, by construction, these increments will be both small in magnitude and relatively insensitive to basis set, particularly if the reactions under investigation have been constructed to minimize differential correlation effects between reactants and products. Thus, the increments computed using the smallest basis sets are also the most rapidly convergent and in many cases are orders of magnitude less than the first-order (MP2) correlation increment. Auxiliary effects arising from core electron correlation, special relativity, first-order non-Born-Oppenheimer terms, and spin-orbit coupling are included as necessary, with the values employed generally of the highest available accuracy, be they of experimental or theoretical origins.

1.5 Prospectus

The focal point procedure produces not only high accuracy results, but also valuable insights into both the magnitude of the higher-order energy increments and the convergence of

the one-particle basis. In this dissertation, extrapolation techniques are applied to molecular systems in a variety of contexts. In Chapter 2, a definitive *ab initio* study on the heats of formation of NCO and the [H, N, C, O] isomers is performed using focal point analysis as the primary computational tool. Chapter 3 presents gradient extrapolation formulas derived from (1.2) and (1.3) which are employed to overcome the prodigious basis set dependence of the molecular geometry of BH_5. Focal point analysis is then utilized to determine the energy of dissociation to BH_3 and H_2, as well as the barriers to internal H_2 rotation and hydrogen scrambling. Lastly, in Chapter 4, energy and gradient extrapolation formulas are applied in conjunction with vibrational perturbation theory to determine a CBS limit quartic force field for BH_3.

REFERENCES

1 W. Kohn and L. J. Sham, Phys. Rev. **140**, A1133 (1965).

2 P. Hohenberg and W. Kohn, Phys. Rev. **136**, B864 (1964).

3 C. C. J. Roothaan, Rev. Mod. Phys. **23**, 69 (1951).

4 A. Szabo and N. S. Ostlund, *Modern Quantum Chemistry: Introduction to Advanced Electronic Structure Theory*, 1st edition, revised ed. (McGraw-Hill, New York, 1989).

5 C. Schwartz, Phys. Rev. **126**, 1015 (1962).

6 C. Schwartz, Meth. Comp. Phys. **2**, 241 (1963).

7 R. Hill, J. Chem. Phys. **83**, 1173 (1985).

8 W. Kutzelnigg and J. D. Morgan III, J. Chem. Phys. **96**, 4484 (1992).

9 W. Kutzelnigg and J. D. Morgan III, J. Chem. Phys. **97**, 8821 (1992).

10 D. P. Carroll, H. J. Silverstone, and R. M. Metzger, J. Chem. Phys. **71**, 4142 (1979).

11 W. Kutzelnigg, Theor. Chim. Acta **68**, 445 (1985).

[12] W. Klopper and W. Kutzelnigg, J. Chem. Phys. **94**, 2020 (1991).

[13] W. Klopper and W. Kutzelnigg, Chem. Phys. Lett. **134**, 17 (1987).

[14] J. Noga and W. Kutzelnigg, J. Chem. Phys. **101**, 7738 (1994).

[15] T. H. Dunning, Jr., J. Chem. Phys. **90**, 1007 (1989).

[16] D. E. Woon and T. H. Dunning, Jr., J. Chem. Phys. **98**, 1358 (1993).

[17] D. E. Woon and T. H. Dunning, Jr., J. Chem. Phys. **100**, 2975 (1994).

[18] D. E. Woon and T. H. Dunning, Jr., J. Chem. Phys. **103**, 4572 (1995).

[19] A. K. Wilson, T. van Mourik, and T. H. Dunning, Jr., J. Mol. Struct. (Theochem) **388**, 339 (1996).

[20] D. Feller, J. Chem. Phys. **98**, 7059 (1993).

[21] T. Helgaker, W. Klopper, H. Koch, and J. Noga, J. Chem. Phys. **106**, 9639 (1997).

[22] A. Halkier, T. Helgaker, P. Jørgensen, W. Klopper, and J. Olsen, Chem. Phys. Lett. **302**, 437 (1999).

[23] J. A. Pople, M. J. Frisch, B. T. Luke, and J. S. Binkley, Int. J. Quant. Chem. Symp. **17**, 307 (1983).

[24] R. J. Bartlett and I. Shavitt, Chem. Phys. Lett. **50**, 190 (1977).

[25] Z. He and D. Cremer, Int. J. Quantum Chem. **59**, 71 (1996).

[26] E. Brindas and O. Goscinski, Phys. Rev. A **1**, 52 (1970).

[27] S. Wilson, D. M. Silver, and R. A. Farrell, Proc. R. Soc. A **356**, 363 (1977).

[28] N. C. Handy, P. J. Knowles, and K. Somasundram, Theor. Chim. Acta **68**, 87 (1985).

[29] W. D. Laidig, G. Fitzgerald, and R. J. Bartlett, Chem. Phys. Lett. **113**, 151 (1985).

[30] P. M. W. Gill and L. Radom, Chem. Phys. Lett. **132**, 16 (1986).

[31] J. Olsen, O. Christiansen, H. Koch, and P. Jørgensen, J. Chem. Phys. **105**, 5082 (1996).

[32] M. L. Leininger, W. D. Allen, H. F. Schaefer, and C. D. Sherrill, J. Chem. Phys. **112**, 9213 (2000).

[33] S. Hirata and R. J. Bartlett, Chem. Phys. Lett. **321**, 216 (2000).

[34] J. Olsen, J. Chem. Phys. **113**, 7140 (2000).

[35] M. Kállay and P. R. Surján, J. Chem. Phys. **113**, 1359 (2000).

[36] G. A. Petersson and M. Braunstein, J. Chem. Phys. **83**, 5129 (1985).

[37] G. A. Petersson, A. Bennett, T. G. Tensfeldt, M. A. Al-Laham, W. A. Shirley, and J. Mantzaris, J. Chem. Phys. **89**, 2193 (1988).

[38] L. A. Curtiss, K. Raghavachari, G. W. Trucks, and J. A. Pople, J. Chem. Phys. **94**, 7221 (1991).

[39] L. A. Curtiss, K. Raghavachari, P. C. Redfern, V. Rassolov, and J. A. Pople, J. Chem. Phys. **109**, 7764 (1998).

[40] L. A. Curtiss, P. C. Redfern, K. Raghavachari, and J. A. Pople, Chem. Phys. Lett. **359**, 390 (2002).

[41] J. M. L. Martin and G. d. Oliveira, J. Chem. Phys. **111**, 1843 (1999).

[42] A. D. Boese, M. Oren, O. Atasoylu, J. M. L. Martin, and M. Kállay, J. Chem. Phys. **120**, 4129 (2004).

[43] W. D. Allen, A. L. L. East, and A. G. Császár, in *Structures and Conformations of Non-Rigid Molecules*, edited by J. Laane, M. Dakkouri, B. van der Vecken, and H. Oberhammer (Kluwer, Dordrecht, 1993), pp. 343.

[44] A. G. Császár, W. D. Allen, and H. F. Schaefer III, J. Chem. Phys. **108**, 9751 (1998).

[45] A. G. Császár, G. Tarczay, M. L. Leininger, O. L. Polyansky, J. Tennyson, and W. D. Allen, in *Spectroscopy from Space*, edited by J. Demaison and K. Sarka (Kluwer, Dordrecht, 2001), pp. 317.

[46] J. M. Gonzales, R. S. Cox III, S. T. Brown, W. D. Allen, and H. F. Schaefer III, J. Phys. Chem. A **105**, 11327 (2001).

[47] J. P. Kenny, W. D. Allen, and H. F. Schaefer, J. Chem. Phys. **118**, 7353 (2003).

CHAPTER 2

TOWARD SUBCHEMICAL ACCURACY IN COMPUTATIONAL THERMOCHEMISTRY: FOCAL POINT ANALYSIS OF THE ENTHALPY OF FORMATION OF NCO AND [H,N,C,O] ISOMERS[1]

[1] Schuurman, M. S.; Muir, S. R.; Allen, W. D.; Schaefer, H. F. *J. Chem. Phys*., **118**, 11293 (2004). Reprinted by permission of the American Institute of Physics.

2.1 ABSTRACT

In continuing pursuit of thermochemical accuracy to the level of 0.1 kcal mol^{-1}, the enthalpies of formation of NCO, HNCO, HOCN, HCNO, and HONC have been rigorously determined using state-of-the-art *ab initio* electronic structure theory, including conventional coupled cluster methods [CCSD, CCSD(T), CCSDT] with large basis sets, conjoined in cases with explicitly-correlated MP2-R12/A computations. Limits of valence and all-electron correlation energies were extrapolated via focal point analysis using correlation consistent basis sets of the form cc-pV*X*Z (*X* = 2-6) and cc-pCV*X*Z (*X* = 2-5), respectively. In order to reach subchemical accuracy targets, core correlation, spin-orbit coupling, special relativity, the diagonal Born-Oppenheimer correction (DBOC), and anharmonicity in zero-point vibrational energies (ZPVEs) were accounted for. Various coupled-cluster schemes for partially including connected quadruple excitations were also explored, although none of these approaches gave reliable improvements over CCSDT theory. Based on numerous, independent thermochemical paths, each designed to balance residual *ab initio* errors, our final proposals are $\Delta_f H_0^\circ$(NCO) = +30.5, $\Delta_f H_0^\circ$(HNCO) = –27.6, $\Delta_f H_0^\circ$(HOCN) = –3.1, $\Delta_f H_0^\circ$(HCNO) = +40.9, and $\Delta_f H_0^\circ$(HONC) = +56.3 kcal mol^{-1}. The internal consistency and convergence behavior of the data suggests accuracies of ±0.2 kcal mol^{-1} in these predictions, except perhaps in the HCNO case. However, the possibility of somewhat larger systematic errors cannot be excluded, and the need for full CCSDTQ computations to eliminate remaining uncertainties is apparent.

2.2 INTRODUCTION

The role of isocyanic acid (HNCO) in the reduction of nitrogenous by-products of combustion processes has been subjected to intense study for some time.[1-9] In large measure this interest has been driven by the role HNCO plays in the RAPRENOx process,[10] by which NO_x in effluent streams is reduced to more innocuous species such as N_2, H_2O and CO_2. In addition, the

cyanato radical (NCO) is a key intermediate in RAPRENOx and other combustion processes and has itself been the subject of extensive investigation.[11-14]

The most common techniques employed to obtain the enthalpy of formation of NCO have involved the photodissociation of HNCO. In 1970, Okabe[15] determined D_0(H-NCO) = 113.0 ± 0.2 kcal mol^{-1} via the direct dissociation of HNCO to NCO($^2\Pi$) + H(^2S). Using the contemporaneous value for the enthalpy of formation of HNCO resulted in $\Delta_f H_0^\circ$(NCO) = 37.8 ± 3.5 kcal mol^{-1}. In 1983, Sullivan and co-workers[16] probed the $\widetilde{B}\,^2\Pi$ state of NCO and found that the fluorescence lifetime of the (100) vibrational state was almost an order of magnitude lower than that of the ground (000) state. These results suggested that the N(^2D) + CO dissociation limit lay somewhere between these two vibrational states, leading to a lower bound of $\Delta_f H_0^\circ$(NCO) ≥ 48 kcal mol^{-1}. In 1986, Spiglanin *et al.*[17] observed an onset energy of 118.7 kcal mol^{-1} for the production of NH($a\,^1\Delta$) and CO($X\,^1\Sigma^+$) via the photodissociation of HNCO. This threshold gave thermochemical values of $\Delta_f H_0^\circ$(HNCO) = –24.9(+0.7, –2.8) kcal mol^{-1} and, using Okabe's value of D_0(H-NCO), corresponds to $\Delta_f H_0^\circ$(NCO) = 36.1(+0.7, –2.8) kcal mol^{-1}. In 1989, Liu and Coombe[18] performed a photolysis study of the reaction $\mathrm{NCO}(^2\Pi) \rightarrow \mathrm{CN}(^2\Sigma^+) + \mathrm{O}(^3P)$ in which CN production was monitored via $X\,^2\Sigma^+ \leftarrow B\,^2\Sigma^+$ laser-induced fluorescence. The upper limit on the internal excitation of the CN($^2\Sigma^+$) fragments, as obtained using a spectral simulation, indicated $\Delta_f H_0^\circ$(NCO) > 37 kcal mol^{-1}.

Beginning with the work of Cyr *et al.*[19] in 1992, significant progress in establishing $\Delta_f H_0^\circ$(NCO) began to be made on what was proving to be a difficult spectroscopic challenge. A fast beam study was performed in which the production of NCO free radicals via photodetachment of NCO^- was followed by excitation to NCO ($\widetilde{B}\,^2\Pi$), for which all vibrational levels were found to predissociate. The kinetic energy distributions of the N and CO products were then measured using time-of-flight mass spectrometry. Variation of the dissociative laser

wavelength bracketed the onset energy at which the dissociation pathway $NCO(^2\Pi) \rightarrow N(^2D) + CO(^1\Sigma^+)$ became energetically accessible, with subsequent analysis yielding $\Delta_f H^\circ_0$(NCO) = 30.5 ± 1 kcal mol^{-1}. This result was significantly lower than all values in the prevailing literature.

In early 1993, East, Johnson and Allen[20] applied high-level *ab initio* techniques in an early focal point analysis scheme to determine and extensively characterize the ground state of HNCO and the relative energies of its low-lying isomers. In their study, $\Delta_f H^\circ_0$(HNCO) was determined from the isogyric reaction $NH_3 + CO_2 \rightarrow H_2O + HNCO$, while $\Delta_f H^\circ_0$(NCO) was computed from the heterolytic bond breaking reaction $HNCO \rightarrow H^+ + NCO^-$. The investigation employed up to a quadruple-zeta quality basis with correlation treatments up to MP4, resulting in $\Delta_f H^\circ_0$(HNCO) = –26.1 kcal mol^{-1} and $\Delta_f H^\circ_0$(NCO) = 35.3 kcal mol^{-1}. In addition, the relative energies (ΔE_e) of the low-lying isomers HOCN, HCNO and HONC were found to be 25.5 ± 1.0, 70 ± 2 and 84.5 ± 1.5 kcal mol^{-1}. Earlier 6-31G** MP2 harmonic frequency data[21] gave zero-point vibrational energy (ZPVE) corrections for these isomerization energies of –0.14, –0.93, and –0.73 kcal mol^{-1}, respectively. Later in 1993 East and Allen performed a more refined *ab initio* study[22] considering five different thermochemical routes and employing coupled-cluster treatments up to CCSD(T), in addition to further MP*n* results. Their revised values were $\Delta_f H^\circ_0$(HNCO) = –27.5 ± 0.5 kcal mol^{-1} and $\Delta_f H^\circ_0$(NCO) = 31.4 ± 0.5, with their value of $\Delta_f H^\circ_0$(NCO) in excellent agreement with that determined by Cyr *et al.*[19]

The past decade has seen numerous groundbreaking studies[19,23-29] examining the fascinating dynamics and attendant thermochemistry in the multiple dissociation channels of HNCO, in particular, three channels which are competitive in the region below 45 000 cm^{-1}:

$$HNCO \rightarrow NH(X\,^3\Sigma^-) + CO(X\,^1\Sigma^+) \quad \text{(I)}$$

$$HNCO \rightarrow H(^2S) + NCO(X\,^2\Pi) \quad \text{(II)}$$

$$\mathrm{HNCO} \rightarrow \mathrm{NH}(a\,^1\Delta) + \mathrm{CO}(X\,^1\Sigma^+) \qquad \text{(III)}$$

A photoionization mass spectrometric study[23] of HNCO and NCO gave D_0(H-NCO) ≤ 110.1 ± 0.3 kcal mol^{-1} in 1994. Then in 1996, Brown *et al.*[24] determined the threshold energies of both channels (II) and (III) by dissociating vibrationally excited HNCO and monitoring the product yields of NCO($X\,^2\Pi$) and NH($a\,^1\Delta$) via laser-induced fluorescence (LIF). From their data and the known singlet/triplet splitting of NH, they determined upper bounds for D_0 in channels (II) and (III) of 109.6 ± 0.4 kcal mol^{-1} and 122.1 ± 0.3 kcal mol^{-1}, respectively. Using $\Delta_f H_0^\circ$(NCO) from Ref. 19 and accepted enthalpies of formation of NH[30,31] and CO[32] yielded an averaged value of $\Delta_f H_0^\circ$(HNCO) ≥ –27.7 ± 1.1 kcal mol^{-1}. Also in 1996, Zyrianov *et al.*[25] obtained accurate dissociation energies for the same two channels employing sequential two-photon excitation of jet-cooled HNCO via the S_1 state. Again, the product yields of the dissociation processes were monitored using LIF. Utilizing the measured D_0(^{1}NH-CO) = 122.5 (+0.03, –0.17) kcal mol^{-1} and the known enthalpies of the formation of NH and CO yielded $\Delta_f H_0^\circ$(HNCO) = −27.8 ± 0.4 kcal mol^{-1}. Additionally, D_0(H-NCO) = 109.7 ± 0.1 kcal mol^{-1} was determined, resulting in $\Delta_f H_0^\circ$(NCO) = 30.3 ± 0.4 kcal mol^{-1}.

The controversy surrounding the enthalpy of formation of NCO was given new life in 1996 when a VUV photolysis study of NCO by Schönnenbeck and Stuhl[33] led to a lower bound of $\Delta_f H_0^\circ$(NCO) ≥ 40 kcal mol^{-1}. This enthalpy of formation, while significantly higher than currently accepted values, was in concert with the aforementioned studies prior to 1992. Thus, in 2001 Hoops *et al.*[29] performed a new experiment on the dissociation of NCO to N(^2D) and CO($^1\Sigma^+$), employing a higher resolution detection scheme to measure product energy distributions. From their determination of D_0(N-CO) = 54.0 ± 0.7 kcal mol^{-1} they obtained $\Delta_f H_0^\circ$(NCO) = 31.4 ± 0.7 kcal mol^{-1}, almost 1 kcal mol^{-1} larger than that derived from the 1992

study in the same group,[19] and in very good agreement with the best existing *ab initio* results, particularly those of Ref. 22.

The interest accorded the thermochemical properties of HNCO and NCO by both experimental and computational chemists makes these molecular systems ideal test beds for next-generation electronic structure methods designed to deliver sub-chemical accuracy (ca. 0.1 kcal mol^{-1}). To achieve these ends, a multi-pronged approach is required that rigorously addresses both the one-particle basis set and *N*-particle electron correlation expansions, as well as numerous auxiliary effects such as core correlation, special relativity, spin-orbit splitting, non-Born-Oppenheimer terms and vibrational anharmonicity. The development of extrapolation techniques utilizing correlation consistent basis sets has emerged as a powerful method for approaching the complete basis set (CBS) limits in electronic structure theory. However, the accuracy obtainable via such extrapolations is dependent on the rate of convergence of the correlation energy in the one-particle expansion, which has been shown to be frustratingly protracted.[34-37]

One of the most promising developments in response to the sluggish convergence rates of the one-particle expansion found in traditional correlation treatments has been the emergence of linear R12 methods.[38-41] These techniques explicitly include the interelectronic distance, R12, in the functional form of the wave function. The result is a wave function that exhibits the proper behavior with respect to electron cusp conditions and more rapid convergence of the correlation energy to the CBS limit. Recent research in our laboratory has focused on the development of efficient linear R12 electronic structure codes, resulting in a powerful MP2-R12/A implementation.[42,43] In addition, our recent investigations[36] have analyzed the convergence behavior of molecular partial wave expansions of conventional and linear R12 correlation energies.

In the present investigation, extrapolations utilizing correlation consistent basis sets, as well as explicit MP2-R12 computations, are employed in order to push the limits of attainable accuracy via *ab initio* methods. Recent studies have demonstrated that computational techniques employing advanced treatments of electron correlation in conjunction with large correlation consistent basis sets have the ability to produce enthalpies of formation that rival the most accurately known experimental results.[44-50] Here we aim to determine *ab initio* results of subchemical accuracy for the enthalpies of formation of NCO, HNCO, HOCN, HCNO and HONC.

2.3 THEORETICAL METHODS

In this investigation we first determine $\Delta_f H^\circ_0(\mathrm{NCO})$ precisely by considering two separate formation reactions:

$$\mathrm{N}(^4S) + \mathrm{CO_2} \rightarrow \mathrm{O}(^3P_2) + \mathrm{NCO}(^2\Pi_{3/2}) \quad (2.1)$$

$$\mathrm{NH}(^3\Sigma^-) + \mathrm{CO_2} \rightarrow \mathrm{OH}(^2\Pi_{3/2}) + \mathrm{NCO}(^2\Pi_{3/2}) \quad (2.2)$$

Then seven additional reactions are employed to pinpoint $\Delta_f H^\circ_0(\mathrm{HNCO})$,

$$\mathrm{NH_3} + \mathrm{CO_2} \rightarrow \mathrm{H_2O} + \mathrm{HNCO} \quad (2.3)$$

$$\mathrm{NH}(^3\Sigma^-) + \mathrm{CO_2} \rightarrow \mathrm{O}(^3P_2) + \mathrm{HNCO} \quad (2.4)$$

$$\mathrm{H}(^2S) + \mathrm{NCO}(^2\Pi_{3/2}) \rightarrow \mathrm{HNCO} \quad (2.5)$$

$$\mathrm{H^+} + \mathrm{NCO^-}(^1\Sigma^+) \rightarrow \mathrm{HNCO} \quad (2.6)$$

$$\mathrm{NH}(^3\Sigma^-) + \mathrm{NCO}(^2\Pi_{3/2}) \rightarrow \mathrm{N}(^4S) + \mathrm{HNCO} \quad (2.7)$$

$$\mathrm{NH_3} + 3\mathrm{NCO}(^2\Pi_{3/2}) \rightarrow \mathrm{N}(^4S) + 3\mathrm{HNCO} \quad (2.8)$$

$$\mathrm{H_2O} + 2\mathrm{NCO}(^2\Pi_{3/2}) \rightarrow \mathrm{O}(^3P_2) + 2\mathrm{HNCO} \quad (2.9)$$

of which the first two are independent of the enthalpy of formation of NCO, and the rest assume the final $\Delta_f H_0^\circ$(NCO) value derived from Reactions (2.1) and (2.2). Finally, the enthalpies of formation of the principal isomers of HNCO are evaluated from Reactions (2.10) – (2.12).

$$\text{HNCO} \rightarrow \text{HOCN} \tag{2.10}$$

$$\text{HNCO} \rightarrow \text{HCNO} \tag{2.11}$$

$$\text{HNCO} \rightarrow \text{HONC} \tag{2.12}$$

The general approach of this work is to ascertain the *ab initio* limits of the reaction energies for (2.1) – (2.12) via dual one- and *N*-particle extrapolations of highest feasible quality within the focal point approach of Allen and co-workers.[22,36,51-54]

After inferring *ab initio* limits for the reaction energies, the precisely established enthalpies of formation listed in Table 2.1 for component species are employed to ascertain our target enthalpies. Whether purely empirical or aided by extremely high levels of theory, the adopted reference enthalpies are the best available, at least to our knowledge. Our thermochemical routes are designed to avoid full atomization reactions in favor of isogyric (or even isoelectronic) comparisons, and thereby to minimize differential errors in *ab initio* predictions, with the goal of achieving subchemical accuracy without empirical parametrizations.

The (aug-)cc-p(C)V*X*Z families of basis sets developed by Dunning and co-workers[55-59] were used exclusively in this investigation for all conventional (non-R12) methods. For computations utilizing the MP2-R12/A approach,[38,39,41-43] a large, uncontracted basis set is required for an adequate resolution of the identity needed in the computation of three- and four-electron integrals in terms of nonstandard two-electron integrals. For C, N and O, the R12 basis is represented as (19*s*13*p*11*d*9*f*7*g*5*h*), while for H it is given by (13*s*11*p*9*d*7*f*5*g*), where both sets were obtained by uncontracting the corresponding cc-pV5Z basis set and adding tight and diffuse

TABLE 2.1: Pertinent gas-phase thermochemical data (kcal mol^{-1})

	$\Delta H^{\circ}_{f,0}$	Ref.	ZPVE[b]	Ref.	ΔE_{so}[f]
H (^2S)	51.634 (002)	expt., 60	0	--	--
C ($^3P_0$)	169.98 (11)	expt., 60	0	--	0.085
N (^4S)	112.53 (02)	expt., 60	0	--	--
O ($^3P_2$)	58.98 (02)	expt., 60	0	--	0.223
N_2	0.0	expt., 60	3.36 (3.37)[c]	61 (61)	--
NH ($^3\Sigma^-$)	85.92 (08)	theory, 48	4.64 (4.69)[c]	61 (61)	--
OH ($^2\Pi_{3/2}$)	8.85 (07)	mixed, 62	5.29 (5.34)[c]	61 (61)	0.180
CO	–27.20 (04)	expt., 60	3.09 (3.10)[c]	61 (61)	--
H_2O	–57.10 (01)	expt., 60	13.26 (13.55)	63 (64)	--
CO_2	–93.97 (01)	expt., 60	7.25 (7.28)	65 (65)	--
NH_3	–9.3 (1)	expt., 60	21.21 (21.65)	66 (67)	--
NCO^-	[50.7]	[a]	6.57 (6.61)	68 (68)	--
NCO ($^2\Pi_{3/2}$)	[30.6]	[a]	6.03 (6.07)[c]	69 (69)[d]	0.137
HNCO	[–27.6]	[a]	13.24 (13.39)	[e]	--
HCNO	[40.4]	[a]	11.16 (12.38)	70 (70)	--
HOCN	[–3.1]	[a]	13.08 (13.18)[c]	70 (70)	--
HONC	[56.0]	[a]	12.49 (12.61)[c]	70 (70)	--
IP(H) = 313.588[g]			EA(NCO)= 83.23(12)[h]		

[a] This work.
[b] Based on explicit anharmonic vibrational analyses for every species; harmonic values in parentheses.
[c] Computed here from reported spectroscopic constants.
[d] Computed using formulae from Ref. 71.
[e] Computed from extrapolated CBS CCSD(T) + core correlation quadratic force field conjoined with complete cc-pVQZ CCSD(T) quartic force field, to be published.
[f] Spin-orbit splitting corrections for C and O are from Ref. 72, OH from Ref. 62, and NCO from Ref. 73.
[g] Ref. 72.
[h] Ref. 73.

shells for every angular momentum value in an even-tempered fashion using the exponent ratio of the original two tightest and two most diffuse functions.[43]

The first focal point extrapolation is of the total energies of reactants and products computed under the frozen-core approximation. For this primary extrapolation, valence correlation consistent basis sets of the form (aug-)cc-pV*X*Z (*X* = 2, 3, 4, 5, 6)[55,56,58] were utilized to determine energies at the RHF and UHF (restricted and unrestricted Hartree-Fock),[74-77] MP2 (second-order Møller-Plesset perturbation theory),[78,79] CCSD (coupled cluster singles and doubles),[80-83] CCSD(T) (CCSD with perturbative triples),[84-86] and CCSDT (full coupled cluster through triple excitations)[87-89] levels of theory. In addition, the cc-pVTZ basis was used to obtain perturbative estimates of the effects of connected quadruple excitations via the Brueckner-orbital coupled-cluster approach BD(TQ)[80,90,91] and the CCSD(2)[92,93] method. For reactions in which only closed-shell species are present, the MP2-R12/A method[38,39,41-43] was employed to obtain the CBS-limit MP2 energy. The second focal point extrapolation involves the determination of the core correlation energy that is neglected in a valence-only treatment. Core-valence basis sets of the form (aug-)cc-pCV*X*Z (*X* = 2, 3, 4, 5)[57] were used in these extrapolations. Energy increments through the CCSDT level were incorporated in the determination of the core correlation energy. All energy computations were performed using a highly accurate, fixed r_e structure for each molecular species, as detailed in Table 2.2.

Details of the focal point extrapolation scheme have been given in several other publications.[36,51,53] The layout of the valence extrapolations is presented in Tables 2.3, 2.4 and 2.5 for the determination of the energies of Reactions (1) – (12). In acknowledgment of space constraints, the secondary extrapolations to ascertain the effects of core correlation are given as supplementary material (Tables A.1-A.3).[103] In the focal point analysis of core correlation effects, the largest basis set used for each level of theory was cc-pCV(*X*–1)Z, where cc-pV*X*Z is

TABLE 2.2: High-quality r_e structural parameters (Å, deg) of relevant species

	Source	Ref.	Geometry
NH ($^3\Sigma^-$)	Expt.	61	r_e(NH) = 1.0362
OH ($^2\Pi_{3/2}$)	Expt.	61	r_e(OH) = 0.96966
CO	Expt.	61	r_e(CO) = 1.1658
H_2O	Expt.	94	r_e(OH) = 0.9572, θ_e(HOH) = 104.52º
CO_2	Expt.	95	r_e(CO) = 1.1600
NH_3	Expt.	96	r_e(NH) = 1.0124, θ_e(HNH) = 106.67º
NCO ($^2\Pi_{3/2}$)	cc-pCVQZ CCSD(T)	[a]	r_e(NC) = 1.2276, r_e(CO) = 1.1744
NCO^-	aug-cc-pCVQZ CCSD(T)	[a]	r_e(NC) = 1.1910, r_e(CO) = 1.2279
HNCO	Expt.(A_0, B_0, C_0) / RHF (α_e)	98	r_e(HN) = 1.0030, r_e(NC) = 1.2146, r_e(CO) = 1.1634, θ_e(HNC) = 123.34º, θ_e(NCO) = 172.22º
HOCN	cc-pVQZ CCSD(T)	[a]	r_e(HO) = 0.9638, r_e(OC) = 1.3031, r_e(CN) = 1.1601, θ_e(HOC) = 109.34º, θ_e(OCN) = 176.81º
HCNO	cc-pVQZ CCSD(T)	97	r_e(HC) = 1.0605, r_e(CN) = 1.1620, r_e(NO) = 1.2039, θ_e(HCN) = 180º, θ_e(CNO) = 180º
HONC	cc-pVQZ CCSD(T)	[a]	r_e(HO) = 0.9658, r_e(ON) = 1.3321, r_e(NC) = 1.1762, θ_e(HON) = 104.61º, θ_e(ONC) = 172.64º

[a] This work.

the largest set used for that level in the corresponding frozen-core focal point table. The information contained in each focal-point table is substantial, and the footnotes to Tables 2.3, 2.4 and 2.5 explain procedures and notations. The functional form adopted for the Hartree-Fock extrapolations[104] is

$$E_{HF}(X) = E_{HF}^{\infty} + ae^{-bX}, \tag{2.13}$$

whereas that used to evaluate correlation energy limits[34] is

$$E_{corr}(X) = a + bX^{-3}. \tag{2.14}$$

The adiabatic approximation is invoked by appending to the energy of the r_e structures the diagonal Born-Oppenheimer correction (DBOC).[105-108] This energy term corresponds to the first-order correction to the Born-Oppenheimer approximation and accounts for finite nuclear mass. The DBOC corrections were computed at the cc-pVDZ CISD level of theory for each molecular species using the code recently developed by Valeev and co-workers.[108]

For atoms with degenerate ground states, spin-orbit splitting corrections were computed using experimentally observed spin-state energies. Specifically, these corrections were computed by taking advantage of the fact that within an atomic LS manifold the spin-orbit operator leaves invariant the degeneracy-weighted energetic center of gravity to which conventional *ab initio* total energies correspond. Empirical spin-orbit corrections were also applied to the OH and NCO radicals using analogous principles for linear molecules.

While relativistic effects for first-row atoms are small, their inclusion is necessary for subchemical accuracy. Thus, the one-electron mass-velocity and Darwin terms[109-113] arising from a scalar relativistic treatment of electronic motion have been computed using the perturbative approach of Ref. 109 at the cc-pCVTZ CCSD(T) level of theory.

TABLE 2.3: Valence focal point analysis of NCO ($^2\Pi$) formation reactions[a]

	ΔE_e[UHF]	$+\delta$[MP2]	$+\delta$[CCSD]	$+\delta$[CCSD(T)]	$+\delta$[CCSDT]	$= \Delta E_e$[CCSDT]
Reaction (1): $N(^4S) + CO_2 \rightarrow O(^3P) + NCO(^2\Pi)$						
cc-pVDZ	66.42	+20.99	–13.34	+0.60	–0.57	74.11
cc-pVTZ	66.46	+20.53	–14.36	+0.98	–0.79	72.81
cc-pVQZ	66.38	+20.74	–14.65	+0.83	–0.64	72.65
cc-pV5Z	66.25	+20.76	–14.71	+0.82	[–0.63]	[72.49]
cc-pV6Z	66.24	+20.76	[–14.72]	[+0.82]	[–0.63]	[72.46]
CBS limit	[66.23]	[+20.76]	[–14.75]	[+0.81]	[–0.62]	[**72.44**]
Reaction (2): $NH(^3\Sigma^-) + CO_2 \rightarrow OH(^2\Pi) + NCO(^2\Pi)$						
cc-pVDZ	49.94	+12.19	–10.89	+0.54	–0.52	51.26
cc-pVTZ	49.53	+10.68	–10.88	+0.39	–0.55	49.17
cc-pVQZ	49.32	+10.51	–10.89	+0.31	–0.55	48.70
cc-pV5Z	49.17	+10.40	–10.86	+0.27	[–0.53]	[48.44]
cc-pV6Z	49.15	+10.38	[–10.88]	[+0.25]	[–0.52]	[48.38]
CBS limit	[49.14]	[+10.36]	[–10.91]	[+0.23]	[–0.51]	[**48.31**]
Extrapolation scheme	$a+be^{-cX}$	$a+bX^{-3}$	$a+bX^{-3}$	$a+bX^{-3}$	$a+bX^{-3}$	
Points (X =)	4, 5, 6	5, 6	4, 5	4, 5	3, 4	

[a] For correlated methods the symbol δ denotes the increment in the relative energy (ΔE_e) with respect to the preceding level of theory in the hierarchy UHF → MP2 → CCSD → CCSD(T) → CCSDT. Brackets signify results obtained from basis set extrapolations detailed in the last rows of the table; all other entries are from explicit electronic structure computations. Final predictions are boldfaced.

TABLE 2.4: Valence focal point analysis of HNCO formation reactions[a]

	ΔE_e[UHF]	$+\delta$[MP2]	$+\delta$[CCSD]	$+\delta$[CCSD(T)]	$+\delta$[CCSDT]	$= \Delta E_e$[CCSDT]
Reaction (3): $NH_3 + CO_2 \rightarrow H_2O + HNCO$						
cc-pVDZ	25.89	+0.23	–0.24	0.00	–0.04	25.84
cc-pVTZ	24.26	–1.94	+0.10	–0.22	+0.00	22.20
cc-pVQZ	23.73	–2.58	+0.31	–0.31	[+0.00]	[21.15]
cc-pV5Z	23.52	–2.86	+0.45	–0.35	[+0.00]	[20.75]
cc-pV6Z	23.46	–2.93	[+0.45]	[–0.37]	[+0.00]	[20.61]
CBS limit	[23.45]	[–3.00][b]	[+0.46]	[–0.40]	[+0.00]	[**20.51**]
Reaction (4): $NH(^3\Sigma^-) + CO_2 \rightarrow O(^3P) + HNCO$						
cc-pVDZ	29.37	+10.93	–1.61	+0.00	+0.00	38.70
cc-pVTZ	29.78	+10.56	–2.30	+0.50	–0.16	38.38
cc-pVQZ	29.77	+10.77	–2.33	+0.36	[–0.16]	[38.42]
cc-pV5Z	29.67	+10.87	–2.31	+0.38	[–0.16]	[38.44]
cc-pV6Z	29.67	+10.91	[–2.30]	[+0.39]	[–0.16]	[38.50]
CBS limit	[29.67]	[+10.96]	[–2.30]	[+0.40]	[–0.16]	[**38.58**]
Reaction (5): $H(^2S) + NCO(^2\Pi) \rightarrow HNCO$						
cc-pVDZ	–84.83	–30.76	+9.51	–1.15	+0.47	–106.76
cc-pVTZ	–87.33	–35.57	+10.10	–1.43	+0.55	–113.67
cc-pVQZ	–87.74	–37.43	+10.50	–1.51	[+0.55]	[–115.61]
cc-pV5Z	–87.87	–38.08	+10.74	–1.52	[+0.55]	[–116.19]
cc-pV6Z	–87.90	–38.36	[+10.84]	[–1.53]	[+0.55]	[–116.40]
CBS limit	[–87.90]	[–38.75]	[+10.97]	[–1.54]	[+0.55]	[**–116.67**]
Reaction (6): $H^+ + NCO^- \rightarrow HNCO$						
aug-cc-pVDZ	–348.20	+5.50	–3.13	+0.61	–0.20	–345.44
aug-cc-pVTZ	–350.26	+5.98	–3.36	+0.92	–0.26	–346.99
aug-cc-pVQZ	–350.62	+6.25	–3.44	+0.98	[–0.26]	[–347.09]
aug-cc-pV5Z	–350.70	+6.50	[–3.62]	[+1.00]	[–0.26]	[–347.07]
aug-cc-pV6Z	–350.70	+6.65	[–3.74]	[+1.01]	[–0.26]	[–347.04]
CBS limit	[–350.71]	[+6.97][b]	[–3.89]	[+1.03]	[–0.26]	[**–346.87**]
Extrapolation scheme	$a+be^{-cX}$	$a+bX^{-3}$	$a+bX^{-3}$	$a+bX^{-3}$	add	
Points (X=)	4, 5, 6	5, 6	4, 5	4, 5	--	

[a] See footnote *a* of Table 2.3. The CCSDT increments given here for the larger basis sets are obtained from a simple additivity approximation.

[b] CBS limit energy obtained via explicit MP2-R12/A computations; cc-pV*X*Z (*X*=5,6) extrapolation yields [–3.03] for Reaction (2.3) and [+6.85] for Reaction (2.6).

TABLE 2.4: Valence focal point analysis of HNCO formation reactions (cont'd)[a]

	ΔE_e[UHF]	$+\delta$[MP2]	$+\delta$[CCSD]	$+\delta$[CCSD(T)]	$+\delta$[CCSDT]	$= \Delta E_e$[CCSDT]
Reaction (7): $NH(^3\Sigma^-) + NCO(^2\Pi) \rightarrow N(^4S) + HNCO$						
cc-pVDZ	–37.05	–10.06	+11.73	–0.60	+0.57	–35.41
cc-pVTZ	–36.67	–9.96	+12.06	–0.49	+0.63	–34.43
cc-pVQZ	–36.61	–9.93	+12.33	–0.47	[+0.63]	[–34.08]
cc-pV5Z	–36.58	–9.89	+12.40	–0.44	[+0.63]	[–33.89]
cc-pV6Z	–36.56	–9.85	[+12.42]	[–0.43]	[+0.63]	[–33.80]
CBS limit	[–36.56]	[–9.80]	[+12.45]	[–0.42]	[+0.63]	[**–33.69**]
Reaction (8): 1/3 $[NH_3 + 3NCO(^2\Pi) \rightarrow N(^4S) + 3HNCO]$						
cc-pVDZ	–20.68	–6.59	+9.55	–0.49	+0.50	–17.71
cc-pVTZ	–20.87	–6.45	+9.41	–0.31	+0.53	–17.69
cc-pVQZ	–20.91	–6.54	+9.52	–0.27	[+0.53]	[–17.67]
cc-pV5Z	–20.88	–6.52	+9.55	–0.25	[+0.53]	[–17.58]
cc-pV6Z	–20.89	–6.52	[+9.57]	[–0.24]	[+0.53]	[–17.55]
CBS limit	[–20.89]	[–6.52]	[+9.59]	[–0.23]	[+0.53]	[**–17.51**]
Reaction (9): 1/2 $[H_2O + 2NCO(^2\Pi) \rightarrow O(^3P) + 2HNCO]$						
cc-pVDZ	–10.76	+0.51	+7.78	–0.44	+0.49	–2.42
cc-pVTZ	–10.21	+1.56	+6.89	+0.14	+0.40	–1.23
cc-pVQZ	–10.04	+1.85	+6.80	+0.16	[+0.40]	[–0.83]
cc-pV5Z	–9.96	+2.02	+6.74	+0.21	[+0.40]	[–0.58]
cc-pV6Z	–9.94	+2.06	[+6.76]	[+0.24]	[+0.40]	[–0.48]
CBS limit	[–9.94]	[+2.11]	[+6.79]	[+0.27]	[+0.40]	[**–0.38**]
Extrapolation scheme	$a+be^{-cX}$	$a+bX^{-3}$	$a+bX^{-3}$	$a+bX^{-3}$	add	
Points (X =)	4, 5, 6	5, 6	4, 5	4, 5	--	

[a] See footnote *a* of Table 2.3. The CCSDT increments given here for the larger basis sets are obtained from a simple additivity approximation.

TABLE 2.5: Valence focal point analysis of HNCO isomerization reactions[a]

	ΔE_e[UHF]	$+\delta$[MP2]	$+\delta$[CCSD]	$+\delta$[CCSD(T)]	$+\delta$[CCSDT]	$=\Delta E_e$[CCSDT]
Reaction (10): HNCO → HOCN						
cc-pVDZ	24.22	+0.12	–2.39	+1.17	+0.14	23.26
cc-pVTZ	24.94	+0.08	–2.07	+0.94	+0.16	23.86
cc-pVQZ	25.16	+0.16	–2.01	+0.94	[+0.16]	[24.41]
cc-pV5Z	25.22	+0.25	–2.01	+0.95	[+0.16]	[24.57]
cc-pV6Z	25.24	+0.30	[–2.02]	[+0.95]	[+0.16]	[24.62]
CBS limit	[25.24]	[+0.35][b]	[–2.04]	[+0.95]	[+0.16]	[**24.65**]
Reaction (11): HNCO → HCNO						
cc-pVDZ	84.87	–16.65	+3.73	–2.19	+0.28	70.05
cc-pVTZ	85.05	–16.95	+4.50	–2.65	+0.37	70.32
cc-pVQZ	85.13	–16.99	+4.80	–2.73	[+0.37]	[70.59]
cc-pV5Z	85.03	–16.94	+4.87	–2.76	[+0.37]	[70.58]
cc-pV6Z	85.02	–16.95	[+4.94]	[–2.77]	[+0.37]	[70.61]
CBS limit	[85.02]	[–16.97][b]	[+5.03]	[–2.79]	[+0.37]	[**70.67**]
Reaction (12): HNCO → HONC						
cc-pVDZ	83.72	+3.37	–6.87	+0.87	–0.02	81.05
cc-pVTZ	84.66	+3.36	–6.03	+0.55	+0.02	82.56
cc-pVQZ	85.11	+3.80	–5.81	+0.50	[+0.02]	[83.63]
cc-pV5Z	85.20	+3.99	–5.78	+0.49	[+0.02]	[83.92]
cc-pV6Z	85.21	+4.10	[–5.79]	[+0.48]	[+0.02]	[84.03]
CBS limit	[85.21]	[+4.21][b]	[–5.80]	[+0.48]	[+0.02]	[**84.12**]
Extrapolation scheme	$a+be^{-cX}$	MP2-R12/A	$a+bX^{-3}$	$a+bX^{-3}$	add	
Points (X =)	4, 5, 6	--	4, 5	4, 5	--	

[a] See footnote *a* of Table 2.3.

[b] cc-pVXZ (X = 5,6) extrapolation yields CBS limit δ[MP2] increments of [+0.38], [–16.97], and [+4.25] for Reactions (2.10), (2.11), and (2.12), respectively.

All CCSD, CCSD(T) and CCSDT energies, as well as the relativistic corrections, were computed using ACES II,[114] while the CCSD(2) computations were performed with Q-CHEM 2.0.[115] The MP2, MP2-R12/A and DBOC computations were performed using PSI3,[116] and the BD(TQ) energies are computed with GAUSSIAN 94.[117]

2.4 Zero-Point Vibrational Energy Corrections

The harmonic approximation for the zero-point vibrational energy (ZPVE) is employed ubiquitously in computational thermochemistry. However, anharmonic terms can comprise several percent of the exact ZPVE, especially for hydrogen-containing molecules. Given the considerable magnitude of total ZPVEs (3 - 21 kcal mol^{-1} for the species of Table 2.1), the addition of anharmonic corrections is therefore necessary to generally ensure subchemical accuracy in thermochemical predictions. In usual practice the question is whether the substantial errors in the harmonic ZPVEs of reactants and products sufficiently cancel. Fortunately, the species of Reactions (2.1) – (2.12) are sufficiently small that the determination of highly accurate, anharmonic ZPVEs is possible.

Based on a critical assessment of the best anharmonic vibrational analyses available in the literature, the ZPVEs in Table 2.1 were compiled. The diatomic data result from the empirical coefficients of higher-order Dunham expansions and include the oft-neglected Y_{00} term.[118,119] For H_2O and NH_3, the values are derived from rigorous variational computations on surfaces of spectroscopic accuracy. For HNCO we computed a ZPVE of near spectroscopic accuracy by applying second-order vibrational perturbation theory (VPT2)[120-125] to a CBS-limit, core-correlated CCSD(T) quadratic force field conjoined with a cc-pVQZ CCSD(T) quartic force field, recently determined in our laboratory.[126] For the isomerization reactions (2.10), (2.11), and

(2.12), an error-balanced set of ZPVEs was adopted from a single study[70] reporting variational (HCNO) and perturbational (HNCO, HOCN, HONC) computations on partial TZ2P MP2 anharmonic force fields.

In the classic expansion of molecular vibrational energies,[127]

$$E(\mathrm{v}) = G_0 + \sum_i \omega_i \left(\mathrm{v}_i + \frac{1}{2} \right) + \sum_{i \geq j} \chi_{ij} \left(\mathrm{v}_i + \frac{1}{2} \right) \left(\mathrm{v}_j + \frac{1}{2} \right) + \ldots \qquad (2.15)$$

the constant term G_0 is almost universally neglected. This practice may be ill-advised in the computation of ZPVEs, because G_0 contains potentially sizable kinetic energy elements as well as cubic potential energy terms which cancel all resonance denominators in the χ_{ij} constants.[128] We evaluated the G_0 term for the molecules of Table 2.1 and found that it is generally less than 5 cm^{-1}, provided that any resonance terms encountered are excluded. However, HNCO was a striking exception, exhibiting G_0 = –33.2 cm^{-1}, mostly due to the existence of a large A_e rotational constant near 30 cm^{-1}. Our inclusion of G_0 in the ZPVE of isocyanic acid effectively shifts our final $\Delta_f H_0^\circ$(HNCO) value by –0.1 kcal mol^{-1}.

Although much care was taken in this study to accurately include anharmonicities in the ZPVEs, the final thermochemical predictions generally did not prove to be very sensitive to the *net* correction beyond the harmonic approximation. With harmonic ZPVEs (Table 2.1) the mean values of $\Delta_f H_0^\circ$(NCO) from Reactions (2.1) and (2.2) and $\Delta_f H_0^\circ$(HNCO) from Reactions (2.3) – (2.9) deviate from those obtained with the best anharmonic ZPVEs by only +0.01 kcal mol^{-1} and −0.05 kcal mol^{-1}, respectively. The corresponding deviations for $\Delta_f H_0^\circ$(HOCN) and $\Delta_f H_0^\circ$(HONC), via Reactions (2.10) and (2.12), are −0.04 and −0.02 kcal mol^{-1}, respectively. However, in the determination of $\Delta_f H_0^\circ$(HCNO), failure to include vibrational anharmonicity gives an error of +1.07 kcal mol^{-1} for Reaction (2.11). This prodigious anharmonic shift results from the extreme quasi-linearity of HCNO.[97,129]

2.5 Relation Of Formation Reactions To Bond Additivity Corrections

The inherent error in describing bond-breaking processes that arises from an incomplete treatment of electron correlation is often addressed by employing empirical bond additivity corrections (BACs), a common technique in computational thermochemistry.[130] This first step in this approach is to compute the *ab initio* reaction energies of homolytic bond-breaking processes whose thermochemistry is known experimentally with high accuracy. Then, the differences between the *ab initio* and experimental bond energies for the calibration reactions are used as BACs to improve theoretical predictions for processes in which bonds of a similar nature are broken and/or formed.

In the previous investigation of $\Delta_f H_0^\circ(\mathrm{NCO})$ by East and Allen,[22] care was taken to construct and employ BACs for N-H and N=C bond fragmentation. Here, however, the overt use of BACs is eschewed by subsuming any BAC into the construction of the formation reactions when necessary. In these cases, the formation reactions may be decomposed into the sum of two half-reactions, as shown in Table 2.6. The given half-reaction decompositions are not necessarily unique; for example, an alternate set for reaction (2.7) is [$\mathrm{H}(^2S) + \mathrm{NCO}(^2\Pi_{3/2}) \rightarrow \mathrm{HNCO}$, $\mathrm{NH}(^3\Sigma^-) \rightarrow \mathrm{N}(^4S) + \mathrm{H}(^2S)$]. Following decomposition, the first half-reaction of each pair can be used to compute $\Delta_f H_0^\circ(\mathrm{NCO})$ from atomic and diatomic fragments alone, while the second half-reaction provides an attendant BAC. However, this two-step, *a posteriori* correction scheme is mathematically identical to utilizing the error-balanced net reactions directly and is a more transparent procedure which does not necessitate overt empirical corrections.

2.6 Focal Point Calibration Of Quadruples Terms

When performing a focal point analysis, one of the primary issues to be addressed is the manner in which correlation increments are chosen. In practice, previous studies[36,43,51,53,54,131,132] have shown that the series HF→MP2→CCSD→CCSD(T) →CCSDT yields highly reliable

TABLE 2.6: Half-reaction decompositions of NCO and HNCO formation reactions

Reaction	Decomposition
(1)	$N(^4S) + CO \rightarrow NCO(^2\Pi_{3/2})$ $CO_2 \rightarrow CO + O(^3P_2)$
(2)	$NH(^3\Sigma^-) + CO \rightarrow H(^2S) + NCO(^2\Pi_{3/2})$ $H(^2S) + CO_2 \rightarrow CO + OH(^2\Pi_{3/2})$
(4)	$NH(^3\Sigma^-) + CO \rightarrow HNCO$ $CO_2 \rightarrow CO + O(^3P_2)$
(7)	$NH(^3\Sigma^-) + CO \rightarrow HNCO$ $NCO(^2\Pi_{3/2}) \rightarrow N(^4S) + CO$
(8)	$3H(^2S) + 3NCO(^2\Pi_{3/2}) \rightarrow 3HNCO$ $NH_3 \rightarrow N(^4S) + 3H(^2S)$
(9)	$2H(^2S) + 2NCO(^2\Pi_{3/2}) \rightarrow 2HNCO$ $H_2O \rightarrow O(^3P_2) + 2H(^2S)$

results. However, a persistent question arises as to the inclusion of increments for connected quadruple excitations, given the dearth of electronic structure codes that incorporate such effects efficiently. In order to address this issue, a number of relevant homolytic bond-breaking reactions (Table 2.7), involving the H, N, C, and O atoms and whose energetics are known to high accuracy, were studied at the outset in order to determine which of five increment schemes would consistently produce the best agreement with experimentally confirmed results. Unlike the principal formation reactions employed here to determine final enthalpies of formation, the calibration reactions have no inherent error balancing and provide more stringent tests of *ab initio* performance.

The first increment scheme was simply to exclude any quadruples correction, leaving CCSDT as the final correlation level. The other schemes used explicit BD(TQ) or CCSD(2) results for post-CCSDT increments, or isolated only the quadruples components of BD(TQ) or CCSD(2) energetics for such corrections. In particular, these four methods computed quadruples increments as: δ[BD(TQ)] = ΔE[BD(TQ)] – ΔE[CCSDT], δ[CCSD(2)] = ΔE[CCSD(2)] – ΔE[CCSDT], δ["CCSDT+(QB)"] = ΔE[BD(TQ)] – ΔE[BD(T)], and δ["CCSDT+(Q2)"] = ΔE[CCSD(2)] – ΔE[CCSD(T)]. Note that the δ[BD(TQ)] and δ[CCSD(2)] cases correspond to merely placing the CBS BD(TQ) and CCSD(2) levels, respectively, as the final targets of the valence focal point extrapolations.

A summary of the focal-point calibrations for the quadruples increments is given in Table 2.7, where all the ΔE_{fp} results involve the same layout as in Table 2.3 before the highest-order increments are considered, as well as identical corrections given by the sum of the DBOC, spin-orbit, and relativistic terms. For those schemes in which a post-CCSDT increment is included, it is evaluated in a cc-pVTZ basis and added to the δ[CCSDT] result.

TABLE 2.7: Summary of correlation increment calibration reactions (kcal mol^{-1})

Reaction	Highest Order Increment[a]	ΔE_{fp}[b]	ΔE_e(expt.)[c]	Error
Single bonds				
$1/2\,[H_2O \rightarrow O(^3P_2) + 2H(^2S)]$	BD(TQ)	116.47	116.30 ± 0.02	+0.17
	CCSDT+(QB)	116.43		+0.13
	CCSD(2)	116.48		+0.18
	CCSDT+(Q2)	116.36		+0.06
	CCSDT	116.49		+0.18
$NH(^3\Sigma^-) \rightarrow N(^4S) + H(^2S)$	BD(TQ)	83.12	82.88 ± 0.08	+0.23
	CCSDT+(QB)	83.25		+0.36
	CCSD(2)	83.00		+0.12
	CCSDT+(Q2)	83.07		+0.19
	CCSDT	83.12		+0.23
$1/3\,[NH_3 \rightarrow N(^4S) + 3H(^2S)]$	BD(TQ)	99.48	99.31 ± 0.03	+0.17
	CCSDT+(QB)	99.47		+0.16
	CCSD(2)	99.46		+0.15
	CCSDT+(Q2)	99.44		+0.13
	CCSDT	99.48		+0.17
Multiple bonds				
$CO_2 \rightarrow CO + O(^3P_2)$	BD(TQ)	128.92	129.89 ± 0.05	–0.97
	CCSDT+(QB)	128.56		–1.33
	CCSD(2)	129.67		–0.22
	CCSDT+(Q2)	129.11		–0.78
	CCSDT	129.72		–0.18
$HNCO \rightarrow NH(^3\Sigma^-) + CO$	BD(TQ)	90.91	91.72 ± 0.20[d]	–0.81
	CCSDT+(QB)	90.49		–1.24
	CCSD(2)	91.38		–0.34
	CCSDT+(Q2)	90.97		–0.75
	CCSDT	91.55		–0.17

[a] The entries labeled CCSDT+(Q) are computed as CCSDT + BD(TQ) – BD(T). The entries labeled CCSDT+(2) are computed as CCSDT + CCSD(2) – CCSD(T).

[b] Includes valence cc-pV*X*Z extrapolation, core-valence cc-pCV*X*Z extrapolation, DBOC correction, spin-orbit correction, and one-electron mass-velocity and Darwin relativistic terms.

[c] Computed from enthalpy of formation and ZPVE data in Table 2.1.

[d] Ref. 25 (Zyrianov).

TABLE 2.7: Summary of correlation increment calibration reactions (kcal mol^{-1}) (cont'd)

Reaction	Highest Order Increment[a]	ΔE_{fp}[b]	ΔE_e(expt.)[c]	Error
Multiple bonds				
$N_2O \rightarrow N_2 + O(^3P_2)$	BD(TQ)	39.63		–2.34
	CCSDT+(QB)	39.15		–2.82
	CCSD(2)	40.69	41.97 ± 0.10	–1.28
	CCSDT+(Q2)	39.90		–2.07
	CCSDT	40.98		–0.99
$CO \rightarrow C(^3P_0) + O(^3P_2)$	BD(TQ)	258.71		–1.05
	CCSDT+(QB)	258.99		–0.77
	CCSD(2)	258.68	259.76 ± 0.11	–1.08
	CCSDT+(Q2)	258.29		–1.47
	CCSDT	258.85		–0.92
$N_2 \rightarrow N(^4S) + N(^4S)$	BD(TQ)	227.20		–1.22
	CCSDT+(QB)	226.82		–1.53
	CCSD(2)	227.70	228.42± 0.01	–0.72
	CCSDT+(Q2)	227.12		–1.30
	CCSDT	227.07		–1.35

[a] The entries labeled CCSDT+(Q) are computed as CCSDT + BD(TQ) – BD(T). The entries labeled CCSDT+(2) are computed as CCSDT + CCSD(2) – CCSD(T).

[b] Includes valence cc-pV*X*Z extrapolation, core-valence cc-pCV*X*Z extrapolation, DBOC correction, spin-orbit correction, and one-electron mass-velocity and Darwin relativistic terms.

[c] Computed from enthalpy of formation and ZPVE data in Table 2.1.

For the single bonds, all schemes essentially achieve subchemical accuracy, generally overestimating the dissociation energies by only 0.1 – 0.2 kcal mol^{-1}. Moreover, the quadruples increments are all significantly less than 0.2 kcal mol^{-1}, so that little preference exists among the methods. However, the errors increase significantly when these methods are applied to reactions in which multiple bonds are broken. For the CO_2 and HNCO fragmentations the BD(TQ) derived quadruples increments are sizable (0.8 – 1.3 kcal mol^{-1}) and always spoil the excellent results given by CCSDT theory alone. The same behavior of BD(TQ) increments is observed in the N_2O case, except that the initial CCSDT error is now almost 1.0 kcal mol^{-1} for this error-unbalanced reaction. The corresponding increments derived from the CCSD(2) method, particularly δ[CCSD(2)], perform significantly better than their BD(TQ) counterparts, but still generally produce larger errors (0.2 – 2.1 kcal mol^{-1} underestimation of bond energies) than the CCSDT scheme in which quadruples increments are neglected altogether. For the extremely challenging CO and N_2 reactions, all schemes underestimate the (enormous) triple bond dissociation energies by 0.7 – 1.5 kcal mol^{-1}. Here the Brueckner quadruples increments do not change the CCSDT results by more than 0.2 kcal mol^{-1}, and no clear preference over CCSDT is seen. On the other hand, the increments based on CCSD(2) theory are not negligible, performing worse than CCSDT for CO but better in the N_2 case.

In summary, the various quadruples estimates show disconcerting inconsistencies and in certain cases give an anomalously large correction of the wrong sign to the bond dissociation energy. Most notable is the N_2O dissociation reaction, where all quadruples increments push the CCSDT result further away from experiment by a sizable amount. The one scheme which is generally competitive in accuracy with CCSDT for the calibration reactions in Table 2.7 is CCSD(2). However, only in the N_2 case does CCSD(2) offer a significant improvement over

CCSDT, and none of our formation reactions or underlying half-reactions (Table 2.6) involve triple-bond fragmentation.

The convergence of atomization energies computed from coupled-cluster expansions has received significant attention in the recent literature.[133-135] It is now documented[134] that the CCSD(T) approach happens to give more accurate atomization energies in general than full CCSDT theory, because iterative T_3 effects consistently decrease molecular binding energies. However, T_4 effects systematically increase the energies of homolytic bond cleavages, so that full CCSDTQ theory yields superior performance when it is not cost prohibitive. For the atomization energies of CH_2, H_2O, HF, N_2, F_2, and CO, Ruden and co-workers[134] found CCSDTQ – CCSDT increments ranging from +0.10 to +0.95 kcal mol^{-1}. In contrast, for these same quantities and with the same basis sets, we compute CCSD(2) – CCSDT and CCSD(2) – CCSD(T) increments in the intervals [−1.42, +0.27] and [−1.61, +0.13] kcal mol^{-1}, respectively. In brief, it appears that T_4 effects cannot be determined reliably via currently available perturbative methods. Because our principal NCO and HNCO formation reactions are error-balanced, it is more important for the final correlation method to be consistent than to provide the best atomization energies on average. Until full CCSDTQ computations on all the species in our formation reactions are feasible with reasonable basis sets, it is advisable to simply omit (Q) additions to the CCSDT energies in our focal-point analyses. In the following sections, we mention the effect of quadruples increments, but the recommended enthalpies of formation are derived with no post-CCSDT corrections.

2.7 Enthalpy of formation Of NCO $\left(X\ ^2\Pi\right)$

The theoretical data for the determination of $\Delta_f H_0^\circ$(NCO) are given in Tables 2.3, 2.8, and supplementary Table A.1.[103] One of the most striking features of Table 2.3 is the rapid

convergence of each increment with respect to the one-particle basis set, attesting to excellent error balancing in the chosen formation reactions. For Reactions (2.1) and (2.2), the largest explicit computation is within 0.03 kcal mol^{-1} of the inferred CBS limit for every increment. With regard to *N*-particle convergence, it is remarkable that the net CCSD and CCSDT energies for Reactions (2.1) and (2.2) differ by less than 0.3 kcal mol^{-1}. The post-CCSDT increments for Reactions (2.1, 2.2) are given in supplementary Table A.4[103] and are equal to (–0.55, –0.50) for the BD(TQ) method, (−1.10, −0.99) for the CCSDT+(QB) scheme, (+0.46, +0.38) for the CCSD(2) approach, and (–0.33, –0.17) for the CCSDT+(Q2) increment. These shifts are large compared to our target accuracy, but the calibrations of Section 2.6 indicate that they are misleading indicators of the *N*-particle, full configuration interaction (FCI) limit.

The core correlation effect on the reaction energies (Table 2.8) does not exceed 0.06 kcal mol^{-1} for Reactions (2.1) and (2.2). The non-Born-Oppenheimer (DBOC) and relativistic corrections, both no larger than 0.10 kcal mol^{-1} in size, are of opposite signs and partially cancel one another for each reaction. The enthalpies of formation (Table 2.8) resulting from the final theoretical reaction energies and the established thermochemical data of Table 2.1 show internal agreement to subchemical accuracy. The accord between the result of Reaction (2.2) versus Reaction (2.1) is dependent upon the recently lowered (by more than 0.5 kcal mol^{-1}) enthalpy of formation of the hydroxyl radical, determined by a positive ion cycle approach and confirmed by rigorous *ab initio* computations.[62,136] Our recommended enthalpy of formation of the cyanato radical, $\Delta_f H_0^\circ$(NCO) = 30.5 kcal mol^{-1}, results from the average focal-point result from the two pathways *sans* post-CCSDT increments. The uncertainty in this result is a few tenths of a kcal mol^{-1}, discussion of which is deferred until Section 2.10.

TABLE 2.8: Determination of the enthalpies of formation for NCO, HNCO, HOCN, HCNO, and HONC (kcal mol^{-1}).

Rxn.	ΔE_{fp}(V)	ΔE_{fp} (CV)	ΔDBOC	ΔRel.	ΔE_{so}	ΔZPVE[a]	ΔE_0	Target	$\Delta H^\circ_{f,0}$
(1)	72.44	+0.05	+0.08	–0.10	–0.36	–1.22	70.89	NCO	30.47
(2)	48.31	+0.02	+0.02	–0.05	–0.32	–0.57	47.42	NCO	30.52
							Mean Result: $\Delta H^\circ_{f,0}$ (NCO) = 30.49 kcal mol		
(3)	20.51	–0.12	–0.04	+0.07	+0.00	–1.96	18.46	HNCO	–27.71
(4)	38.58	–0.25	–0.10	–0.02	–0.22	+1.34	39.33	HNCO	–27.70
(5)	–116.67	–0.46	–0.13	+0.16	+0.09	+7.21	–109.76	HNCO	–27.64
(6)	–346.86	–0.08	+0.10	+0.01	+0.00	+6.67	–340.17	HNCO	–27.68
(7)	–33.69	–0.30	–0.18	+0.09	+0.09	+2.56	–31.39	HNCO	–27.51
(8)	–17.51	–0.21	–0.09	+0.07	+0.09	+0.14	–17.46	HNCO	–27.58
(9)	–0.38	–0.22	–0.07	+0.02	–0.02	+0.58	–0.05	HNCO	–27.59
							Mean Result: $\Delta H^\circ_{f,0}$ (HNCO) = –27.63 kcal mol		
(10)	24.65	+0.11	–0.02	–0.01	+0.00	–0.15	24.58	HOCN	–3.05
(11)	70.67	–0.12	+0.01	+0.04	+0.00	–2.08	68.51	HCNO	40.88
(12)	84.16	+0.59	+0.00	–0.03	+0.00	–0.74	83.97	HONC	56.34

[a] Determined from anharmonic ZPVE values in Table 2.1.

The experimental values for $\Delta_f H_0^\circ$(NCO) in closest agreement with our new theoretical proposal are 30.5 ± 1 kcal mol^{-1} determined in Ref. 19 from D_0(N-CO), and 30.3 ± 0.4 kcal mol^{-1} ascertained in Ref. 25 from D_0(H-NCO) and D_0(HN-CO). The most recent experimental enthalpy of formation, 31.4 ± 0.7 kcal mol^{-1} from the refined D_0(N-CO) measurement of Hoops *et al*.,[29] appears to be a little too high, although its lower limit broadly lies within the uncertainty of our theoretical proposal. We can envision no scenarios under which the Schönnenbeck and Stuhl[33] lower bound, $\Delta_f H_0^\circ$(NCO) ≥ 40 kcal mol^{-1}, is plausible given the level of rigor underpinning our theoretical result of 30.5 kcal mol^{-1}.

2.8 Enthalpy of formation Of HNCO

The theoretical determination of $\Delta_f H_0^\circ$(HNCO) via Reactions (2.3) – (2.9) is detailed in Tables 2.4, 2.8 and supplementary Table A.2. The general features of the data are the same as found for Reactions (2.1) and (2.2), except even more favorable for pinpointing the target enthalpy of formation. No CCSD → CCSDT change in reaction energy exceeds 1 kcal mol^{-1}, and most of these higher-order correlation effects are substantially less. The only increments in the focal point tables for which CBS extrapolation produces a change greater than 0.1 kcal mol^{-1} over the largest explicit computation are δ[MP2] and δ[CCSD] for both Reactions (2.5) and (2.6); yet these extrapolation shifts still do not exceed 0.5 kcal mol^{-1} in magnitude and partially cancel one another. Finally, the difference between the δ[MP2] limits determined by the explicit R12/A approach versus extrapolation of the cc-pV*X*Z series of correlation energies is only 0.03 and 0.12 kcal mol^{-1} for Reactions (2.3) and (2.6), respectively.

A superior balance of errors is found for Reaction (2.3), which is an isogyric equation consisting of isoelectronic reactant-product pairs. In this case the CBS net MP2 reaction energy lies within 0.1 kcal mol^{-1} of the inferred CCSDT limit, due to rapid correlation convergence, not

fortuitous cancellation of errors. Unless undetected errors exist in the accepted enthalpies of formation of NH_3, CO_2, and H_2O, Reaction (2.3) provides a definitive path to the theoretical determination of $\Delta_f H_0^\circ$(HNCO).

Reaction (2.5) involves a direct evaluation of D_0(H-NCO). The valence focal point limit $\Delta E_e(2.5) = -116.67$ kcal mol^{-1}, conjoined with the auxiliary terms of Table 2.8, yields D_0(H-NCO) = 109.8 kcal mol^{-1}, in remarkable agreement with the best experimental value of 109.7 ± 0.1 kcal mol^{-1}, reported by Reisler and co-workers.[25] This accord precisely fixes the difference between $\Delta_f H_0^\circ$(HNCO) and $\Delta_f H_0^\circ$(NCO) with high confidence.

Reaction (2.6), measuring the gas-phase acidity of HNCO, involves direct heterolytic bond cleavage. As expected, the requirements for saturation of the one-particle basis are considerable, requiring use of the aug-cc-pV*X*Z series, but the correlation convergence is rapid. The inclusion of this reaction provides an important cross-check on the consistency of D_0(H-NCO) and the experimental electron affinity of NCO (3.609 ± 0.005 eV).[73]

The remaining reactions [(2.4), (2.7), (2.8), and (2.9)] for HNCO formation are decomposable into half-reactions (Table 2.6) and in effect have built-in bond additivity corrections. In addition, Reaction (2.4) is another isogyric transformation comprised of isoelectronic reactant-product pairs. Accordingly, the focal point convergence behavior of these four reactions is excellent, even better than in Reactions (2.5) and (2.6).

The cc-pVTZ post-CCSDT increments computed for the energies of Reactions (2.3) – (2.9) are given in supplementary Table A.4.[103] The range of these values is [–0.16, +0.39] for the BD(TQ) method, [–0.14, +1.01] for the CCSDT+(QB) scheme, [–0.33, +0.20] for the CCSD(2) approach, and [–0.03, +0.34] for the CCSDT+(Q2) increment. These shifts highlight the fact that post-CCSDT effects are our largest source of uncertainty, but again the calibrations

of Section 2.6 suggest that CCSDT theory without modification is probably the most reliable estimator of the full configuration interaction limit for our error-balanced formation reactions.

As shown in Table 2.8, the core correlation shifts for the reaction energies of Reactions (2.3) – (2.9) are the most important auxiliary terms but are generally only a few tenths of a kcal mol^{-1}. The effect is greatest (–0.46 kcal mol^{-1}) for the simple N-H bond fission reaction (2.5) and least (–0.08 kcal mol^{-1}) for the proton extraction reaction (2.6). The DBOC and relativistic corrections are 0.01-0.18 kcal mol^{-1} in size, the largest shifts being displayed by Reactions (2.7) and (2.5), respectively.

The consistency observed in the computation of $\Delta_f H_0^\circ$(HNCO) from Reactions (2.3) through (2.9) is encouraging (Table 2.8). The high and low values for the computed enthalpies of formation of HNCO are –27.51 for Reaction (2.7) and –27.71 for Reaction (2.3), a range of only 0.2 kcal mol^{-1}. Our final recommendation is $\Delta_f H_0^\circ$(HNCO) = –27.6 kcal mol^{-1}, taken from the mean value of Reactions (2.3) – (2.9). Again, final assessment of the uncertainty of this result is given in Section 2.10. As a result of the uniformity in the above computed enthalpies of formation, the standard deviation between the seven reactions is only 0.07 kcal mol^{-1}. Our new enthalpy of formation validates the theoretical result of East and Allen,[22] $\Delta_f H_0^\circ$(HNCO) = –27.5 ± 0.5 kcal mol^{-1}, derived a decade ago with more limited means of converging to *ab initio* limits.

An aforementioned experimental value, $\Delta_f H_0^\circ$(HNCO) = –27.8 ± 0.4 kcal mol^{-1}, was deduced in 1996 by Zyrianov *et al.*[25] from precise measurements of D_0(^{1}NH-CO). Remarkable agreement between this experiment and our best theory is thus apparent. However, this appealing confluence of results is tempered somewhat by a later 1999 paper from the Reisler group,[27] wherein photofragment ion imaging techniques were used to probe (*inter alia*) product energy distributions in the vicinity of the ^{1}NH + CO threshold. The best fits to the CO velocity distributions were obtained with D_0(^{1}NH+CO) = 122.23 ± 0.07 kcal mol^{-1}, corresponding to

$D_0(^3\text{NH+CO})$ = 85.95 kcal mol^{-1}. The authors did not choose to report a revised enthalpy of formation of HNCO, but if $D_0(^3\text{NH+CO})$ from Ref. 27 is conjoined with the thermochemical reference data we have adopted (Table 2.1), then the empirical $\Delta_f H_0^\circ$(HNCO) value is lowered by 0.6 kcal mol^{-1}, and the agreement with theory is diminished.

2.9 Isomerization Energies Of HOCN, HCNO And HONC

The relative energies of the [H, N, C, O] isomers, which have long intrigued chemists,[20,21] were determined to within 1-2 kcal mol^{-1} in the 1993 study of East, Johnson, and Allen.[20] A 1999 G2 study[137] reproduced these predictions to ± 1 kcal mol^{-1}, specifically giving ΔE_0 = 25.4, 70.1, and 83.8 kcal mol^{-1} for the formation of HOCN, HCNO, and HONC, respectively, from HNCO. The new theoretical data reported in Tables 2.5, 2.8, and A.3 allow the uncertainties in these isomerization energies to be substantially reduced.

Among the [H, N, C, O] isomers, fulminic acid (HCNO) has proved to be the most problematic species. The extreme quasi-linearity of HCNO has provided a fertile ground for numerous computational studies of both its electronic structure[21,70,97,138-142] and vibrational dynamics.[70,143-147] Over the years electronic structure computations have predicted both linear and bent r_e geometries for HCNO, with the system demonstrating a strong dependence on both the level of electron correlation and basis set. In 1989 Teles *et al.*[21] predicted a linear structure based on computations at the 6-31G** MP3 level of theory. Two years later, Nguyen, Pierloot and Vanquickenborne[141] obtained optimized geometries using the MCSCF, CISD, and MP*n* (*n* = 2, 3, 4) methods and DZP, 6-311G**, and 6-31G* basis sets. They found that the MP2, MP4, and MCSCF methods predicted bent structures with H-C-N angles between 145.5° and 158.0°, while MP3 and CISD yielded linear minimum energy geometries. MRCI energy points computed using moderately large ANO basis sets at the 6-311G** MP2 and 6-311G** MP3

geometries failed to produce conclusive results. The quartic force field study reported in 1993 by Handy and co-workers[70] determined that at the highest level of theory employed (TZ2P MP2) the minimum energy structure was bent, with the linear structure 98 cm^{-1} higher in energy. Later that same year Rendell, Lee, and Lindh[142] predicted the linear structure to be lower in energy by 87 cm^{-1} using CCSD(T) single-point energies with a modest ANO basis set at TZ2P CCSD(T) optimized geometries. In 1996, Koput, Winnewisser, and Winnewisser[97] found that a bent structure, with θ_e(H-C-N) = 165.1°, was lower in energy at the cc-pVQZ CCSD(T) level of theory. Furthermore, the energy difference between the linear and bent forms decreased with increasing cardinal number of the cc-pV*X*Z basis set, to a minuscule 7 cm^{-1} barrier to linearity with the cc-pVQZ basis set. Given the exceedingly small energy difference between the two forms, the linear cc-pVQZ CCSD(T) structure of Ref. 97 was adopted in this work for the sake of computational efficiency. This choice assigns any remaining geometric effects to the highly anharmonic zero-point vibrational energy.

The ZPVEs for the isomers HOCN and HONC were obtained using *ab initio* fundamental frequencies and VPT2 anharmonic constants,[70] computed at the TZ2P MP2//DZP MP2 level of theory. For HCNO, however, a perturbative approach is not appropriate and is unable to yield the desired accuracy in the determination of the ZPVE (*cf.* the harmonic and anharmonic values in Table 2.1). Rather, a variational result[70] was employed.

The enthalpies of formation for all the isomers were computed using the simple isomerization reactions (2.10) – (2.12) and the enthalpy of formation of HNCO determined in Section 2.7. As shown in Table 2.5, the rate of convergence for the Hartree-Fock increments is rapid, such that the largest explicitly computed increment is within 0.01 kcal mol^{-1} of the extrapolated limit in all cases. Furthermore, the basis set convergence of the correlation increments is similarly swift, with the largest explicitly computed increment always within 0.15

kcal mol^{-1} of the extrapolated limit. Not surprisingly, differential correlation effects are largest for the isomerization to fulminic acid, where the CBS values for δ[MP2], δ[CCSD], and δ[CCSD(T)] are –17.0, +5.0, and –2.8 kcal mol^{-1}, respectively. However, none of the quadruples increments in Table A.4 for HCNO formation are larger than 0.24 kcal mol^{-1} in magnitude. The HNCO $\rightarrow$ HOCN reaction exhibits the sharpest contrast to the HCNO isomerization, as no correlation increment for Reaction (2.10) exceeds 2.4 kcal mol^{-1} in magnitude, yet the quadruples increments scatter from –0.26 to –0.95 kcal mol^{-1} (Table A.4).[103]

As shown in Table 2.8, core correlation effects on the HNCO isomerization energies are not negligible, particularly in the HONC case, where a shift in relative energy of almost +0.6 kcal mol^{-1} is observed. On the other hand, the relativistic and non-Born-Oppenheimer terms have little discernible effect (shifts less than 0.05 kcal mol^{-1} in size). For the HOCN and HONC isomerization energies, the ZPVE contribution is less than 0.8 kcal mol^{-1} and is not sensitive to anharmonicity. Such is not the case for HCNO, whose quasilinearity leads to a –2.08 kcal mol^{-1} ZPVE correction, over half of which arises from anharmonicity (see Table 2.1). Therefore, in addition to poorer focal-point convergence behavior, ZPVE effects complicate the precise determination of the HCNO isomerization energy.

Our final results for the HOCN, HCNO, and HONC isomerization energies are ΔE_0 (ΔE_e) = 24.6 (24.7), 68.5 (70.6), and 84.0 (84.7) kcal mol^{-1}, respectively. The ΔE_e values of Ref. 20 show discrepancies with our improved values of less than 1 kcal mol^{-1} in each case, well within the stated uncertainties of the 1993 investigation. Also, the ΔE_0 results given by G2 theory[137] are removed by +0.8, +1.6, and –0.2 kcal mol^{-1}, respectively, from our corresponding HOCN, HCNO, and HONC values. Adopting $\Delta_f H_0^\circ$(HNCO) = –27.6 kcal mol^{-1} from Section 2.8 above, our revised isomerization energies lead to $\Delta_f H_0^\circ$(HOCN) = –3.1 kcal mol^{-1}, $\Delta_f H_0^\circ$(HCNO) = +40.9 kcal mol^{-1}, and $\Delta_f H_0^\circ$(HONC) = +56.3 kcal mol^{-1}.

2.10 SUMMARY

In this study we have pushed *ab initio* quantum chemistry to its current limits for the species NCO, HNCO, HOCN, HCNO, and HONC, all in pursuit of subchemical accuracy (ca. 0.1 – 0.2 kcal mol^{-1}) in thermochemical predictions. By means of systematic focal point analyses, the complete basis set limits of CCSDT theory have been pinpointed for a total of 12 chemical reactions, in cases with the aid of explicitly-correlated MP2-R12/A computations. The chosen reactions [(2.1) – (2.12)] provide independent thermochemical paths to the enthalpies of formation of the target chemical species and are specifically constructed to minimize differential errors in *ab initio* total energies. Explicit account was made for a number of auxiliary effects often neglected in computational thermochemistry, including core correlation, spin-orbit coupling, special relativity, the diagonal Born-Oppenheimer correction (DBOC), and anharmonicity in zero-point vibrational energies (ZPVEs). The purpose of the investigation is not only to obtain definitive thermochemistry for species of combustion significance, but also to gain further insight into the requirements for breaking past the chemical accuracy benchmark (ca. 1 kcal mol^{-1}).

For cyanato radical and isocyanic acid, we determine $\Delta_f H_0^\circ$(NCO) = +30.5 kcal mol^{-1} and $\Delta_f H_0^\circ$(HNCO) = –27.6 kcal mol^{-1}. The considerable breadth and remarkable internal consistency of our data suggests errors bars of ±0.2 kcal mol^{-1} for these quantities. Among the numerous experimental determinations of these enthalpies of formation, our conclusions best compare with the 1996 spectroscopic results of Zyrianov *et al.*,[25] $\Delta_f H_0^\circ$(NCO) = +30.3 ± 0.4 kcal mol^{-1} and $\Delta_f H_0^\circ$(HNCO) = –27.8 ± 0.4 kcal mol^{-1}. Such accord between theory and experiment would be virtually unparalleled for species with more than 20 electrons. Based on our enthalpy of formation of isocyanic acid, we ascertain $\Delta_f H_0^\circ$(HOCN) = –3.1, $\Delta_f H_0^\circ$(HCNO) = +40.9, and $\Delta_f H_0^\circ$(HONC) = +56.3 kcal mol^{-1}, with uncertainties of only a few tenths of a kcal

mol^{-1} in the first and last cases. For fulminic acid (HCNO) the uncertainty is somewhat larger, owing to poorer correlation convergence in the computed isomerization energy and an enormous anharmonicity in the zero-point vibrational energy of this quasilinear molecule.

Enthusiasm for the apparent near-achievement of subchemical accuracy in this study for the target enthalpies of formation must be tempered by admission of possible sources of significant systematic error. First, the adopted empirical reference enthalpies in Table 2.1 may have errors considerably larger than the stated uncertainties, as demonstrated by the recent work of numerous collaborators which revised the enthalpy of formation of the hydroxyl radical by 0.5 kcal mol^{-1}.[62,136] Second, our calibrations on dissociation energies of multiple bonds indicate that several available schemes for partially including connected quadruple excitations within the coupled-cluster formalism not only fail to provide reliable improvements over CCSDT theory but often significantly deteriorate the excellent bond-energy predictions already given by this established method. Therefore, we have based our conclusions on energies for our error-balanced reactions discerned for CCSDT theory in the complete basis set limit, even though scattered quadruples increments of several tenths of a kcal mol^{-1} were often observed. With the advent of correlation-consistent basis set extrapolations and the development of explicitly correlated methods, the practical determination of accurate post-CCSDT corrections is now perhaps the chief obstacle to the achievement of true subchemical accuracy in computational thermochemistry. It is encouraging that meaningful full CCSDTQ computations may become possible for systems with 3-4 heavy atoms in the near future. However, highlighting the problem of post-CCSDT effects in numerous computational applications should promote further research in this area and perhaps spawn novel ideas applicable to larger systems.

2.11 Acknowledgements

The research presented here was supported by the U. S. Department of Energy, Office of Basic Energy Sciences, Combustion Program (Grant No. DE-FG02-00ER14748) and SciDAC Computational Chemistry Program (Grant No. DE-FG02-01ER15226).

References

[1] J. A. Miller and C. T. Bowman, Prog. Energy Comb. Sci. **15**, 287 (1989).

[2] J. D. Mertens, A. Y. Chang, R. K. Hanson, and C. T. Bowman, Int. J. Chem. Kin. **21**, 1049 (1989).

[3] J. D. Mertens, K. Kohse-Höinghaus, R. K. Hanson, and C. T. Bowman, Int. J. Chem. Kin. **23**, 655 (1991).

[4] J. D. Mertens, A. Y. Chang, R. K. Hanson, and C. T. Bowman, Int. J. Chem. Kin. **24**, 279 (1992).

[5] Y. He, X. Liu, M. C. Lin, and C. F. Melius, Int. J. Chem. Kin. **23**, 1129 (1991).

[6] J. A. Miller and C. T. Bowman, Int. J. Chem. Kin. **23**, 289 (1991).

[7] M. Lin, Y. He, and C. Melius, J. Phys. Chem. **97**, 9124 (1993).

[8] P. Glarborg, P. Kristensen, S. Jensen, and K. Damjohansen, Combust. Flame **98**, 241 (1994).

[9] M. Wooldridge, R. Hanson, and C. Bowman, Int. J. Chem. Kinet. **28**, 361 (1996).

[10] R. A. Perry and D. L. Siebers, Nature **324**, 657 (1986).

[11] R. A. Perry, J. Chem. Phys. **82**, 5485 (1985).

[12] W. R. Anderson, J. A. Vanderhoff, A. J. Kotlar, M. A. Dewilde, and R. A. Beyer, J. Chem. Phys. **77**, 1677 (1982).

[13] K.-Y. Du and D. W. Setser, Chem. Phys. Lett. **153**, 393 (1988).

[14] S. Wategaonkar and D. W. Setser, J. Phys. Chem. **97**, 10028 (1993).

[15] H. Okabe, J. Chem. Phys. **53**, 3507 (1970).

[16] B. J. Sullivan, G. P. Smith, and D. R. Crosley, Chem. Phys. Lett. **96**, 307 (1983).

[17] T. A. Spiglanin, R. A. Perry, and D. W. Chandler, J. Phys. Chem. **90**, 6184 (1986).

[18] X. Liu and R. D. Coombe, J. Chem. Phys. **91**, 7543 (1989).

[19] D. R. Cyr, R. E. Continetti, R. B. Metz, D. L. Osborn, and D. M. Neumark, J. Chem. Phys. **97**, 4937 (1992).

[20] A. L. L. East, C. S. Johnson, and W. D. Allen, J. Chem. Phys. **98**, 1299 (1993).

[21] J. H. Teles, G. Maier, B. A. Hess, Jr., L. J. Schaad, M. Winnewisser, and B. P. Winnewisser, Chem. Ber. **122**, 753 (1989).

[22] A. L. L. East and W. D. Allen, J. Chem. Phys. **99**, 4638 (1993).

[23] B. Ruscic and J. Berkowitz, J. Chem. Phys. **100**, 4498 (1994).

[24] S. S. Brown, H. L. Berghout, and F. F. Crim, J. Chem. Phys. **105**, 8103 (1996).

[25] M. Zyrianov, T. Droz-Georget, A. Sanov, and H. Reisler, J. Chem. Phys. **105**, 8111 (1996).

[26] H. L. Berghout, S. S. Brown, R. Delgado, and F. F. Crim, J. Chem. Phys. **109**, 2257 (1998).

[27] M. Zyrianov, T. Droz-Georget, and H. Reisler, J. Chem. Phys. **110**, 2059 (1999).

[28] M. Zyrianov, A. Sanov, T. Droz-Georget, and H. Reisler, J. Chem. Phys. **110**, 10774 (1999).

[29] A. A. Hoops, R. T. Bise, J. R. Gascooke, and D. M. Neumark, J. Chem. Phys. **114**, 9020 (2001).

[30] C. R. Brazier, R. S. Ram, and P. F. Bernath, J. Mol. Spectrosc. **120**, 381 (1986).

[31] W. R. Anderson, J. Phys. Chem. **93**, 530 (1989).

[32] M. W. Chase, Jr., C. A. Davies, J. R. Downey, Jr., D. J. Frurip, R. A. McDonald, and A. N. Syverud, *JANAF Thermochemical Tables*, 3rd ed. (1985).

[33] G. Schönnenbeck and F. Stuhl, Chem. Phys. Lett. **264**, 199 (1997).

[34] T. Helgaker, W. Klopper, H. Koch, and J. Noga, J. Chem. Phys. **106**, 9639 (1997).

[35] A. Halkier, T. Helgaker, P. Jørgensen, W. Klopper, H. Koch, J. Olsen, and A. K. Wilson, Chem. Phys. Lett. **286**, 243 (1998).

[36] J. P. Kenny, W. D. Allen, and H. F. Schaefer, J. Chem. Phys. **118**, 7353 (2003).

[37] E. F. Valeev, W. D. Allen, R. Hernandez, C. D. Sherrill, and H. F. Schaefer, J. Chem. Phys. **118**, 8594 (2003).

[38] W. Klopper and W. Kutzelnigg, Chem. Phys. Lett. **134**, 17 (1987).

[39] W. Kutzelnigg and W. Klopper, J. Chem. Phys. **94**, 1985 (1991).

[40] J. Noga and W. Kutzelnigg, J. Chem. Phys. **101**, 7738 (1994).

[41] W. Klopper and C. C. M. Samson, J. Chem. Phys. **116**, 6397 (2002).

[42] E. F. Valeev and H. F. Schaefer, J. Chem. Phys. **113**, 3990 (2000).

[43] E. F. Valeev, W. D. Allen, H. F. Schaefer, and A. G. Császár, J. Chem. Phys. **114**, 2875 (2001).

[44] D. Feller and D. A. Dixon, J. Phys. Chem. A **103**, 6413 (1999).

[45] D. A. Dixon, D. Feller, and G. Sandrone, J. Phys. Chem. A **103**, 4744 (1999).

[46] D. Feller and D. A. Dixon, J. Phys. Chem. A **104**, 3048 (2000).

[47] D. A. Dixon and K. A. Peterson, J. Chem. Phys. **115**, 6327 (2001).

[48] D. A. Dixon, D. Feller, and K. A. Peterson, J. Chem. Phys. **115**, 2576 (2001).

[49] D. A. Dixon, W. A. d. Jong, K. A. Peterson, and J. S. Francisco, J. Phys. Chem. A **106**, 4725 (2002).

[50] D. Feller, D. Dixon, and J. Francisco, J. Phys. Chem. A **107**, 1604 (2003).

[51] J. M. Gonzales, C. Pak, R. S. Cox, W. D. Allen, H. F. Schaefer, G. Tarczay, and A. G. Császár, Chem. Eur. J. **9**, 2173 (2003).

[52] W. D. Allen, A. L. L. East, and A. G. Császár, in *Structures and Conformations of Non-Rigid Molecules*, edited by J. Laane, M. Dakkouri, B. van der Vecken, and H. Oberhammer (Kluwer, Dordrecht, 1993), pp. 343.

[53] A. G. Császár, W. D. Allen, and H. F. Schaefer III, J. Chem. Phys. **108**, 9751 (1998).

[54] A. G. Császár, G. Tarczay, M. L. Leininger, O. L. Polyansky, J. Tennyson, and W. D. Allen, in *Spectroscopy from Space*, edited by J. Demaison and K. Sarka (Kluwer, Dordrecht, 2001), pp. 317.

[55] T. H. Dunning, Jr., J. Chem. Phys. **90**, 1007 (1989).

[56] R. A. Kendall, T. H. Dunning, Jr., and R. J. Harrison, J. Chem. Phys. **96**, 6796 (1992).

[57] D. E. Woon and T. H. Dunning, Jr., J. Chem. Phys. **103**, 4572 (1995).

[58] A. K. Wilson, T. van Mourik, and T. H. Dunning, Jr., J. Mol. Struct. (Theochem) **388**, 339 (1996).

[59] Basis sets were obtained from the Extensible Computational Chemistry Environment Basis Set Database, Version 2/12/03, as developed and distributed by the Molecular Science Computing Facility, Environmental and Molecular Sciences Laboratory which is part of the Pacific Northwest Laboratory, P.O. Box 999, Richland, Washington 99352, USA, and funded by the U.S. Department of Energy. The Pacific Northwest Laboratory is a multi-program laboratory operated by Battelle Memorial Institue for the U.S. Department of Energy under contract DE-AC06-76RLO 1830. Contact David Feller or Karen Schuchardt for further information.

[60] M. W. Chase, *NIST-JANAF Thermochemical Tables*, 4th ed. (1998).

[61] K. P. Huber and G. Herzberg, *Molecular Spectra and Molecular Structure. IV. Constants of Diatomic Molecules*. (Van Nostrand, Princeton, NJ, 1979).

[62] B. Ruscic, A. F. Wagner, L. B. Harding, R. L. Asher, D. Feller, D. A. Dixon, K. A. Peterson, Y. Song, X. Qian, C.-Y. Ng, J. Liu, W. Chen, and D. W. Schwenke, J. Phys. Chem. A **106**, 2727 (2002).

[63] O. L. Polyansky, A. G. Császár, S. V. Shirin, N. F. Zobov, P. Barletta, J. Tennyson, D. W. Schwenke, and P. J. Knowles, Science **299**, 539 (2003).

[64] I. M. Mills and A. G. Császár, Spectrochim. Acta A **53**, 1101 (1997).

[65] S. A. Tashkun, V. I. Perevalov, J. L. Teffo, L. S. Rothman, and V. G. Tyuterev, J. Quant. Spectrosc. Radiat. Transfer **60**, 785 (1998).

[66] T. Rajamaki, A. Miani, and L. Halonen, J. Chem. Phys. **118**, 6358 (2003).

[67] J. M. L. Martin, T. J. Lee, and P. R. Taylor, J. Chem. Phys. **97**, 8361 (1992).

[68] Y. Pak, R. C. Woods, and K. A. Peterson, J. Chem. Phys. **106**, 5123 (1997).

[69] D. Patel-Misra, D. G. Sauder, and P. J. Dagdigian, J. Chem. Phys. **93**, 5448 (1990).

[70] N. Pinnavaia, M. J. Bramley, M.-D. Su, W. H. Green, and N. C. Handy, Mol. Phys. **78**, 319 (1993).

[71] J. M. Brown and F. Jorgensen, Adv. Chem. Phys. **LII**, 117 (1983).

[72] C. E. Moore, *Atomic Energy Levels*. (Office of Standard Reference Data, National Bureau of Standards, U. S. GPO, Washington, D. C., 1971).

[73] S. E. Bradforth, E. H. Kim, D. W. Arnold, and D. M. Neumark, J. Chem. Phys. **98**, 800 (1993).

[74] C. C. J. Roothaan, Rev. Mod. Phys. **23**, 69 (1951).

[75] J. A. Pople and R. K. Nesbet, J. Chem. Phys. **22**, 571 (1954).

[76] W. J. Hehre, L. Radom, P. v. R. Schleyer, and J. A. Pople, *Ab initio molecular orbital theory*. (Wiley-Interscience, New York, 1986).

[77] A. Szabo and N. S. Ostlund, *Modern Quantum Chemistry: Introduction to Advanced Electronic Structure Theory*, 1st edition, revised ed. (McGraw-Hill, New York, 1989).

[78] C. Møller and M. S. Plesset, Phys. Rev. **46**, 618 (1934).

[79] J. A. Pople, J. S. Binkley, and R. Seeger, Int. J. Quant. Chem. Symp. **10**, 1 (1976).

[80] G. D. Purvis and R. J. Bartlett, J. Chem. Phys. **76**, 1910 (1982).

[81] G. E. Scuseria, A. C. Scheiner, T. J. Lee, J. E. Rice, and H. F. Schaefer III, J. Chem. Phys. **86**, 2881 (1987).

[82] G. E. Scuseria, C. L. Janssen, and H. F. Schaefer, J. Chem. Phys. **89**, 7382 (1988).

[83] M. Rittby and R. J. Bartlett, J. Phys. Chem. **92**, 3033 (1988).

[84] K. Raghavachari, G. W. Trucks, J. A. Pople, and M. Head-Gordon, Chem. Phys. Lett. **157**, 479 (1989).

[85] G. E. Scuseria and T. J. Lee, J. Chem. Phys. **93**, 5851 (1990).

[86] G. E. Scuseria, Chem. Phys. Lett. **176**, 27 (1991).

[87] J. Noga and R. J. Bartlett, J. Chem. Phys. **86**, 7041 (1987).

[88] J. Noga and R. J. Bartlett, J. Chem. Phys. **89**, 3401 (1988).

[89] J. D. Watts and R. J. Bartlett, J. Chem. Phys. **93**, 6104 (1990).

[90] N. C. Handy, J. A. Pople, M. Head-Gordon, K. Raghavachari, and G. W. Trucks, Chem. Phys. Lett. **164**, 185 (1989).

[91] T. J. Lee, R. Kobayashi, N. C. Handy, and R. D. Amos, J. Chem. Phys. **96**, 8931 (1992).

[92] S. R. Gwaltney, C. D. Sherrill, M. Head-Gordon, and A. I. Krylov, J. Chem. Phys. **113**, 3548 (2000).

[93] S. R. Gwaltney and M. Head-Gordon, J. Chem. Phys. **115**, 2014 (2001).

[94] A. R. Hoy, I. M. Mills, and G. Strey, Mol. Phys. **24**, 1265 (1972).

[95] I. Suzuki, J. Mol. Spectrosc. **25**, 479 (1968).

[96] W. S. Benedict and E. K. Plyler, Can. J. Phys. **35**, 1235 (1957).

[97] J. Koput, B. P. Winnewisser, and M. Winnewisser, Chem. Phys. Lett. **225**, 357 (1996).

[98] The equilibrium geometrical parameters for HNCO are obtained from the Kraitchman equations [Refs. 99, 100] using vibration-rotation interaction constants computed via ab initio methods [Ref. 20] and empirical rotational constants [Refs. 101, 102].

[99] J. Kraitchman, Am. J. Phys. **21**, 17 (1953).

[100] C. C. Costain, J. Chem. Phys. **29**, 864 (1958).

[101] K. Yamada, J. Mol. Spectrosc. **79**, 323 (1980).

[102] W. H. Hocking, M. C. L. Gerry, and G. Winnewisser, Can. J. Phys. **53**, 1869 (1975).

[103] See Appendix A for focal point extrapolations of the core correlation energy corrections, as well as the post-CCSDT perturbative quadruples corrections, for Reactions (2.1) - (2.12).

[104] D. Feller, J. Chem. Phys. **98**, 7059 (1993).

[105] N. C. Handy, Y. Yamaguchi, and H. F. Schaefer, J. Chem. Phys. **84**, 4481 (1986).

[106] A. G. Ioannou, R. D. Amos, and N. C. Handy, Chem. Phys. Lett. **251**, 52 (1996).

[107] N. C. Handy and A. M. Lee, Chem. Phys. Lett. **252**, 425 (1996).

[108] E. F. Valeev and C. D. Sherrill, J. Chem. Phys. **118**, 3921 (2003).

[109] S. A. Perera and R. J. Bartlett, Chem. Phys. Lett. **216**, 606 (1993).

[110] K. Balasubramanian, *Relativistic Effects in Chemistry: Part A, Theory and Techniques*. (Wiley, New York, 1997).

[111] K. Balasubramanian, *Relativistic Effects in Chemistry: Part B, Applications*. (Wiley, New York, 1997).

[112] R. D. Cowan and D. C. Griffin, J. Opt. Soc. Am. **66**, 1010 (1976).

[113] G. Tarczay, A. G. Császár, W. Klopper, and H. M. Quiney, Mol. Phys. **99**, 1769 (2001).

[114] J. F. Stanton, J. Gauss, W. J. Lauderdale, J. D. Watts, and R. J. Bartlett, ACES II Stanton version.

[115] J. Kong, C. A. White, A. I. Krylov, C. D. Sherrill, R. D. Adamson, T. R. Furlani, M. S. Lee, A. M. Lee, S. R. Gwalteny, T. R. Adams, C. Ochsenfeld, A. T. B. Gilbert, G. S. Kedziora, V. A. Rassolov, D. R. Maurice, N. Nair, Y. Shao, N. A. Besley, P. E. Maslen, J. P. Dombroski, H. Daschel, W. Zhang, P. P. Korambath, J. Baker, E. F. C. Byrd, T. V. Voorhis, M. Oumi, S. Hirata, C.-P. Hsu, N. Ishikawa, J. Florian, A. Warshel, B. G. Johnson, P. M. W. Gill, M. Head-Gordon, and J. A. Pople, J. Comput. Chem. **21**, 1532 (2000).

[116] T. D. Crawford, C. D. Sherrill, E. F. Valeev, J. T. Fermann, R. A. King, M. L. Leininger, S. T. Brown, C. L. Janssen, E. T. Seidl, J. P. Kenny, and W. D. Allen, PSI3 3.2 (2003).

[117] M. J. Frisch, G. W. Trucks, M. Head-Gordon, P. M. W. Gill, M. W. Wong, J. B. Foresman, B. G. Johnson, H. B. Schlegel, M. A. Robb, E. S. Replogle, R. Gomperts, J. L. Andres, K. Raghavachari, J. S. Binkley, C. Gonzalez, R. L. Martin, D. J. Fox, D. J. Defrees, J. Baker, J. J. P. Stewart, and J. A. Pople, Gaussian 94, Revision C (Gaussian Inc., Pittsburgh, PA, 1995).

[118] J. L. Dunham, Phys. Rev. **41**, 721 (1932).

[119] G. Herzberg, *Molecular Spectra and Molecular Structure: I. Spectra of Diatomic Molecules*, 2nd ed. (Van Nostrand, New York, 1950).

[120] H. H. Nielsen, Rev. Mod. Phys. **23**, 90 (1951).

[121] I. M. Mills, in *Molecular Spectroscopy: Modern Research*, edited by K. N. Rao and C. W. Mathews (Academic Press, New York, 1972), Vol. 1, pp. 115.

[122] D. Papousek and M. R. Aliev, *Molecular Vibrational-Rotational Spectra*. (Elsevier, Amsterdam, 1982).

[123] W. D. Allen, Y. Yamaguchi, A. G. Császár, D. A. Clabo, Jr., R. B. Remington, and H. F. Schaefer, Chem. Phys. **145**, 427 (1990).

[124] J. K. G. Watson, in *Vibrational Spectra and Structure*, edited by J. R. Durig (Elsevier, Amsterdam, 1977), Vol. 6, pp. 1.

[125] D. A. Clabo, Jr., W. D. Allen, R. B. Remington, Y. Yamaguchi, and H. F. Schaefer, Chem. Phys. **123**, 187 (1988).

[126] H. L. Woodcock, A. G. Császár, W. D. Allen, and H. F. Schaefer III, to be published.

[127] G. Herzberg, *Molecular Spectra and Molecular Structure. II. Infrared and Raman Spectra of Polyatomic Molecules*. (Van Nostrand, Princeton, NJ, 1945).

[128] According to general formulas for the G0 term which have been derived in our laboratory, to be published.

[129] S. Albert, K. K. Albert, M. Winnewisser, and B. P. Winnewisser, J. Mol. Struct. **599**, 347 (2001).

[130] K. Irikura and D. J. Frurip, *Computational Thermochemistry*. (American Chemical Society, Washington D.C., 1998).

[131] N. D. K. Petraco, W. D. Allen, and H. F. Schaefer, J. Chem. Phys. **116**, 10229 (2002).

[132] G. Tarczay, A. G. Császár, W. Klopper, V. Szalay, W. D. Allen, and H. F. Schaefer III, J. Chem. Phys. **110**, 11971 (1999).

[133] D. Feller, J. Chem. Phys. **111**, 4373 (1999).

[134] T. A. Ruden, T. Helgaker, P. Jorgensen, and J. Olsen, Chem. Phys. Lett. **371**, 62 (2003).

[135] J. Olsen, J. Chem. Phys. **113**, 7140 (2000).

[136] B. Ruscic, D. Feller, D. A. Dixon, K. A. Peterson, L. B. Harding, R. L. Asher, and A. F. Wagner, J. Phys. Chem. A **105**, 1 (2001).

[137] W. A. Shapley and G. B. Backsay, J. Phys. Chem. **103**, 6624 (1999).

[138] A. D. McLean, G. H. Loew, and D. S. Berkowitz, J. Mol. Spectrosc. **64**, 184 (1977).

[139] L. Farnell, R. H. Nobes, and L. Radom, J. Mol. Spectrosc. **93**, 271 (1982).

[140] N. C. Handy, C. W. Murray, and R. D. Amos, Phil. Mag. B **69**, 755 (1994).

[141] M. T. Nguyen, K. Pierloot, and L. G. Vanquickenborne, Chem. Phys. Lett. **181**, 83 (1991).

[142] A. P. Rendell, T. J. Lee, and R. Lindh, Chem. Phys. Lett. **194**, 84 (1992).

[143] K. Yamada, B. P. Winnewisser, and M. Winnewisser, J. Mol. Spectrosc. **56**, 449 (1975).

[144] P. R. Bunker, B. M. Landsberg, and B. P. Winnewisser, J. Mol. Spectrosc. **74**, 9 (1979).

[145] B. P. Winnewisser, M. Winnewisser, and C. W. Mathews, J. Mol. Spectrosc. **126**, 460 (1987).

[146] S. Albert, M. Winnewisser, and B. P. Winnewisser, Ber. Bunsen-Ges. Phys. Chem. **101**, 1165 (1997).

[147] S. Albert, K. K. Albert, M. Winnewisser, and B. P. Winnewisser, Ber. Bunsen-Ges. Phys. Chem. **102**, 1428 (1998).

CHAPTER 3

THE HIGHLY ANHARMONIC BH_5 POTENTIAL ENERGY SURFACE CHARACTERIZED IN THE *AB INITIO* LIMIT[1]

[1] Schuurman, M. S.; Allen, W. D.; Schleyer, P. v.R. Schaefer, H. F. Submitted to the *Journal of Chemical Physics* (2004).

3.1 ABSTRACT

The strong sensitivity to level of theory of the salient features of the ground state potential energy surface of BH_5 has been overcome by rigorously converged *ab initio* computations employing correlation-consistent basis sets cc-p(C)V*X*Z (X = 2-6), explicitly-correlated R12 corrections, and coupled-cluster theory complete through quadruple excitations (CCSDTQ). Our focal-point extrapolations yield a C_s-symmetry global minimum of $BH_3 - H_2$ type featuring interfragment B – H distances of (1.401, 1.414) Å, an H_2 bond length elongated to 0.803 Å, and a $BH_3 + H_2$ dissociation energy D_e (D_0) = 6.6 (1.2) kcal mol^{-1}. The classical barriers for H_2 internal rotation and hydrogen scrambling are 0.07 and 5.81 kcal mol^{-1}, respectively. Our thermochemical computations yield $\Delta_f H_0^\circ[BH_5(g)] = -111.3 \pm 0.2$ kcal mol^{-1} $+ \Delta_f H_0^\circ[B(g)]$, which is limited in accuracy only by persistent uncertainties in the enthalpy of formation of gaseous boron. As a first step in investigating the extremely anharmonic 12-dimensional vibrational dynamics of BH_5, a complete quartic force field has been computed at the all-electron cc-pCVQZ CCSD(T) level of theory. Previous matrix isolation infrared assignments of the ν_2 and ν_9 stretching modes of BH_5 compare favorably with our computed vibrational fundamentals, but the experimental assignment of the ν_6 bending mode of the BH_3 moiety is not supported by computed isotopic shifts.

3.2 INTRODUCTION

The existence of BH_5 was predicted long before it could be experimentally or theoretically confirmed. Beginning in 1961, a number of investigations[1-3] into the protonation of aqueous BH_4^- lead experimentalists to postulate a stable BH_5 intermediate. This hypothesis was primarily based on observed hydrogen-deuterium scrambling in the $H_2/D_2 + BDH_2/BHD_2$

products when the reaction was performed in D_2O/H_2O. In lieu of these results, early theoretical studies were undertaken to gauge the viability of this fascinating intermediate. In 1971, an early computational study[4] determined that BH_5 was not stable with respect to dissociation into BH_3 and H_2 at the Hartree-Fock (HF) level of theory. A year later, Olah and co-workers[5] predicted a C_s minimum energy structure using the CNDO (complete neglect of differential overlap) method,[6] but did not report dissociation energies with respect to BH_3 and H_2. These early results were elaborated upon by Hoheisel and Kutzelnigg,[7] who confirmed the absence of a Hartree-Fock BH_5 minimum, but also found that the inclusion of CEPA (coupled electron pair approximation) correlation energy led to a C_s minimum energy structure that was analogous to CH_5^+ and stable (D_e = 2 kcal mol^{-1}) with respect to dissociation. In 1976, Collins *et al.*[8] computed the binding energy of BH_3-H_2 to be 1.70 kcal mol^{-1} on the basis of 6-31G** UMP2 (unrestricted second-order Möller-Plesset perturbation theory) single-point computations (excluding zero-point vibrational effects), while Pepperberg and co-workers[9] were unable to find any tenable BH_5 structure less than 10 kcal mol^{-1} above the $BH_3 + H_2$ dissociation products using the PRDDO (partial retention of diatomic differential overlap) and PRDDO-CI methods.

In 1989 Stanton *et al.*[10] performed a thorough *ab initio* study employing MP2 and coupled-cluster theory (CCSD[T]) with moderately sized basis sets. They discovered a pronounced dependence of the geometric and energetic properties of the system on both the basis set and electron correlation treatment. For example, a repulsive intermolecular BH_3-H_2 interaction is observed at the CCSD[T] level of theory if a double zeta (DZ) quality, unpolarized basis set is employed, whereas a polarized DZP basis set gave rise to a vibrationless binding energy of 2.7 kcal mol^{-1}. The largest computations, performed at the [5s4p3d1f/4s2p1d] CCSD[T] level of theory, predicted a binding energy of D_e = 5.4 kcal mol^{-1}. However, the zero-

point vibrational energy correction (computed using scaled MP2 harmonic frequencies) works to lower the binding energy by a significant 4.5 kcal mol^{-1}, yielding D_0 = 0.9 kcal mol^{-1}. Moreover, the Gibbs free energy for dissociation at 298 K was computed as $\Delta G_0^{298K} = -4.1$ kcal mol^{-1}, suggesting that BH_5 is not thermodynamically stable at room temperature.

In 1994, Tague and Andrews[11] reported the first observation of BH_5 and its deuterated analog in a cryogenic argon matrix. BH_5 was generated by reacting boron atoms, produced via pulsed-laser ablation, with H_2 diluted in excess argon gas. The reported $^{11}BH_5$ ($^{11}BD_5$) fundamental frequencies of 2475.2 (1866.2) and 1134.3 (883.0) were observed to correspond, respectively, to the degenerate bond-stretch (ν_3) and out-of-plane bend (ν_2) vibrations found in the BH_3 subunit and were in general agreement with the results reported by Stanton *et al.*[10] However, the degeneracy of the bond stretch mode should be lifted in the lowest-energy (C_s) conformer BH_5, yet no frequency splitting was observed.

Shortly thereafter, new *ab initio* results were reported by Schreiner *et al.*[12] and Watts and Bartlett.[13] The former investigation included an extensive survey of the low-energy BH_5 isomers and yielded equilibrium structures and harmonic frequencies up to the triple-zeta plus polarization (TZ2P) CCSD(T) level of theory. In addition to predicting D_e = 6.3 kcal mol^{-1} and D_0 = 0.9 kcal mol^{-1}, the barrier to internal rotation of the H_2 subunit was found to be only 0.03 kcal mol^{-1}. In broad agreement with these results, Watts and Bartlett[13] reported BSSE-corrected values of D_e (D_0) = 5.8 (0.1) kcal mol^{-1} obtained via computations up to the polarized valence quadruple-zeta (PVQZ) CCSD(T) level of theory. Both authors noted that the experimentally observed peak at 2544 cm^{-1}, tentatively assigned by Tague and Andrews[11] to a higher-order B_xH_y species, was in good agreement with the computed BH_5 ν_9 mode. This mode corresponds to the second component of the degenerate BH_3 stretch.

The past decade has seen a number of computational studies on BH_5 employing an array of standard *ab initio* methods, including MP2,[14,15] CBS/G2,[16] and density functional theory (DFT).[17] The majority of these studies predicted D_e = 3.5 - 6.5 kcal mol^{-1} and D_0 = 0.0 - 1.4 kcal mol^{-1} for dissociation to BH_3 + H_2. Most recently, multicoefficient correlated methods (MCCMs),[18,19] techniques that scale basis set and correlation increments using empirically fitted coefficients to approximate full configuration interaction results with large basis sets, have been used to compute dissociation energies (5.8 - 6.2 kcal mol^{-1}), as well as hydrogen scrambling barrier heights (5.6 - 5.8 kcal mol^{-1})[20] and rate constants.[21] Thus, there have been many approaches to computing D_e; however, an accurate determination of D_0 has not been forthcoming since all zero-point vibrational energy (ZPVE) corrections have simply involved the scaling of harmonic frequencies. In this report, in addition to accurate focal point analyses of the binding energy of BH_5 and relative energies of two low-lying isomers, anharmonicity is considered explicitly using an *ab initio* quartic force-field to compute anharmonic ZPVEs and fundamental frequencies.

3.3 Theoretical Methods

This investigation is primarily concerned with the precise determination of the dissociation energy of BH_5 into BH_3 + H_2, the barrier to internal rotation of the H_2 moiety, and the barrier to hydrogen scrambling in the gas phase. In order to achieve the highest possible accuracy, focal point analyses were executed to determine all reaction energies. This extrapolation scheme has been discussed in detail elsewhere[22-26] and will only be briefly summarized below. In addition, anharmonic zero-point vibrational energies (ZPVEs) were determined for BH_5, BH_3, and H_2 by computing quartic force fields for each of these species.

These results are of particular interest for the computation of the $BH_5 \rightarrow BH_3 + H_2$ dissociation energy and for comparison to the experimentally observed BH_5 fundamental frequencies.[11] Lastly, a host of auxiliary terms, including core-correlation, diagonal Born-Oppenheimer (DBOC), and special relativistic corrections, were included additively to obtain a final prediction for each reaction energy.

Focal-point analyses entail the layout of a two-dimensional extrapolation grid for the basis set dependence of the correlation energy in order to carefully track increments to the reaction energy toward the complete basis set (CBS) full configuration interaction (FCI) limit. No empirical corrections are embedded. The functional form adopted for the Hartree-Fock extrapolations[27] is

$$E_{HF}(X) = E_{HF}^{\infty} + ae^{-bX}, \tag{3.1}$$

whereas that used to evaluate correlation energy limits[28] is

$$E_{corr}(X) = E_{corr}^{\infty} + bX^{-3}. \tag{3.2}$$

The first focal point extrapolation is of the total energies of reactants and products computed under the frozen-core approximation. For this primary extrapolation, valence correlation consistent basis sets of the form cc-pV*X*Z (*X* = D, T, 4, 5, 6)[29-31] were utilized to determine energies at the RHF (restricted Hartree-Fock),[32-34] MP2,[35,36] CCSD (coupled cluster singles and doubles),[37-39] CCSD(T) (CCSD with perturbative triples),[40,41] and CCSDT (full coupled cluster through triple excitations)[42,43] levels of theory. In addition, the effects of connected quadruple excitations were evaluated using a cc-pVDZ basis with the full CCSDTQ[44-46] method via a string-based algorithm. In order to precisely determine the δ[MP2] energy increment, explicitly correlated MP2-R12/A[47-51] computations were performed. The large, uncontracted basis set required for the resolution of the identity was obtained by uncontracting

the cc-pV6Z basis set and adding a tight and diffuse function to each angular momentum shell in an even-tempered fashion. The functions in this R12 basis are (18*s*13*p*7*d*6*f*5*g*4*h*3*i*) for B and (12*s*7*p*6*d*5*f*4*g*3*h*) for H.

The second focal point extrapolation involves the determination of the core correlation energy that is neglected in a valence-only treatment. Core-valence basis sets of the form cc-pCV*X*Z (*X* = 2, 3, 4, 5)[52] were used in these extrapolations. Energy increments through the CCSDT level were incorporated in the determination of the core correlation energy.

To obtain highly accurate r_e structures, all-electron CCSD(T) gradient optimizations were performed, both with the cc-pCV*X*Z (*X* = D, T, Q) basis sets and for the extrapolated CBS limit, i.e., the sum $E_{HF}^{\infty} + E_{corr}^{\infty}$ from Eqs. (3.1) and (3.2). The requisite input for evaluation of each CBS CCSD(T) gradient was a set of three cc-pCV*X*Z (*X* = T, Q, 5) HF gradients and a pair of cc-pCV*X*Z (*X* = T, Q) CCSD(T) gradients. The nonlinear relationship between (E_{HF}^{∞}, *a*, *b*) and $E_{HF}(X)$ in Eq. (3.1) requires numerical solution of a set of nonlinear equations for ∇E_{HF}^{∞} (see supplementary material),[53] but ∇E_{corr}^{∞} is trivially computed because Eq. (3.2) is linear. The CBS Cartesian gradients were converged to less than 10^{-5} hartree/bohr at the extrapolated r_e structures. Table 3.1 collects the all-electron CCSD(T) optimum geometric parameters of the three BH_5 stationary points of concern within the basis set series cc-pCV*X*Z (*X* = D, T, Q, ∞). The analogous series for the equilibrium bond distance of isolated BH_3 and H_2 are (1.207, 1.189, 1.187, 1.186) Å and (0.7609, 0.7426, 0.7419, 0.7417) Å, respectively. For BH_3 the addition of relativistic and DBOC corrections changes the equilibrium length by only 0.0001 Å, and we anticipate similar shifts for BH_5.

The adiabatic approximation was invoked by appending to the energy of the r_e structures the diagonal Born-Oppenheimer correction (DBOC).[54-57] This energy term corresponds to the

first-order correction to the Born-Oppenheimer approximation for finite nuclear mass. The DBOC corrections were computed at the cc-pVDZ CISD level of theory for each molecular species. While relativistic effects for first-row atoms are small, their inclusion is necessary for subchemical accuracy. Thus, the one-electron mass-velocity and Darwin terms[58-62] arising from a scalar relativistic treatment of electronic motion have been computed using the perturbative approach of Ref. 58 at the all-electron cc-pCVQZ CCSD(T) level of theory.

All CCSD, CCSD(T) and CCSDT energies, as well as the relativistic corrections, were computed using ACES II,[63] and the MP2 and DBOC computations were performed using PSI3.[64] The CCSDTQ energy increments were determined using the MRCC code of Kallay and co-workers.[44-46]

The harmonic vibrational frequencies for the principal BH_5 stationary points (i.e. the C_s(I) minimum and C_s(II) and C_{2v} transition states) are listed in Table 3.2. To determine anharmonic zero-point vibrational energies (ZPVEs), quartic force fields for BH_5, BH_3 and H_2 were computed at the cc-pCVQZ CCSD(T) level of theory and employed in concert with second-order vibrational perturbation theory (VPT2)[65-67] to determine anharmonic constants. Adopting the atomic labeling of Figure 3.1, the internal coordinate set chosen for BH_5 was:

$S_1(a') = \frac{r_1 + r_2 + r_3}{\sqrt{3}}$	(BH_3 sym. str.)	$S_7(a') = r_5$	(B-H interfragment str.)
$S_2(a') = \frac{\gamma_1 + \gamma_2 + \gamma_3}{\sqrt{3}}$	(BH_3 out-of-plane bend)	$S_8(a') = R$	(H_2 str.)
$S_3(a') = \frac{2r_1 - r_2 - r_3}{\sqrt{6}}$	(BH_3 asym. str.)	$S_9(a'') = \frac{r_2 - r_3}{\sqrt{2}}$	(BH_3 asym. str.)
$S_4(a') = \frac{2\theta_{23} - \theta_{13} - \theta_{12}}{\sqrt{6}}$	(BH_3 asym. bend)	$S_{10}(a'') = \frac{\theta_{13} - \theta_{12}}{\sqrt{2}}$	(BH_3 asym. bend)
$S_5(a') = \frac{2\theta_{14} - \theta_{24} - \theta_{34}}{\sqrt{6}}$	(BH_3 – H_2 rock)	$S_{11}(a'') = \frac{\theta_{24} - \theta_{34}}{\sqrt{2}}$	(BH_3 – H_2 wag)
$S_6(a') = r_4$	(B-H interfragment str.)	$S_{12}(a'') = \tau_{RB1}$	(BH_3 – H_2 torsion)

TABLE 3.1: Optimum geometric parameters of principal BH_5 stationary points, as predicted by all-electron cc-pCV*X*Z (*X* = D, T, Q, ∞) CCSD(T) theory.[a]

	C_s(I)				C_s(II)				C_{2v}			
X =	D	T	Q	∞(CBS)	D	T	Q	∞(CBS)	D	T	Q	∞(CBS)
R_1	1.216	1.201	1.200	1.199	1.207	1.191	1.189	1.189	1.290	1.267	1.265	1.263
$r_2 = r_3$	1.209	1.192	1.191	1.190	1.213	1.197	1.196	1.195	1.202	1.185	1.184	1.183
R_4	1.470	1.414	1.406	1.401	1.484	1.426	1.417	1.411	1.274	1.250	1.247	1.246
R_5	1.487	1.429	1.420	1.414	1.484	1.426	1.417	1.411	1.290	1.267	1.265	1.263
r_{45}	0.809	0.801	0.802	0.803	0.807	0.799	0.800	0.801	1.101	1.088	1.088	1.088
θ_{12}	116.4	115.8	115.7	115.7	118.8	118.6	118.5	118.5	106.0	105.9	105.9	105.9
θ_{14}	79.2	79.5	79.4	79.4	101.3	102.1	102.2	102.3	50.9	51.2	51.3	51.4
θ_{23}	120.2	120.1	120.1	120.1	115.5	114.7	114.6	114.5	128.1	128.0	128.1	128.1
θ_{45}	31.8	32.7	33.0	33.2	31.6	32.5	32.8	33.0	50.9	51.2	51.3	51.4
γ_1	27.0	29.4	29.7	29.9	25.5	27.6	27.9	28.1	50.9	51.2	51.3	51.4

[a] Bond lengths are given in Å, bond angles in degrees. See Fig. 3.1 for atomic labeling and a description of the structures.

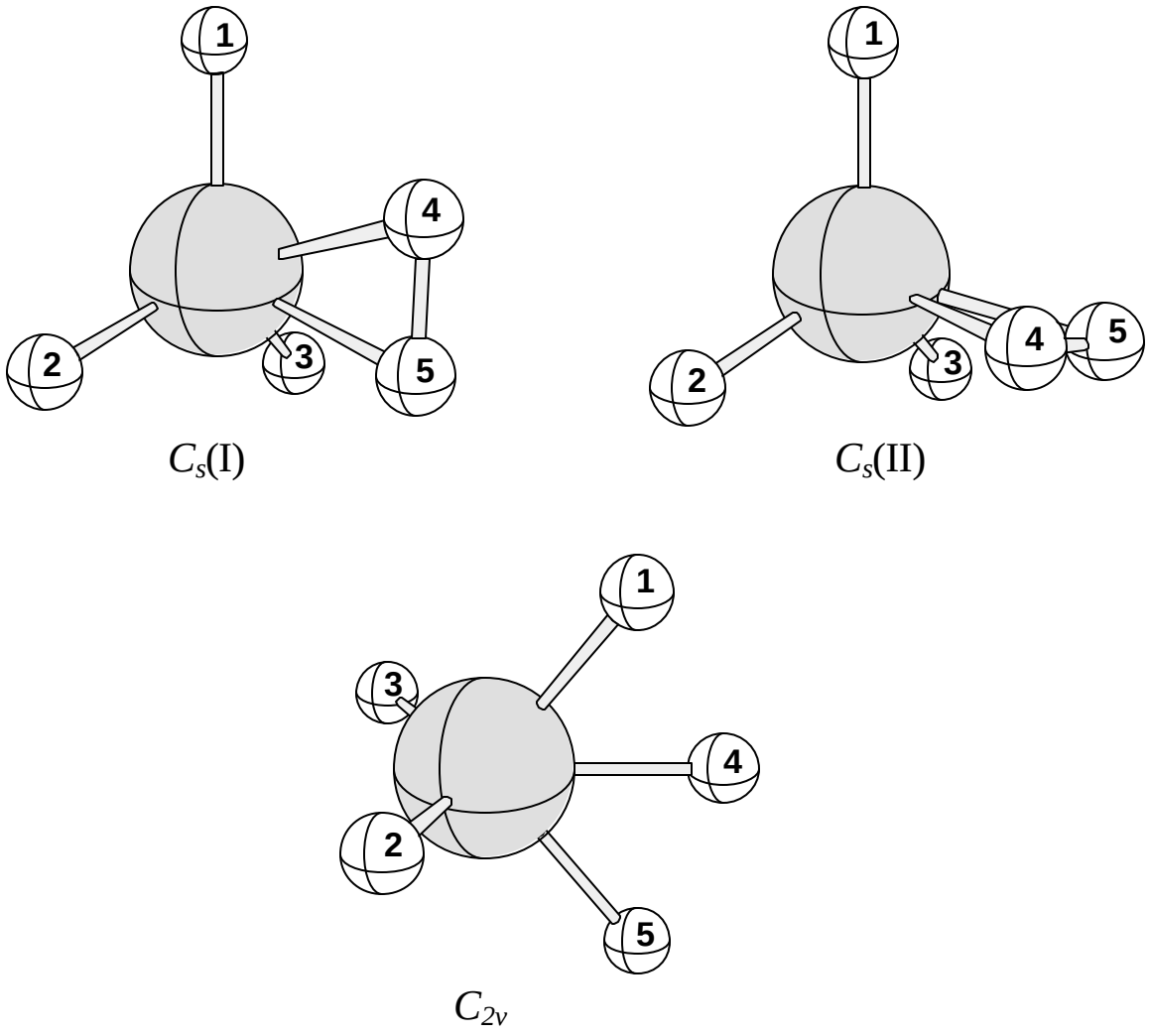

FIGURE 3.1: The lowest energy minimum [C_s (I)], internal rotation transition state [C_s (II)], and hydrogen scrambling transition state [C_{2v}] of BH_5.

where r_i and R denote the B-H_i and H_4-H_5 bond distances, θ_{ij} is the H_i-B-H_j angle, γ_i is the B-H_i out-of-plane angle with respect to the B – H_j – H_k plane, and τ_{RB1} is the (H-H-B-H) torsional angle defined by the H_2 moiety and B – H_1. S_1, S_2, S_3, S_4, S_9 and S_{10} involve atoms in the BH_3 fragment only, and these were the internal coordinates used in the BH_3 force field, where the indices are mapped as $1 \rightarrow 1\ (a_1')$, $2 \rightarrow 2\ (a_2'')$, $3 \rightarrow 3\ (e')$, $4 \rightarrow 4\ (e')$, $9 \rightarrow 5\ (e')$, $10 \rightarrow 6\ (e')$.

The full quartic force field for BH_3 was determined by computing analytic energy gradients at 92 displaced geometries, while the force field for BH_5 was computed via 2062 single-point energies. The program INTDIF2004[68] was employed to determine the required displacements as well as compute the force constants in internal coordinates. The transformation of the force constants from internal to normal coordinates and the computation of spectroscopic constants were performed using the programs INTDER2000 (Refs. 69-72) and ANHARM (Ref. 72), respectively.

3.4 Anharmonic Vibrational Analysis

Computed *ab initio* vibrational frequencies played an integral role in the identification of BH_5 from the experimental spectrum obtained by Tague and Andrews.[11] However, since the assignment of the observed peaks was based largely on (scaled) harmonic vibrational frequencies, more conclusive evidence for this assignment may be obtained via high level computations that explicitly account for anharmonicity. Anharmonicity constants derived from second-order vibrational perturbation theory (VPT2) and *ab initio* force fields, have proven extremely successful in predicting fundamental frequencies of semi-rigid molecules. However, as has been previously noted and is further discussed in this report, the interaction of the H_2

TABLE 3.2: All-electron cc-pCVQZ CCSD(T) harmonic vibrational frequencies, IR intensities, and total vibrational energy distributions for the principal BH_5 stationary points.

		$^{11}BH_5$			$^{11}BD_5$		
	mode	freq.	IR Int.[a]	TED[b]	freq.	IR Int.[a]	TED[b]
C_s(I)	ω_1	3574	20.4	$S_8(98)$	2531	10.1	$S_8(97)$
	ω_2	2625	74.9	$S_3(94)-S_1(6)$	1953	39.1	$S_3(98)$
	ω_3	2531	9.5	$S_1(94)+S_3(6)$	1801	5.7	$S_1(99)$
	ω_4	1796	7.0	$S_6(54)-S_7(41)-S_5(4)$	1281	4.6	$S_6(54)-S_7(40)-S_5(5)$
	ω_5	1210	11.7	$S_4(65)+S_7(14)-S_2(14)+S_6(5)$	872	3.6	$S_4(85)+S_5(12)$
	ω_6	1195	36.1	$S_2(64)+S_4(15)-S_7(10)+S_5(5)$	874	35.8	$S_2(96)$
	ω_7	979	45.0	$S_7(33)-S_5(32)+S_2(14)+S_6(11)$	745	18.5	$S_7(48)-S_5(29)+S_6(17)$
	ω_8	776	18.3	$S_5(46)+S_6(23)-S_4(13)+S_7(11)$	589	9.6	$S_5(57)+S_6(23)-S_4(13)+S_7(7)$
	ω_9	2669	102.1	$S_9(100)$	1996	55.1	$S_9(100)$
	ω_{10}	1196	3.5	$S_{10}(93)+S_7(16)-S_{12}(9)$	855	1.2	$S_{10}(104)-S_{12}(8)$
	ω_{11}	1027	0.1	$S_{11}(90)-S_{10}(11)$	767	0.1	$S_{11}(101)$
	ω_{12}	190	5.0	$S_{12}(109)+S_{11}(5)+S_{10}(4)$	134	2.0	$S_{12}(109)+S_{11}(5)+S_{10}(4)$
C_s(II)	ω_1	3600	12.8	$S_8(96)$	2557	6.4	$S_8(97)$
	ω_2	2666	103.5	$S_3(97)$	1997	56.6	$S_3(99)$
	ω_3	2536	7.6	$S_1(96)$	1808	6.0	$S_1(99)$
	ω_4	1200	21.1	$S_2(77)-S_7(10)-S_6(10)$	877	38.9	$S_2(94)$
	ω_5	1194	22.0	$S_4(73)+S_5(22)$	860	1.9	$S_4(84)+S_5(8)$
	ω_6	1029	27.4	$S_5(55)-S_4(18)+S_2(10)+S_6(7)$	780	10.0	$S_5(66)+S_6(12)+S_7(12)+S_{12}(5)$
	ω_7	831	30.5	$S_6(31)+S_7(31)+S_2(13)-S_5(12)$	643	14.7	$S_6(33)+S_7(33)-S_5(17)-S_4(10)$
	ω_8	2627	76.6	$S_9(100)$	1963	37.9	$S_9(100)$
	ω_9	1778	7.6	$S_9(100)$	1272	4.8	$S_6(49)-S_7(45)-S_{11}(5)$
	ω_{10}	1205	7.4	$S_{10}(84)-S_{11}(15)$	871	2.7	$S_{10}(89)-S_{11}(8)$
	ω_{11}	945	0.9	$S_{11}(71)-S_{12}(16)\ )+S_{10}(9)$	697	1.2	$S_{11}(78)-S_{12}(14)$
	ω_{12}	185i	--	$S_{12}(75)+S_{11}(10)+S_{10}(8)-S_5(8)$	132i	--	$S_{12}(75)+S_{11}(10)+S_{10}(8)-S_5(8)$
C_{2v}	ω_1	2639	14.3	$S_1(50)-S_3(23)-S_6(22)$	1938	11.8	$S_1(40)-S_6(31)-S_3(28)$
	ω_2	2528	21.2	$S_6(58)-S_3(28)-S_7(12)$	1796	10.9	$S_6(57)-S_3(29)-S_7(11)$
	ω_3	2282	12.4	$S_1(24)+S_7(24)+S_8(20)+S_6(14)$	1641	7.2	$S_1(35)+S_7(26)+S_8(16)+S_3(9)$
	ω_4	1394	7.5	$S_5(34)+S_8(29)-S_7(13)+S_2(7)$	1039	8.1	$S_8(33)+S_5(28)-S_4(11)-S_7(11)$
	ω_5	1156	20.9	$S_2(71)+S_4(16)-S_8(16)$	851	8.2	$S_2(70)+S_4(16)-S_8(14)$
	ω_6	1204	0.0	$S_{10}(100)$	854	0.0	$S_{10}(100)$
	ω_7	2735	70.7	$S_9(96)$	2058	37.2	$S_9(98)$
	ω_8	1140	2.0	$S_{12}(70)-S_4(26)$	830	0.3	$S_{12}(77)-S_4(17)$
	ω_9	893	2.7	$S_{11}(46)-S_{12}(22)-S_4(21)-S_5(5)$	660	1.8	$S_{11}(43)-S_4(22)-S_{12}(21)-S_5(7)$
	ω_{10}	2304	86.1	$S_7(44)-S_3(32)-S_1(16)+S_8(6)$	1703	40.0	$S_7(43)-S_3(32)-S_1(16)+S_8(6)$
	ω_{11}	1143	44.6	$S_{11}(71)-S_{12}(16)\ )+S_{10}(9)$	845	15.6	$S_{11}(56)+S_4(32)-S_2(6)$
	ω_{12}	1095i	--	$S_5(54)-S_8(29)-S_2(8)-S_4(6)$	811i	--	$S_5(53)-S_8(30)-S_2(7)-S_4(6)$

[a] Infrared intensity given in units of km mol^{-1}.

[b] Total energy decomposition. The percentage proportions k of the total energy (kinetic and potential) of each normal vibration attributable to the individual internal coordinates S_i defined in the text are indicated as $S_i(k)$. The signs preceding these entries denote the relative phases of the internal coordinates in the normal-mode eigenvectors. See Refs. 73 and 74.

fragment with BH_3 is sufficiently weak to allow for large amplitude motion of the H_2 moiety – motion that cannot be appropriately treated using perturbation theory. Thus, accurate fundamental frequencies for these large amplitude modes of BH_5 may not be obtained using a VPT2 approach. What may be determined, however, are approximate anharmonicities for the remaining modes.

An accounting of the anharmonicities of small-amplitude modes may be accomplished within perturbation theory by employing contact transformations.[67,75] Consider the similarity-transformed Hamiltonian

$$\tilde{H} = e^{i\lambda\hat{S}}\hat{H}e^{-i\lambda\hat{S}}, \tag{3.3}$$

whose eigenspectrum is identical to that of the original Watson Hamiltonian $\hat{H}$. The operator $\hat{S}$ which removes the predominant coupling among the SA modes is well known:[67]

$$\hat{S} = \frac{1}{6}\sum_{ijk}\frac{\phi_{ijk}}{\Delta_{ijk}}\left[2\omega_i\omega_j\omega_k p_i p_j p_k + 3\omega_j\left(\omega_i^2 - \omega_j^2 + \omega_k^2\right)q_i p_j q_k\right] \tag{3.4}$$

where the q_i are reduced normal coordinates, the p_i are associated momentum operators, the ω_i are harmonic vibrational frequencies, the ϕ_{ijk} are cubic force constants in the reduced normal coordinate space, and

$$\Delta_{ijk} = \left(\omega_i + \omega_j + \omega_k\right)\left(\omega_i + \omega_j - \omega_k\right)\left(\omega_i - \omega_j + \omega_k\right)\left(\omega_i - \omega_j - \omega_k\right). \tag{3.5}$$

While rigorous diagonalization of $\tilde{H}$ is necessary for a description of the large-amplitude interfragment modes of BH_5, a perturbative treatment of $\tilde{H}$ yields anharmonic corrections within the SA space. The usual VPT2 formulas[65-67,76,77] result for the anharmonic constants χ_{ij}, except that all summations are restricted to the small-amplitude coordinates. The large-amplitude interfragment modes which require exclusion from the VPT2 treatment are ν_4, ν_7, ν_8, and ν_{12}, which correspond to an interfragment antisymmetric stretch ($S_6 - S_7$), two BH_3-H_2 rocks

mixed with interfragment stretches ($S_7 + S_6 - S_5$, $S_5 + S_6 + S_7$), and the BH_3-H_2 torsion mode (S_{12}).

The full quartic force field in the internal coordinate space for BH_5 [C_s(I)] at the all-electron cc-pCVQZ CCSD(T) level is given as supplementary material (Tables B.1 – B.3).[53] The anharmonic constants χ_{ij} for BH_5, determined from the reduced-dimensionality SA treatment, are given in Table 3.3. The corresponding fundamental frequencies for BH_5, as well as their BH_3 analogs, are given in Tables 3.4 and 3.5. Anharmonic zero-point vibrational energies (ZPVEs) also appear in these tables. The complete anharmonic force field of BH_3 is reported in a concurrent paper.

The saga of the CH_5^+ ion,[78] isoelectronic with BH_5, bears directly on the current investigation. *Ab initio* studies[79,80] attempting to determine the lowest energy isomer of CH_5^+ focused on structures analogous to the C_s(I), C_s(II) and C_{2v} species shown in Figure 3.1. While CCSD(T)-R12 (explicitly correlated coupled-cluster singles and doubles with perturbative triples) results[80] definitively assigned the C_s(I) structure as the lowest energy form (by 0.10 and 0.82 kcal mol^{-1} below the C_s(II) and C_{2v} transition states, respectively), questions remained as to the fluxional nature of the CH_5^+ geometry. Subsequent molecular dynamics computations[81,82] have addressed this issue, and a recent 12 (fully) dimensional molecular dynamics investigation[82] has concluded that CH_5^+ indeed has an effective structure comprised of CH_3^+ and H_2 subunits. Further work on BH_5 would provide an interesting comparison to the CH_5^+ story, particularly given the differences in bonding of the subunits. In CH_5^+, ion-molecule interactions contribute to the significant binding of the two moieties (D_e = 48 kcal mol^{-1}),[80] while the bonding observed in neutral BH_5 is strictly covalent and much smaller (D_e = 6.2 kcal mol^{-1}), arguably making the dynamics even more fascinating. Another key difference is that the B-H bonds in borane are

TABLE 3.3: Vibrational anharmonicity constants for BH_5 [C_s(I)] (cm^{-1}).[a,b]

i	j	χ_{ij}		i	j	χ_{ij}		i	j	χ_{ij}	
		$^{11}BH_5$	$^{11}BD_5$			$^{11}BH_5$	$^{11}BD_5$			$^{11}BH_5$	$^{11}BD_5$
1	1	−130.18	−62.50	7	6	0.03	0.23	10	8	0.59	0.57
2	1	−6.00	−5.14	7	7	0.00	0.00	10	9	−13.28	−8.74
2	2	−16.06	−12.13	8	1	0.81	0.66	10	10	−3.20	−3.69
3	1	−9.26	−4.93	8	2	0.22	0.01	11	1	−6.09	−3.50
3	2	−61.05	−32.04	8	3	1.11	0.77	11	2	−5.97	−2.30
3	3	−16.98	−6.91	8	4	0.88	0.50	11	3	−1.94	−0.48
4	1	5.12	2.49	8	5	0.75	0.04	11	4	0.82	0.36
4	2	0.02	0.02	8	6	0.28	0.31	11	5	−1.29	0.15
4	3	0.14	0.08	8	7	1.51	0.48	11	6	−1.55	−0.51
4	4	0.00	0.00	8	8	0.00	0.00	11	7	1.40	0.76
5	1	−9.59	−6.63	9	1	−2.87	−2.00	11	8	2.24	1.09
5	2	−14.03	−8.13	9	2	−51.85	−20.27	11	9	−9.99	−5.05
5	3	−5.68	19.94	9	3	−31.64	−23.54	11	10	−2.20	−1.04
5	4	0.31	0.06	9	4	0.03	0.04	11	11	−0.36	0.28
5	5	−4.16	−7.23	9	5	−10.40	−7.22	12	1	63.08	31.97
6	1	−13.68	−3.95	9	6	−15.56	−7.02	12	2	0.29	0.24
6	2	−6.93	−9.80	9	7	0.95	0.08	12	3	3.73	1.60
6	3	0.84	0.30	9	8	4.10	1.89	12	4	18.17	9.20
6	4	0.16	0.18	9	9	−24.54	−14.96	12	5	0.96	0.04
6	5	0.90	0.70	10	1	−4.14	−1.23	12	6	0.39	0.01
6	6	−3.35	−2.43	10	2	−15.00	−8.74	12	7	3.84	2.28
7	1	1.35	0.73	10	3	−4.28	−5.80	12	8	0.42	0.53
7	2	1.41	0.69	10	4	0.21	3.60	12	9	0.29	0.12
7	3	1.98	0.61	10	5	−1.52	0.13	12	10	0.00	0.24
7	4	0.44	0.31	10	6	0.45	0.55	12	11	0.20	0.11
7	5	0.10	0.01	10	7	0.76	0.20	12	12	0.00	0.00

[a] Anharmonicity constants computed assuming a resonance cutoff of 25 cm^{-1}.

[b] From treatment of small-amplitude motion only.

TABLE 3.4: Harmonic and fundamental frequencies for BH_3.

	cc-pCVQZ CCSD(T)[a]				Ref. 83[b]	Matrix isolation[c]				Gas phase
	$^{11}BH_3$	$^{11}BD_3$[d]	$^{10}BH_3$	$^{10}BD_3$[d]	$^{11}BH_3$	$^{11}BH_3$	$^{11}BD_3$	$^{10}BH_3$	$^{10}BD_3$	$^{11}BH_3$
ω_1 (a_1')	2575.4	1821.8	2575.4	1821.8	2568.3	--	--	--	--	--
ω_2 (a_2'')	1160.0	904.5	1172.3	920.3	1158.0	--	--	--	--	--
ω_3 (e')	2708.1	2026.8	2723.9	2048.7	2700.3	--	--	--	--	--
ω_4 (e')	1222.5	901.0	1228.4	906.9	1220.0	--	--	--	--	--
ν_1	2503.2	1767.3	2506.8	1767.0	2499.9	--	--	--	--	--
ν_2	1149.4	897.1	1161.3	912.5	1134.2	1129	879	1141	898	1147.5[e]
ν_3	2601.7	1965.4	2615.9	1985.7	2590.4	2587	1953	2601	1974	2601.6[f]
ν_4	1198.7	887.5	1204.2	893.2	1196.4	--	--	--	--	1196.7[e]
ZPVE	5724.6	4250.4	5751.7	4285.4	5704.0	--	--	--	--	--

[a] All-electron results from this work.
[b] *ab initio* results: pVQZ CCSD(T) harmonic; pVTZ CCSD(T) anharmonic.
[c] Ref. 11, fundamental frequencies observed in argon matrix at 20 – 27 K.
[d] (ν_1, $2\nu_2$) and (ν_1, $2\nu_4$) resonances removed for computation of fundamental frequencies.
[e] Gas phase IR results, Ref. 84.
[f] Gas phase IR results, Ref. 85.

TABLE 3.5: Fundamental frequencies for BH_5 [C_s(I)] (cm^{-1}).

Fundamental	This work				Experiment[a]			
	$^{11}BH_5$	$^{11}BD_5$	$^{10}BH_5$	$^{10}BD_5$	$^{n}BH_5$[b]	$^{n}BD_5$[b]	$^{10}BH_5$	$^{10}BD_5$
ν_1 (a')	3322	2418	3324	2419	--	--	--	--
ν_2 (a')	2513	1893	2525	1910	2475	1866	2488	1885
ν_3 (a')	2444	1775	2447	1787	--	--	--	--
ν_4 (a')	--	--	--	--	--	--	--	--
ν_5 (a')	1182	861	1185	869	--	--	--	--
ν_6 (a')	1171	861	1174	863	1134	883	1146	901
ν_7 (a')	--	--	--	--	--	---	--	--
ν_8 (a')	--	--	--	--	--	--	--	--
ν_9 (a'')	2555	1935	2569	1955	2544	--	2556	1936
ν_{10} (a'')	1170	842	1171	844	--	--	--	--
ν_{11} (a'')	1015	764	1022	770	--	--	--	--
ν_{12} (a'')	--	--	--	--	--	--	--	--
ZPVE	9793.7	7169.9	9823.9	7207.5	--	--	--	--

[a] Ref. 11.

[b] Index n refers to boron sample containing natural isotopic ratios of ^{11}B (80%) and ^{10}B (20%).

much weaker than the H-H bond in the hydrogen molecule, causing the H_2 subunit to remain more intact and the hydrogen scrambling barrier to be higher in BH_5, as compared to CH_5^+.

As shown in Table 3.4, the all-electron cc-pCVQZ CCSD(T) fundamentals for BH_3 compare extremely well to the gas-phase infrared frequencies,[84,85] as well as previous computational results.[83] The deviation of our results from experimental data for modes ν_2, ν_3, and ν_4 is only 1.9, 0.1 and 2.0 cm^{-1}, respectively. Matrix effects may be estimated using the BH_3 fundamentals assigned by Tague and Andrews,[11] which are presented in Table 3.4. One observes a distinct red-shift for the matrix fundamental frequencies of roughly 19 cm^{-1} for ν_2 and 15 cm^{-1} for ν_3 in comparison to the gas-phase results.

In their 1994 matrix-isolation study, Tague and Andrews[11] assigned the peaks at 2475.2 (1866.2) and 1134.3 (883.0) to BH_5 (BD_5) largely based on the general agreement with scaled *ab initio* harmonic frequencies.[10] The observed frequencies (identified here as the BH_5 ν_2 and ν_6 modes, respectively) correspond to vibrational modes predominantly localized on the BH_3 subunit and descendent from the degenerate stretch (e') and out-of-plane bend (a_2'') of isolated BH_3. Schreiner *et al.*[12] were in agreement with this assignment of ν_2 and ν_6 (based on scaled TZ2P CCSD(T) harmonic frequencies), and further noted that the frequency at 2544 cm^{-1}, assigned by Tague and Andrews to higher-order B_xH_y species, corresponded well with ν_9, the degeneracy-lifted companion frequency of ν_2. The assignments were further assessed by Watts and Bartlett,[13] who also noted the good agreement between the computed and observed fundamentals ν_2 and ν_9, but questioned the assignment of ν_6 based on a smaller computed $^{11}BH_5$ - $^{10}BH_5$ isotopic shift than observed experimentally.

Our anharmonic analysis strongly supports the previous experimental assignments of ν_2, as well as the correspondence of ν_9 (BH_5) to the observed frequency at 2544 cm^{-1}. First, the

infrared intensities in Table 3.2 reveal that ν_9 should be the strongest band of BH_5, about ⅓ more intense than ν_2. Thus, ν_9 absorptions should be observable if the nearby ν_2 band is seen. The computed BH_5 stretching fundamentals $\nu_2 = 2513$ and $\nu_9 = 2555$ cm^{-1} lie above the experimental absorptions by 38 and 11 cm^{-1}, respectively, and a substantial part of this difference can be attributed to a matrix red shift, which is 15 cm^{-1} for the antisymmetric stretch of BH_3. Therefore, accounting for SA anharmonicity and matrix effects reduces the disparity between theory and experiment for (ν_2, ν_9) of BH_5 from (+150, +125) cm^{-1} to only about (+23, −4) cm^{-1}. Pending full 12-dimensional variational vibrational analyses on a global BH_5 surface, this level of agreement should be considered excellent.

The theoretical isotopic shifts for the stretching fundamentals of BH_5 also lend remarkable support for the ν_2 and ν_9 assignments. Including anharmonicity, the computed $^{11}BH_5 \rightarrow {}^{10}BH_5$ blue shifts for (ν_2, ν_9) are (+12, +14) cm^{-1}, whereas the corresponding experimental shifts are (+13, +12) cm^{-1}. Similarly, the computed red shifts of ν_2 due to complete deuteration of $^{11}BH_5$ and $^{10}BH_5$ are 620 and 615 cm^{-1}, respectively, which differ by less than 2% from the corresponding experimental shifts of 609 and 603 cm^{-1}. Finally the computed $^{10}BH_5 \rightarrow {}^{10}BD_5$ red shift of ν_9 is 614 cm^{-1}, within 6 cm^{-1} of the observed value.

In contrast to the confirmation of the observed BH_5 stretching fundamentals, our anharmonic analysis further vitiates the set of experimental assignments for the BH_5 out-of-plane bending mode ν_6. For $^{11}BH_5$ the computed anharmonic frequency is 37 cm^{-1} above the measure absorption at 1134 cm^{-1}, but application of the observed matrix red shift $\nu_2(a_2'')$ of BH_3 reduces this disparity to only 19 cm^{-1}. This agreement by itself supports the experimental assignment ν_6 ($^{11}BH_5$). According to the data in Table 3.2, ν_6 is the fourth most intense IR band of $^{11}BH_5$, or about half the strength of ν_2, making the observation of ν_6 plausible. However, the isotopic

shifts within the set of experimental assignments once again raise serious doubts. The computed $^{11}BH_5 \rightarrow {}^{10}BH_5$ blue shift for ν_6 is 3 cm^{-1}, much smaller than the observed 12 cm^{-1} shift. Moreover, the computed red shift of ν_6 upon complete deuteration of ($^{11}BH_5$, $^{10}BH_5$) is (310, 311) cm^{-1}, substantially larger than the experimentally assigned shifts of (251, 245) cm^{-1}. In fact, the matrix-isolation absorptions assigned to ν_6 of $^{11}BD_5$ and $^{10}BD_5$ are 22 and 38 cm^{-1} *larger* than the theoretical gas-phase anharmonic fundamentals, counter to expectation and against the trends observed for the other frequencies of BH_5 and BH_3. In the face of these numerous inconsistencies, our anharmonic analysis leads us to question the ν_6 assignments of BH_5, particularly those of the BD_5 species.

An interesting question of chemical significance is the extent of splitting of the degenerate vibrational modes of BH_3 upon complexation with H_2. At the rigorous all-electron cc-pCVQZ CCSD(T) level, the harmonic frequencies of the paired bond stretches (ω_2, ω_9) and angle bends (ω_5, ω_{10}) of the BH_3 moiety of BH_5 are split by 44 and 14 cm^{-1}, respectively. Explicit consideration of SA anharmonicity has only a marginal effect on these splittings, decreasing both by 2 cm^{-1}. Thus, a model in which the degeneracy splitting within the BH_3 unit is reduced significantly by a large anharmonicity in the interfragment $BH_3 - H_2$ stretch does not seem to hold. Of course, full resolution of this issue must await large-scale investigations of the large-amplitude 12-dimensional vibrational dynamics of BH_5.

The BH_5 system is unique in that over ¾ of the binding energy relative to the lowest energy fragments is lost when ZPVE corrections are applied, leaving $D_0(BH_5 \rightarrow BH_3 + H_2) < 2$ kcal mol^{-1}. Accordingly, the anharmonicity of zero-point vibrations is an unusually important concern in establishing the thermochemistry of BH_5. Anharmonic zero-point vibrational

energies of BH_3 and BH_5 were computed using an expression recently derived from VPT2 by inclusion of the oft-neglected G_0 term:[86-89]

$$ZPVE = \frac{1}{2}\sum_i \omega_i - \frac{1}{32}\sum_{ijk} \frac{\phi_{iik}\phi_{jjk}}{\omega_k} - \frac{1}{48}\sum_{ijk} \frac{\phi_{ijk}^2}{\omega_i + \omega_j + \omega_k} + \frac{1}{32}\sum_{ij} \phi_{iijj} + Z_{kinetic}\ , \qquad (3.6)$$

where

$$Z_{kinetic} = -\frac{1}{4}\sum_{\alpha} B_\alpha^\circ \left[1 + \sum_{i>j} \left(\zeta_{ij}^\alpha\right)^2 \frac{\left[B_\alpha^\circ\left(\omega_i + \omega_j\right) - \left(\omega_i - \omega_j\right)^2\right]}{\omega_i \omega_j} \right]. \qquad (3.7)$$

This ZPVE expression is particularly appealing because it is devoid of resonance denominators. The resulting ZPVE values given by all-electron cc-pCVQZ CCSD(T) theory for BH_5, BH_3 and H_2 are 28.00, 16.37, and 6.21 kcal mol^{-1} respectively. For BH_5, the same $\phi_{ijk(l)}$ constants associated with the large-amplitude interfragment modes (ν_4, ν_7, ν_8, and ν_{12}) neglected in the determination of the fundamental frequencies were excluded from the ZPVE computation, with only the harmonic component of these modes included. This approximation will no doubt introduce some error into the BH_5 zero-point energy. However, only a 12-dimensional variational vibrational analysis will be able to fully capture the fluxional character of this species, and thus produce a better determination of the ZPVE.

3.5 Binding Energy Of BH_5

The dissociation energy of BH_5, as well as its equilibrium geometry, has been shown to exhibit a pronounced dependence on both the correlation treatment and basis set employed. In particular, the H_2 moiety has been observed to move in closer to the central boron atom as the size of the basis set is increased, especially through the addition of polarization functions.[10,12] Since a single r_e structure is employed in all focal point computations, care is required to ensure

that this structure is close to the true minimum. As shown in Table 3.1, successive all-electron CCSD(T) optimizations using the cc-pCV*X*Z family of basis sets, where X = D, T, and Q, produced r_e structures in which R_4 = 1.470, 1.414, and 1.406 Å, and R_5 = 1.487, 1.429, and 1.420 Å, respectively. The gradient extrapolation procedure described in Section 3.3 yields CBS (complete basis set) limit bond distances of 1.401 and 1.414 Å for R_4 and R_5, respectively. The all-electron CBS CCSD(T) structure of Table 3.1 was employed for all subsequent focal point analyses.

The lack of a minimum on the Hartree-Fock potential energy surface (PES) corresponding to BH_5 [C_s(I)] is demonstrated by the repulsive complete basis set (CBS) limit Hartree-Fock dissociation energy of −7.2 kcal mol^{-1} shown in Table 3.6. However, a sizable, positive MP2-R12/A correlation increment yields a BH_5 species stable with respect to $BH_3 + H_2$, with D_e = 6.4 kcal mol^{-1} at the CBS limit. While the higher-order δ[CCSD] and δ[CCSD(T)] increments exceed 1 kcal mol^{-1}, they largely cancel, and full CCSDTQ theory only adds 0.15 kcal mol^{-1} to the CCSD(T) binding energy. Thus, the valence focal point extrapolation result D_e = 6.179 kcal mol^{-1} is only a couple of tenths of a kcal mol^{-1} removed from the MP2 limit.

The separate focal point extrapolations (Table B.4)[53] for the core correlation effect on the D_e($BH_5 \rightarrow BH_3 + H_2$) exhibit definitive convergence past the 0.01 kcal mol^{-1} level and yield a significant 0.37 kcal mol^{-1} increase in the binding energy. As shown in Table 3.7, the one-electron relativistic contribution to D_e is −0.02 kcal mol^{-1}, whereas the DBOC shift for BH_5 is +0.06 kcal mol^{-1}. The final prediction for the classical dissociation energy is thus D_e = 6.62 kcal mol^{-1} for $^{11}BH_5$, or 6.59 for $^{11}BD_5$. It is fascinating that the bulk of the binding energy disappears when zero-point vibrations are considered. The anharmonic ZPVEs from Section 3.4

TABLE 3.6: Valence-only focal point extrapolations of reaction energies (kcal mol^{-1}).[a]

	ΔE_e[RHF]	$+\delta$[MP2]	$+\delta$[CCSD]	$+\delta$[CCSD(T)]	$+\delta$[CCSDT]	$+\delta$[CCSDTQ]	$=\Delta E_e$[CCSDTQ]
BH_5 [C_s(I)] $\rightarrow$ $BH_3 + H_2$							
cc-pVDZ	−7.227	11.199	−1.693	0.993	0.113	0.033	3.418
cc-pVTZ	−7.292	12.932	−1.987	1.473	0.111	[0.033]	[5.270]
cc-pVQZ	−7.262	13.411	−2.014	1.594	[0.111]	[0.033]	[5.873]
cc-pV5Z	−7.248	13.542	−2.021	1.628	[0.111]	[0.033]	[6.045]
cc-pV6Z	−7.244	13.603	[−2.028]	[1.642]	[0.111]	[0.033]	[6.117]
CBS limit	[−7.243]	[13.651][a]	[−2.036]	[1.663]	[0.111]	[0.033]	**[6.179]**
BH_5 [C_s(I)] $\rightarrow$ BH_5 [C_s(II)]							
cc-pVDZ	−0.045	0.113	−0.018	0.011	0.001	0.0002	0.062
cc-pVTZ	−0.046	0.100	−0.019	0.010	0.000	[0.0002]	[0.046]
cc-pVQZ	−0.049	0.108	−0.022	0.012	[0.000]	[0.0002]	[0.050]
cc-pV5Z	−0.049	0.112	−0.023	0.013	[0.000]	[0.0002]	[0.054]
cc-pV6Z	−0.049	0.113	[−0.022]	[0.013]	[0.000]	[0.0002]	[0.056]
CBS limit	[−0.049]	[0.118][a]	[−0.020]	[0.014]	[0.000]	[0.0002]	**[0.063]**
BH_5 [C_s(I)] $\rightarrow$ BH_5 [C_{2v}]							
cc-pVDZ	11.915	−5.881	0.884	−0.523	−0.038	0.0003	6.357
cc-pVTZ	11.969	−6.199	1.079	−0.672	−0.012	[0.0003]	[6.165]
cc-pVQZ	11.990	−6.289	1.108	−0.703	[−0.012]	[0.0003]	[6.094]
cc-pV5Z	11.988	−6.290	1.112	−0.710	[−0.012]	[0.0003]	[6.089]
cc-pV6Z	11.989	−6.298	[1.122]	[−0.712]	[−0.012]	[0.0003]	[6.089]
CBS limit	[11.989]	[−6.303][a]	[1.136]	[−0.716]	[−0.012]	[0.0003]	**[6.094]**
$BH_3 \rightarrow B + 3H$							
cc-pVDZ	229.768	32.971	1.106	0.390	−0.015	0.026	264.065
cc-pVTZ	233.796	40.949	0.829	0.675	−0.029	[0.026]	[276.245]
cc-pVQZ	234.244	43.394	0.517	0.741	[−0.029]	[0.026]	[278.892]
cc-pV5Z	234.348	44.185	0.277	0.760	[−0.029]	[0.026]	[279.566]
cc-pV6Z	234.361	44.549	[0.156]	[0.768]	[−0.029]	[0.026]	[279.831]
CBS limit	[234.364]	[45.049][b]	[−0.009]	[0.780]	[−0.029]	[0.026]	**[280.179]**
Function	$A + be^{-cX}$	MP2R12	$a + bX^{-3}$	$a + bX^{-3}$	add	add	
Points, X	(4,5,6)	--	(4,5)	(4,5)	--	--	

[a] All reference structures correspond to ∞(CBS) geometries listed in Table 3.1.

[a] The corresponding $X = 5, 6$ extrapolations for these increments are 13.687, 0.113, and −6.310 kcal mol^{-1}, for the dissociation, internal rotation and hydrogen scrambling reactions, respectively.

[b] CBS limit increment obtained via $X = 5, 6$ extrapolation using two parameter fit.

TABLE 3.7: Contributions to the dissociation energy of BH_5 [C_s(I)] (kcal mol^{-1}).

ΔE_{fp}(FC)	ΔE_{fp}(core)	ΔRel.	ΔDBOC[b]	ΔE_e[b]	ΔZPVE[a,b]	ΔE_0[b]
BH_5 [C_s(I)] → $BH_3 + H_2$						
+6.179	+0.365	−0.016	+0.055	+6.615	−5.434	+1.181
			+0.028	+6.588	−3.871	+2.717
BH_5 [C_s(I)] → BH_5 [C_s(II)]						
+0.063	+0.005	+0.000	+0.000	+0.068	−0.224	−0.156
			+0.000	+0.068	+0.039	+0.107
BH_5 [C_s(I)] → BH_5 [C_{2v}]						
+6.094	−0.267	+0.004	−0.017	+5.814	−0.500	+5.314
			−0.009	+5.822	−0.121	+5.701
BH_3 → B +3H						
+280.179	+1.232	−0.021	−0.019	281.371	−16.363	+265.008
			−0.010	281.380	−12.150	+269.230

[a] Anharmonic ZPVE computed using full quartic force-field computed at the cc-pCVQZ CCSD(T) level of theory (see text for details). ΔZPVE for H_2 internal rotation and hydrogen scrambling taken from harmonic frequencies of BH_5 structures.

[b] Results in top row are for isotopomers comprised exclusively of H atoms, bottom row for species involving D atoms only.

yield a 5.43 kcal mol^{-1} reduction in D_e for $^{11}BH_5$, or a 3.87 kcal mol^{-1} decrease for $^{11}BD_5$. In conclusion, our final predictions for D_0 are 1.2 kcal mol^{-1} for $^{11}BH_5$ and 2.7 kcal mol^{-1} for $^{11}BD_5$. The former value lies in the middle of the range of recently computed, but less definitive values (0.9 – 1.4 kcal mol^{-1})[10,12,13,20] for $^{11}BH_5$.

In order to determine $\Delta_f H_0^\circ(BH_5)$ from the dissociation reaction, $\Delta_f H_0^\circ(BH_3)$ is required. The computation of the BH_3 enthalpy of formation by means of a complete atomization route is detailed in the focal point layout in Table 3.6. The convergence of the correlation increments in the table is compelling, as CCSD(T) and CCSDTQ theory agree on the atomization energy to 0.01 kcal mol^{-1}. Employing the auxiliary corrections shown in Table 3.7 yields a final atomization energy of ΔE_0 = 265.01 kcal mol^{-1}.

While the error in our computed atomization energy should not exceed 0.2 kcal mol^{-1}, the accuracy of $\Delta_f H_0^\circ(BH_3)$ is limited by uncertainty in the enthalpy of formation of gaseous elemental boron. The current CODATA listing[90] is $\Delta_f H_0^\circ(B)$ = 133.8 ± 1.2 kcal mol^{-1}, which is identical to the Gurvich[91] recommendation based on a review of five measurements[92-96] over the period 1964 – 1991. A more recent value[97] of 135.1 kcal mol^{-1}, with error bars of ± 0.75 kcal mol^{-1} or less, has been determined from the empirical enthalpy of formation[90] of BF_3(g) [−271.2 ± 0.2 kcal mol^{-1}] by means of high-level *ab initio* computations[97,98] of the atomization energy of boron trifluoride. Employing an accurately known value of $\Delta_f H_0^\circ(H)$ [51.633 ± 0.001 kcal mol^{-1}],[90] our computed atomization energy yields $\Delta_f H_0^\circ(BH_3)$ = −110.10 kcal mol^{-1} + $\Delta_f H_0^\circ(B)$. If the CODATA enthalpy of formation for boron is used, one obtains $\Delta_f H_0^\circ(BH_3)$ = 23.70 ± 1.3 kcal mol^{-1} (with the errors taking into account both experimental and theoretical uncertainties), while substituting the value for Ref. 97 yields $\Delta_f H_0^\circ(BH_3)$ = 25.00 ± 1.0 kcal mol^{-1}. This shift is quite substantial. However, both values are in broad agreement with previous experimental

[$\Delta_f H_0^\circ(BH_3)$ = 25.8 ± 1.7 kcal mol^{-1}][99] and theoretical (25.8 ± 0.7 kcal mol^{-1})[100] studies. The final enthalpy of formation of BH_5 is given by $\Delta_f H_0^\circ(BH_5)$ = −111.26 ± 0.2 kcal mol^{-1} + $\Delta_f H_0^\circ(B)$, which upon the application of the CODATA and alternative values[97] of $\Delta_f H_0^\circ(B)$ yields $\Delta_f H_0^\circ(BH_5)$ = 22.54 ± 1.3 and 23.84 ± 1.0 kcal mol^{-1}, respectively.

3.6 Barrier To H_2 Rotation

As discussed in Section 3.4, the small barrier to rotation of the H_2 moiety leads to large amplitude BH_3 – H_2 interfragment modes for which second-order vibrational perturbation theory (VPT2) is not applicable. Given the miniscule energy differences (≤ 0.2 kcal mol^{-1}) between the C_s(I) and C_s(II) structures, previous *ab initio* studies[10,12] have been unable to determine the H_2 barrier to rotation with certainty. Clearly, the H_2 unit is essentially a free rotor, even at low temperature. Focal point analysis provides a rigorous framework on which energy differences of this scale may be accurately resolved.

The diminutive barrier for H_2 internal rotation, constituted by the C_s(II) structure, is analyzed in Table 3.6. First, note that Hatree-Fock theory places the C_s(II) structure 0.05 kcal mol^{-1} *below* the C_s(I) complex. While the addition of electron correlation reverses the HF energetic ordering, only the δ[MP2] increment is larger than 0.1 kcal mol^{-1}. The higher-order δ[CCSD(T)] and δ[CCSDTQ] corrections are less than 0.0005 kcal mol^{-1}! The rate of convergence of the H_2 internal rotation barrier with respect to both the one- and *N*-particle expansions is indeed striking, due to the lack of differential correlation effects between the C_s(I) and C_s(II) forms. As shown in Table 3.7, core correlation raises the H_2 internal rotation barrier a mere +0.01 kcal mol^{-1}, and the relativistic and DBOC corrections are inconsequential. The final focal point result is ΔE_e[CCSDTQ] = 0.063 kcal mol^{-1}, an incredibly small barrier.

The harmonic zero-point vibrational energy in the ν_{12} mode of the C_s(I) minimum is 0.27 kcal mol^{-1} for the $^{11}BH_5$ isotopomer, an amount easily exceeding the 0.07 kcal mol^{-1} classical barrier. If complementary vibrations are assumed to behave adiabatically, the effective one-dimensional barrier for H_2 internal rotation remains minute (+0.12 kcal mol^{-1}). If zero-point effects are evaluated in the traditional manner by simply excluding the imaginary frequency in the transition state, a negative barrier (−0.15 kcal mol^{-1}) is obtained, again suggesting that in the vibrational ground state, the H_2 internal rotation barrier is readily surmounted. Upon complete deuteration, the situation changes, as shown by the positive ΔE_0 = +0.11 kcal mol^{-1} entry in Table 3.7.

3.7 Hydrogen Scrambling In BH_5

The mechanism for hydrogen scrambling in the BH_5 intermediate has been long posited to proceed via the C_{2v} transition state shown in Figure 3.1. However, the difficulty with this proposed pathway is that the C_{2v} structure lies substantially above the BH_5 dissociation energy. In order to accurately evaluate this mechanism the barrier height of the C_{2v} transition state must first be conclusively determined.

As shown in Table 3.1, the C_{2v} geometric structure exhibits much weaker basis set dependence than the two C_s forms. For example, the differences in the cc-pCVQZ and CBS CCSD(T) bond distances and angles do not exceed 0.002 Å and 0.1°, respectively. In the hydrogen-scrambling transition state, the H_2 distance is elongated by almost 0.3 Å and the interfragment distances R_4 and R_5 are shortened by roughly 0.15 Å relative to the C_s(I) minimum.

Table 3.6 gives the valence focal-point results for the C_{2v} hydrogen-scrambling barrier. The differential correlation effects for this barrier are smaller than those observed for the BH_5 →

$BH_3 + H_2$ dissociation; in particular, δ[MP2], δ[CCSD], and δ[CCSD(T)] for the $C_s(I) \rightarrow C_{2v}$ transformation are all about half their corresponding magnitude for the $C_s(I)$ dissociation. Full CCSDTQ theory changes the CCSDT result by only 0.0003 kcal mol^{-1}. Thus, with some confidence we conclude that the valence focal point limit is 6.1 ± 0.1 kcal mol^{-1}. Upon addition of the auxiliary corrections given in Table VII, the final barrier predictions are ΔE_e = 5.81 (5.82) kcal mol^{-1} and ΔE_0 = 5.31 (5.70) kcal mol^{-1} for $^{11}BH_5$ ($^{11}BD_5$). Therefore, the C_{2v} hydrogen scrambling transition state lies 4.1 kcal mol^{-1} above the dissociation energy of BH_5, but only 3.0 kcal mol^{-1} above the BD_5 limit.

Recent variational transition state theory (VTST) computations[21] determined that tunneling effects play an important role in the scrambling rate of BH_5. Utilizing MCCMs[18] to compute the potential energy surfaces yielded $D_e(BH_5 \rightarrow BH_3 + H_2)$ = 5.76 kcal mol^{-1} and a classical hydrogen scrambling barrier of 5.71 kcal mol^{-1}.[21] At 300 K the rate of unimolecular dissociation of BH_5 was found to be three orders of magnitude larger than that for hydrogen scrambling. While the hydrogen scrambling barrier utilized in the VTST computations is in very good agreement with the results presented here, the dissociation energy is almost 1 kcal mol^{-1} smaller than our focal point result. Therefore the relative rate of hydrogen scrambling with respect to dissociation may actually be larger than determined in the VTST study.

The barrier to hydrogen scrambling in CH_5^+ is significantly smaller than that of isoelectronic BH_5. The CCSD(T)-R12 computed barrier[80] of $V_e^{\ddagger}$ = 0.82 kcal mol^{-1} is much smaller than the dissociation energy, D_e = 48 kcal mol^{-1}. In fact, inclusion of harmonic zero-point vibrational effects inverts the energetic ordering of the $C_s(I)$ and C_{2v} structures.[80] A recent 12-dimensional dynamics study[82] has determined CH_5^+ bond length distributions by employing both diffusion Monte Carlo methods and classical molecular dynamics simulations. The

distributions are in qualitative internal agreement and indicate that the effective dynamical structure of CH_5^+ is comprised of CH_3^+ and H_2 subunits, as represented by the C_s(I) minimum.

3.8 SUMMARY

The limits of ab initio electronic structure have been approached to the subchemical accuracy regime (0.1 kcal mol^{-1}) in characterizing the highly anharmonic BH_5 potential energy surface. The geometric parameters of the key stationary points have been fully optimized at the extrapolated, complete basis set (CBS) all-electron CCSD(T) level of theory. Focal point determinations of the prominent energetic features have been performed using both correlation-consistent cc-p(C)V*X*Z (X = 2-6) basis set extrapolations and explicitly-correlated R12 computations, conjoined with coupled-cluster theory extending through complete quadruple excitations (CCSDTQ). The BH_5 species adopts a C_s(I) structure of $BH_3 - H_2$ type, as shown in Figure 1. The C_s(I) minimum of BH_5 lies 6.6 ± 0.1 kcal mol^{-1} below the lowest-energy $BH_3 + H_2$ fragments. Strikingly, the bulk of this binding energy is lost when zero-point vibrational energy is included; specifically, D_0 = 1.2 kcal mol^{-1} for the parent isotopomer $^{11}BH_5$, with inclusion of anharmonicity estimates. Within the $BH_3 - H_2$ well, the H_2 moiety is essentially a free rotor, exhibiting a minute classical barrier to internal rotation of 0.07 ± 0.01 kcal mol^{-1}. In contrast the transition state for hydrogen scrambling lies 5.81 ± 0.05 kcal mol^{-1} above the C_s(I) minimum, or 0.82 ± 0.10 kcal mol^{-1} below the $BH_3 + H_2$ fragments. However, when zero-point vibrational effects are accounted for, the hydrogen scrambling barrier is pushed to 4.2 kcal mol^{-1} above the dissociation asymptote. Certainly the BH_5 system will display a wealth of fascinating, large-amplitude quantum dynamics if subjected to a full 12-dimensional variational vibrational analysis on a global potential energy surface. The essential thermochemical results of our study

are $\Delta_f H_0^\circ[BH_3] = -110.10 \pm 0.20$ kcal mol^{-1} + $\Delta_f H_0^\circ[B_{(g)}]$ and $\Delta_f H_0^\circ[BH_5] = -111.26 \pm 0.20$ kcal mol^{-1} + $\Delta_f H_0^\circ[B_{(g)}]$. If the enthalpy of formation of gaseous boron is taken as $\Delta_f H_0^\circ[B_{(g)}] = 133.8 \pm 1.2$ kcal mol^{-1},[90] then our results yield $\Delta_f H_0^\circ[BH_3] = 23.70 \pm 1.3$ kcal mol^{-1} and $\Delta_f H_0^\circ[BH_5] = 22.54 \pm 1.3$ kcal mol^{-1}.

An anharmonic vibrational analysis of the interfragment ($BH_3 - H_2$) fundamental frequencies of BH_5 and its isotopomers has been performed on the basis of a complete quartic force field computed at the all-electron cc-pCVQZ CCSD(T) level of theory. For BH_3 this approach yields fundamental frequencies within 2 cm^{-1} of the high resolution gas-phase spectroscopic values for the infrared-active modes. For the BH_5 system there exist four interfragment modes (ν_4, ν_7, ν_8, and ν_{12}) whose internal anharmonicities and coupling to small-amplitude intrafragment vibrations will require rigorous full-dimensional variational vibrational treatments. Nonetheless, our anharmonic treatment of intrafragment vibrations provides compelling assessments of the matrix-isolation assignments on which the experimental identification of the BH_5 intermediate was made. For the antisymmetric B-H stretching fundamentals of the BH_3 moiety, the assignment of (ν_2, ν_9) = (2475, 2544) cm^{-1} is supported by both small absolute deviations of (+23, –4) cm^{-1} with respect to theory, as well as excellent agreement between theory and experiment for $^{11}B \rightarrow {}^{10}B$ and $H \rightarrow D$ isotopic shifts. For the out-of-plane bending mode of the BH_3 unit, the observed peak at 1134 cm^{-1} is within 19 cm^{-1} of our predicted ν_2 fundamental of $^{11}BH_5$. However, as noted previously,[13] the $^{11}B \rightarrow {}^{10}B$ and $H \rightarrow D$ isotopic shifts in the experimentally assigned frequencies are brought into serious question by theory. The vibrational spectroscopy of BH_5 across the full infrared region is a rich and largely unexplored area which presents many challenges for both current experimental techniques and first-principles theoretical methods.

3.9 Acknowledgments

The research presented here was supported by the U. S. Department of Energy, Office of Basic Energy Sciences, by both the Combustion Program (Grant No. DE-FG02-00ER14748) and the Chemical Sciences, Geosciences and Biosciences Division (Grant No. DE-FG02-01ER15226). The authors thank Professors Lester Andrews, Peter Schreiner, and Attila Császár for helpful discussions.

References

1 R. E. Mesmer and W. L. Jolly, Inorg. Chem. **1**, 608 (1962).

2 A. N. Well, J. T. New, and K. S. Pitzer, J. Chem. Phys. **17**, 1007 (1964).

3 M. M. Kreevoy and J. E. C. Hutchins, J. Am. Chem. Soc. **94** (1972).

4 H. H. Michels, F. E. Harris, and J. B. Addison, Int. J. Quantum Chem. Symp. **4**, 149 (1971).

5 G. A. Olah, P. W. Westerman, Y. K. Mo, and G. Klopman, J. Am. Chem. Soc. **94**, 7859 (1972).

6 J. A. Pople and G. A. Segal, J. Chem. Phys. **44**, 3289 (1966).

7 C. Hoheisel and W. Kutzelnigg, J. Am. Chem. Soc. **97**, 6970 (1975).

8 J. B. Collins, P. v. R. Schleyer, J. S. Binkley, J. A. Pople, and L. Radom, J. Am. Chem. Soc. **98**, 3436 (1976).

9 I. M. Pepperberg, T. A. Halgren, and W. N. Lipscomb, J. Am. Chem. Soc. **98**, 3442 (1976).

10 J. F. Stanton, W. N. Lipscomb, and R. J. Bartlett, J. Am. Chem. Soc. **111**, 5173 (1989).

11 T. J. Tague and L. Andrews, J. Am. Chem. Soc. **116**, 4970 (1994).

12 P. R. Schreiner, H. F. Schaefer, and P. v. R. Schleyer, J. Chem. Phys. **101**, 7625 (1994).

13 J. D. Watts and R. J. Bartlett, J. Am. Chem. Soc. **117**, 825 (1995).

[14] S. Fau and G. Frenking, Mol. Phys. **96**, 519 (1999).

[15] R. Custelcean, J. Mol. Struct. **505**, 95 (2000).

[16] B. S. Jursic, J. Mol. Struct. **492**, 97 (1999).

[17] B. S. Jursic, J. Mol. Struct. **505**, 67 (2000).

[18] P. L. Fast, J. C. Corchado, M. L. Sanchez, and D. G. Truhlar, J. Phys. Chem. A **103**, 5129 (1999).

[19] P. L. Fast, M. L. Sanchez, and D. G. Truhlar, Chem. Phys. Lett. **306**, 407 (1999).

[20] Y. Kim, J. Kim, and K. H. Kim, J. Phys. Chem. A **107**, 301 (2003).

[21] K. H. Kim and Y. Kim, J. Chem. Phys. **120**, 623 (2004).

[22] W. D. Allen, A. L. L. East, and A. G. Császár, in *Structures and Conformations of Non-Rigid Molecules*, edited by J. Laane, M. Dakkouri, B. van der Vecken, and H. Oberhammer (Kluwer, Dordrecht, 1993), pp. 343.

[23] A. L. L. East and W. D. Allen, J. Chem. Phys. **99**, 4638 (1993).

[24] A. G. Császár, W. D. Allen, and H. F. Schaefer III, J. Chem. Phys. **108**, 9751 (1998).

[25] A. G. Császár, G. Tarczay, M. L. Leininger, O. L. Polyansky, J. Tennyson, and W. D. Allen, in *Spectroscopy from Space*, edited by J. Demaison and K. Sarka (Kluwer, Dordrecht, 2001), pp. 317.

[26] J. M. Gonzales, C. Pak, R. S. Cox, W. D. Allen, H. F. Schaefer, G. Tarczay, and A. G. Császár, Chem. Eur. J. **9**, 2173 (2003).

[27] D. Feller, J. Chem. Phys. **98**, 7059 (1993).

[28] T. Helgaker, W. Klopper, H. Koch, and J. Noga, J. Chem. Phys. **106**, 9639 (1997).

[29] T. H. Dunning, Jr., J. Chem. Phys. **90**, 1007 (1989).

[30] R. A. Kendall, T. H. Dunning, Jr., and R. J. Harrison, J. Chem. Phys. **96**, 6796 (1992).

[31] A. K. Wilson, T. van Mourik, and T. H. Dunning, Jr., J. Mol. Struct. (Theochem) **388**, 339 (1996).

[32] C. C. J. Roothaan, Rev. Mod. Phys. **23**, 69 (1951).

[33] W. J. Hehre, L. Radom, P. v. R. Schleyer, and J. A. Pople, *Ab initio molecular orbital theory*. (Wiley-Interscience, New York, 1986).

[34] A. Szabo and N. S. Ostlund, *Modern Quantum Chemistry: Introduction to Advanced Electronic Structure Theory*, 1st edition, revised ed. (McGraw-Hill, New York, 1989).

[35] C. Møller and M. S. Plesset, Phys. Rev. **46**, 618 (1934).

[36] J. A. Pople, J. S. Binkley, and R. Seeger, Int. J. Quant. Chem. Symp. **10**, 1 (1976).

[37] G. D. Purvis and R. J. Bartlett, J. Chem. Phys. **76**, 1910 (1982).

[38] G. E. Scuseria, A. C. Scheiner, T. J. Lee, J. E. Rice, and H. F. Schaefer III, J. Chem. Phys. **86**, 2881 (1987).

[39] G. E. Scuseria, C. L. Janssen, and H. F. Schaefer, J. Chem. Phys. **89**, 7382 (1988).

[40] K. Raghavachari, G. W. Trucks, J. A. Pople, and M. Head-Gordon, Chem. Phys. Lett. **157**, 479 (1989).

[41] G. E. Scuseria and T. J. Lee, J. Chem. Phys. **93**, 5851 (1990).

[42] J. Noga and R. J. Bartlett, J. Chem. Phys. **86**, 7041 (1987).

[43] J. Noga and R. J. Bartlett, J. Chem. Phys. **89**, 3401 (1988).

[44] M. Kállay and P. R. Surján, J. Chem. Phys. **113**, 1359 (2000).

[45] M. Kállay and P. R. Surján, J. Chem. Phys. **115**, 2945 (2001).

[46] M. Kállay, P. G. Szalay, and P. R. Surján, J. Chem. Phys. **117**, 980 (2002).

[47] W. Klopper and W. Kutzelnigg, Chem. Phys. Lett. **134**, 17 (1987).

[48] W. Kutzelnigg and W. Klopper, J. Chem. Phys. **94**, 1985 (1991).

[49] W. Klopper and C. C. M. Samson, J. Chem. Phys. **116**, 6397 (2002).

[50] E. F. Valeev and H. F. Schaefer, J. Chem. Phys. **113**, 3990 (2000).

[51] E. F. Valeev, W. D. Allen, H. F. Schaefer, and A. G. Császár, J. Chem. Phys. **114**, 2875 (2001).

[52] D. E. Woon and T. H. Dunning, Jr., J. Chem. Phys. **103**, 4572 (1995).

[53] See Appendix B for Hartree-Fock and correlated gradient extrapolation formulas; quadratic, cubic, and quartic force constants of the C_s(I) BH_5 minimum; and focal point extrapolations of the core correlation effect for the reactions shown in Table 3.7.

[54] N. C. Handy, Y. Yamaguchi, and H. F. Schaefer, J. Chem. Phys. **84** (1986).

[55] A. G. Ioannou, R. D. Amos, and N. C. Handy, Chem. Phys. Lett. **251**, 52 (1996).

[56] N. C. Handy and A. M. Lee, Chem. Phys. Lett. **252**, 425 (1996).

[57] E. F. Valeev and C. D. Sherrill, J. Chem. Phys. **118**, 3921 (2003).

[58] S. A. Perera and R. J. Bartlett, Chem. Phys. Lett. **216**, 606 (1993).

[59] K. Balasubramanian, *Relativistic Effects in Chemistry: Part A, Theory and Techniques*. (Wiley, New York, 1997).

[60] K. Balasubramanian, *Relativistic Effects in Chemistry: Part B, Applications*. (Wiley, New York, 1997).

[61] R. D. Cowan and D. C. Griffin, J. Opt. Soc. Am. **66**, 1010 (1976).

[62] G. Tarczay, A. G. Császár, W. Klopper, and H. M. Quiney, Mol. Phys. **99**, 1769 (2001).

[63] J. F. Stanton, J. Gauss, W. J. Lauderdale, J. D. Watts, and R. J. Bartlett, ACES II Stanton version.

[64] T. D. Crawford, C. D. Sherrill, E. F. Valeev, J. T. Fermann, M. L. Leininger, R. A. King, S. T. Brown, C. L. Janssen, E. T. Seidl, Y. Yamaguchi, W. D. Allen, C. B. Kellogg, and H. F. S. III, (2002).

[65] H. H. Nielsen, Rev. Mod. Phys. **23**, 90 (1951).

[66] J. K. G. Watson, in *Vibrational Spectra and Structure*, edited by J. R. Durig (Elsevier, Amsterdam, 1977), Vol. 6, pp. 1.

[67] D. Papoušek and M. R. Aliev, *Molecular Vibrational-Rotational Spectra*. (Elsevier, Amsterdam, 1982).

[68] INTDIF2004 is an abstract program written by Wesley D. Allen for *Mathematica* (Wolfram Research, Inc., Champaign, Illinois) to perform general numerical differentiations to high orders of electronic structure data.

[69] INTDER is a general program written by W. D. Allen which performs sundry vibrational analyses and higher-order nonlinear transformations among force field representations.

[70] W. D. Allen and A. G. Császár, J. Chem. Phys. **98**, 2983 (1993).

[71] W. D. Allen, A. G. Császár, V. Szalay, and I. M. Mills, Mol. Phys. **89**, 1213 (1996).

[72] see program descriptions in K. Sarka and J. Demaison, in *Computational Molecular Spectroscopy*, edited by P. Jensen and P. R. Bunker (Wiley, Chichester, 2000), pp. 255

[73] P. Pulay and F. Török, Acta Chim. Acad. Sci. Hung. **44**, 287 (1965).

[74] W. D. Allen, A. G. Császár, and D. A. Horner, J. Am. Chem. Soc. **114**, 6834 (1992).

[75] W. H. Shaffer, H. H. Nielsen, and L. H. Thomas, Phys. Rev. **56**, 895 (1939).

[76] I. M. Mills, in *Molecular Spectroscopy: Modern Research*, edited by K. N. Rao and C. W. Mathews (Academic Press, New York, 1972), Vol. 1, pp. 115.

[77] D. A. Clabo, Jr., W. D. Allen, R. B. Remington, Y. Yamaguchi, and H. F. Schaefer, Chem. Phys. **123**, 187 (1988).

[78] P. R. Schreiner, Angew. Chem. Int. Ed. **39**, 3239 (2000).

[79] P. R. Schreiner, S.-J. Kim, H. F. Schaefer, and P. v. R. Schleyer, J. Chem. Phys. **99**, 3716 (1993).

[80] H. Müller, W. Kutzelnigg, J. Noga, and W. Klopper, J. Chem. Phys. **106**, 1863 (1997).

[81] D. Marx and M. Parrinello, Z. Phys. D **41**, 253 (1997).

[82] A. B. McCoy, B. J. Braams, A. Brown, X. Huang, Z. Jin, and J. M. Bowman, J. Phys. Chem. A **108**, 4991 (2004).

[83] J. M. L. Martin and T. J. Lee, Chem. Phys. Lett. **200**, 502 (1992).

[84] K. Kawaguchi, J. Chem. Phys. **96**, 3411 (1992).

[85] K. Kawaguchi, Can. J. Phys. **72**, 925 (1994).

[86] J. L. Dunham, Phys. Rev. **41**, 721 (1932).

[87] I. N. Levine, *Molecular Spectroscopy*. (Allyn and Bacon, Boston, 1970).

[88] R. D. Levine and S.-F. Wu, Chem. Phys. Lett. **11**, 557 (1971).

[89] W. H. Shaffer and R. P. Schuman, J. Chem. Phys. **12**, 504 (1944).

[90] J. D. Cox, D. D. Wagman, and V. A. Medvedev, *CODATA Key Values for Thermodynamics*. (Hemisphere Publishing Corp., New York, 1989).

[91] *Thermodynamic properties of individual substances*, edited by L. V. Gurvich, I. V. Veyts, and C. B. Alcock (CRC Press, Boca Raton, FL, 1994).

[92] H. E. Robson and P. W. Gilles, J. Phys. Chem. **68**, 983 (1964).

[93] D. L. Hildenbrand and W. F. Hall, J. Phys. Chem. **68**, 989 (1964).

[94] R. W. Mar and R. G. Bedford, High Temp. Sci. **8**, 365 (1976).

[95] E. Storms and B. Mueller, J. Phys. Chem. **81**, 318 (1977).

[96] P. C. Nordine, J. K. R. Weber, S. Krishnan, and R. A. Schiffman, High Temp. Sci. **30**, 163 (1991).

[97] C. W. Bauschlicher, J. M. L. Martin, and P. R. Taylor, J. Phys. Chem. A **103**, 7715 (1999).

[98] J. M. L. Martin and P. R. Taylor, J. Phys. Chem. A **102**, 2995 (1998).

[99] B. Ruscic, C. A. Mayhew, and J. Berkowitz, J. Chem. Phys. **88**, 5580 (1988).

[100] D. Feller, D. A. Dixon, and K. A. Peterson, J. Phys. Chem. A **102**, 7053 (1998).

CHAPTER 4

THE EXTRAPOLATED COMPLETE BASIS SET LIMIT QUARTIC FORCE FIELD OF BH_3[1]

[1] Schuurman, M. S.; Allen, W. D.; Schaefer, H. F. To be submitted to the *Journal of Molecular Spectroscopy*.

4.1 ABSTRACT

Ab initio quartic force fields have been computed for BH_3 using high levels of electronic structure theory, including extrapolated complete basis set (CBS) limit CCSD(T) (coupled-cluster singles and doubles with perturbative triples). Conventional quartic force fields, determined using a single basis set, were obtained employing core-valence correlation-consistent basis sets of the form cc-pCV*X*Z (*X* = T, Q, 5) and all-electron CCSD(T) theory via displacements about stationary point reference structures. In addition, CBS limit CCSD(T) force constants were evaluated via the extrapolation of electronic energies at each requisite displaced geometry. The reference structure (r_e = 1.18642 Å) for this force field was optimized using gradient extrapolation formulas derived from widely employed correlation-consistent basis set energy functional forms. The extrapolated CCSD(T) quartic force field yielded vibrational frequencies given by ν_1 = 2502.5 cm^{-1}, ν_2 = 1147.4 cm^{-1}, ν_3 = 2602.7 cm^{-1}, and ν_4 = 1196.3 cm^{-1}. These results are in excellent agreement with spectroscopic gas-phase fundamentals, displaying a mean absolute error with experiment of only 0.5 cm^{-1}.

4.2 INTRODUCTION

Experimental detection of borane (BH_3), the simplest of the boron hydrides, was long hindered by its high reactivity. BH_3 is a powerful reducing agent and plays a central role in many families of reactions, particularly the reduction of multiple bonds.[1-4] The earliest spectroscopic observation of BH_3 was achieved by Kaldor and Porter[5], who were able to isolate borane produced by BH_3CO pyrolysis in an argon matrix. The IR-active ν_2, ν_3, and ν_4 fundamental frequencies were assigned as 1125, 2808, and 1604 cm^{-1}, respectively. However, the gas-phase infrared spectrum wasn't observed until 1987, when Kawaguchi *et al.*[6] detected

BH_3 produced by the photolysis of B_2H_6 and BH_3CO using infrared diode laser spectroscopy. The authors analyzed the rotational structure of the ν_2 band (out-of-plane bending mode) and were able to determine ν_2 = 1140.88 cm^{-1}, nearly 16 cm^{-1} larger than the matrix-isolation result.

These early experimental studies were followed by a number of *ab initio* investigations in which optimized r_e structures and harmonic frequencies were computed employing a number of electronic structure methods of varying sophistication, including the CEPA[7], Møller-Plesset perturbation theory,[8] configuration interaction,[9] and coupled-cluster methods.[8,9] While none of these studies explicitly considered anharmonic effects, the computed harmonic frequencies displayed only a moderate dependence on the level of theory employed.

In 1992, Kawaguchi[10] returned to the vibrational spectrum of BH_3, this time studying the ν_3 (degenerate stretch) mode via FT-IR (Fourier transform infrared) spectroscopy. Upon analysis of these results, vibrational and rotational parameters were determined for the both the excited ν_3 and ground vibrational states, with the $^{11}BH_3$ ($^{10}BH_3$) vibrational fundamentals given by ν_3 = 2601.57 (2615.79) cm^{-1}, and the vibrationally averaged B – H bond distance by r_0 = 1.9001(1) Å. That same year, Martin and Lee[11] determined the first *ab initio* fundamental frequencies employing a quartic force field computed using coupled-cluster methods and correlation-consistent basis sets. Their frozen-core cc-pVQZ CCSD(T) harmonic force field and cc-pVTZ CCSD(T) anharmonic force field results were in good agreement with the observed ν_2 and ν_3 modes, with the vibrational fundamentals ν_1, ν_2, ν_3, and ν_4 computed to be 2494.9, 1134.2, 2587.5, and 1196.4 cm^{-1}, respectively.

In 1994, Kawaguchi[12] reported both the observation of the ν_4 (degenerate angle bend) band, as well as revised results for the ν_2 band using FT-IR spectroscopy. The vibrational fundamental frequencies were given as ν_4 = 1196.66 cm^{-1} and ν_2 = 1147.50 cm^{-1}. Most recently,

variationally computed rovibrational energy levels of BH_3 were reported by Schwenke,[13] who employed a potential energy function derived from the quartic force field of Martin and Lee. The vibrational band origins displayed a small degree of deviation from the earlier VPT2 (second-order vibrational perturbation theory)[14-16] results of Martin and Lee, with the reported fundamentals ν_1, ν_2, ν_3, and ν_4 given by 2491.9, 1148.1, 2591.5, and 1199.1 cm^{-1}, respectively.

The current study aims to compute definitive *ab initio* vibrational and rotational constants via VPT2. This investigation will employ both large, single basis set CCSD(T) geometries and force constants, we well as investigating the efficacy of employing extrapolated CBS limit CCSD(T) geometries and force fields to compute spectroscopic parameters.

4.3 Quartic Force Field

The six symmetrized internal coordinates used for this study are identical to those employed to describe the BH_3 localized modes of BH_5 in Chapter 3. Shown below,

$$S_1(a_1') = \frac{r_1 + r_2 + r_3}{\sqrt{3}} \quad \text{(symmetric stretch.)} \qquad S_4(e') = \frac{2\theta_1 - \theta_2 - \theta_3}{\sqrt{6}} \quad \text{(asymmetric bend)}$$

$$S_2(a_2'') = \frac{\gamma_1 + \gamma_2 + \gamma_3}{\sqrt{3}} \quad \text{(out-of-plane bend)} \qquad S_5(e') = \frac{r_2 - r_3}{\sqrt{2}} \quad \text{(asymmetric stretch)}$$

$$S_3(e') = \frac{2r_1 - r_2 - r_3}{\sqrt{6}} \quad \text{(asymmetric stretch)} \qquad S_6(e') = \frac{\theta_2 - \theta_3}{\sqrt{2}} \quad \text{(asymmetric bend}$$

these coordinates are also consistent with previous *ab initio* studies.[11] In the above definitions, r_i is the B – H_i internuclear distance, θ_i is the bond angle opposite r_i, and γ_i is the H_i – BH_2 out-of-plane angle. S_1 and S_2 correspond to the symmetric stretch and out-of-plane angle bend, while linear combinations of S_3, S_5, and S_4, S_6 yield the degenerate bond stretch and degenerate angle

bend, respectively. The force constants were computed via internal coordinate displacements from the reference structure employing step sizes of 0.01 Å and 0.02 radians for the bond stretching and angle bending coordinates, respectively.

The full quartic force field for BH_3 required the computation of 183 single-point energies. While this number may be reduced if one factors in the symmetry relationships between force constants for symmetric top molecules,[17,18] the independent determination of each force constant served as a useful check of the consistency of the force field data. The requisite displaced geometries and resultant force constants were computed using the *Mathematica*[19] script INTDIF,[20] while the coordinate transformation and computation of spectroscopic constants were performed using the programs INTDER2000[21-24] and ANHARM.[24] All electronic energies and energy gradients were computed using the MOLPRO[25] computation package.

The equilibrium geometries and force constants were computed employing two independent techniques. The first was the straightforward application of a single level of theory at a stationary point geometry to determine a full quartic force field. For this approach, correlation-consistent basis sets[26,27] that have been augmented with core-correlating functions for use in all-electron computations (denoted cc-pCV*X*Z) were employed in conjunction with all-electron CCSD(T)[28,29] energies. In order to minimize numerical round-off errors, all energies were tightly converged to 10^{-10} hartree. Stationary point reference geometries were optimized with a similar rigor, resulting in r_e structures for which the internal coordinate forces are less than 10^{-9} hartree bohr^{-1}.

A second, more theoretically rigorous approach, involved the computation of CBS (complete basis set) limit CCSD(T) geometries and energies via basis set extrapolation. The extrapolation of electronic energies computed using the correlation-consistent family of basis

sets has been studied extensively.[30,31] These investigations have resulted in a widely accepted phenomenological exponential decay profile for the Hartree-Fock (HF) energy described by a three-parameter functional form (4.1),[30]

$$E_{HF}(X) = E_{HF}^{\infty} + ae^{-bX} \tag{4.1}$$

while the correlation energy displays a more protracted convergence that may be fit to a physically motivated inverse cubic function:[31]

$$E_{corr}(X) = E_{corr}^{\infty} + aX^{-3}. \tag{4.2}$$

In both expressions, X is the cardinal number of the correlation-consistent basis set. For the CBS limit results, expressions (4.1) and (4.2) were employed to compute the extrapolated total CCSD(T) energies at each displaced geometry.

The reference structure chosen for the CBS limit force field was obtained via a geometry optimization in which the forces were extrapolated using two- and three-point formulas obtained via the differentiation of (4.1) and (4.2) with respect to nuclear coordinates. The correlated gradient expression has a linear functional form,

$$g_{CBS,corr} = \left(\frac{X^3}{3X^2 - 3X + 1}\right) g_{X,corr} - \left(\frac{(X-1)^3}{3X^2 - 3X + 1}\right) g_{X-1,corr} \tag{4.3}$$

where X is again the cardinality of the basis set, $g_{X,corr}$ is the correlation energy gradient in the cc-pCVXZ basis, and $g_{X-1,corr}$ is the correlated gradient in the cc-pCV(X-1)Z basis set. The non-linear SCF gradient extrapolation formula was first presented in Chapter 3, while the mathematical details of the extrapolation procedure are given in Appendix B.

Geometry optimizations were performed by computing a CBS limit Hessian matrix at each optimization step via the extrapolation of the cc-pCVXZ (X = Q, 5) CCSD(T) and (X = T, Q, 5) SCF (self-consistent field) energies at each displaced geometry required for a harmonic

force field. Employing CBS limit gradients determined using (4.3) and the expressions found in Appendix B, subsequent Newton-Raphson steps were taken until the forces were tightly converged to less than 10^{-9} hartree bohr^{-1}. The rate of convergence of the optimization procedure was very rapid, with the gradients achieving the desired threshold within three iterations from the cc-pCV5Z CCSD(T) optimized minimum energy structure.

4.4 Discussion

The BH_3 full quartic force fields are presented in Table 4.1. These results show near complete convergence with respect to basis set, with the difference between the cc-pCVQZ and CBS CCSD(T) force constants sets rarely exceeding 0.02 (in units consistent with energy in aJ, bond distance in Å, and angles in degrees). The number of significant figures displayed in these tabulated results was restricted to no more than the number of digits of agreement shown between the independently computed symmetry related force constants. While for the majority of the force constants this allowed for at least four digits of precision, the computed force constants F_{4411} and F_{6611} were highly inconsistent and only a single digit of precision could be determined. This discrepancy is attributable to numerical round-off errors coupled with the small magnitude of the force constants.

Turning to the spectroscopic constants shown in Table 4.2, it is apparent that this study has achieved convergence of the vibrational parameters to better than 1 cm^{-1} with respect to basis set. Addressing first the molecular geometry, the 1.18742 Å equilibrium bond length computed at the cc-pCVQZ CCSD(T) level of theory is within 0.001 Å of the complete basis set result of 1.18642 Å. Taking into account zero point vibrational energy effects results in a bond

TABLE 4.1: CCSD(T) computed force constants in symmetrized internal coordinates.[a]

	cc-pCVQZ	cc-pCV5Z	CBS
F_{11}	3.93850	3.93958	3.94041
F_{22}	0.09820	0.09799	0.09777
$F_{33} = F_{55}$	3.85278	3.85566	3.85851
F_{43}	−0.10268	−0.10275	−0.10289
$F_{44} = F_{66}$	0.37258	0.37182	0.37099
F_{111}	−11.0393	−11.0489	−11.0632
F_{221}	−0.0318	−0.0322	−0.0326
$F_{331} = F_{551}$	−11.2554	−11.2630	−11.2751
$F_{333} = -F_{553}$	−8.0549	−8.0603	−8.0685
$F_{431} = F_{651}$	0.0371	0.0370	0.0372
$F_{433} = -F_{554} = -F_{653}$	−0.1644	−0.1644	−0.1643
$F_{441} = F_{661}$	−0.1534	−0.1549	−0.1563
$F_{443} = -F_{654} = -F_{663}$	0.0478	0.0483	0.0488
$F_{444} = -F_{664}$	−0.1600	−0.1586	−0.1572
F_{1111}	27.535	27.614	27.633
F_{2211}	−0.020	−0.021	−0.023
F_{2222}	0.060	0.061	0.061
$F_{3311} = F_{5511}$	29.299	29.321	29.288
$F_{3322} = F_{5522}$	−0.036	−0.037	−0.039
$F_{3331} = -F_{5531}$	21.188	21.194	21.160
$F_{3333} = 3F_{5533} = F_{5555}$	45.384	45.378	45.290
$F_{4311} = F_{6511}$	0.121	0.127	0.134
$F_{4322} = F_{6522}$	−0.018	−0.019	−0.020
$F_{4331} = -F_{5541} = -F_{6531}$	0.092	0.093	0.094
$F_{4333} = 3F_{5543} = 3F_{6533} = F_{6555}$	0.269	0.276	0.285
$F_{4411} = F_{6611}$	0.004	0.002	0.006
$F_{4422} = F_{6622}$	0.057	0.056	0.055
$F_{4431} = -F_{6541} = -F_{6631}$	0.003	0.001	−0.003
$F_{4433} = F_{6655}$	−0.106	−0.108	−0.110
$F_{4441} = -F_{6641}$	0.072	0.067	0.062
$F_{4443} = -3F_{5543} = -3F_{6533} = F_{6555}$	−0.118	−0.114	−0.108
$F_{4444} = 3F_{6644} = F_{6666}$	0.033	0.029	0.024
$F_{5544} = F_{6633}$	−0.340	−0.343	−0.346
F_{6543}	0.120	0.117	0.111

[a] Units are consistent with energy in aJ, distances in Å, and angles in degrees, with respect to internal coordinates defined in the text.

TABLE 4.2: CCSD(T) computed spectroscopic parameters for $^{11}BH_3$[a]

	Ref. 7	cc-pCVQZ	cc-pCV5Z	CBS	Exp.[b]
r_e	1.1899	1.18742	1.18688	1.18642	1.18716[c]
r_0	1.1926	1.19427	1.19374	1.19329	1.19001(1)
ω_1	2568.3	2575.4	2575.8	2576.0	
ω_2	1158.0	1160.0	1159.2	1158.4	
ω_3	2700.3	2708.1	2709.1	2710.1	
ω_4	1220.0	1222.5	1221.8	1220.9	
Δ_1	−73.4	−72.2	−72.7	−73.5	
Δ_2	−23.8	−10.6	−10.9	−11.0	
Δ_3	−112.8	−106.4	−106.6	−107.4	
Δ_4	−23.6	−23.8	−23.9	−24.5	
ν_1	2494.9	2503.2	2503.1	2502.5	
ν_2	1134.2	1149.4	1148.4	1147.4	1147.4986(12)
ν_3	2587.5	2601.7	2602.4	2602.7	2601.5743(15)
ν_4	1196.4	1198.7	1197.6	1196.3	1196.66(12)
χ_{11}	−12.86	−13.01	−12.75	−12.81	
χ_{21}	7.72	5.08	6.88	6.55	
χ_{22}	−5.81	−4.62	−4.76	−4.58	
χ_{31}	−54.03	−54.50	−53.84	−54.11	
χ_{32}	−23.75	−12.69	−12.01	−12.16	
χ_{33}	−24.61	−24.66	−24.56	−24.68	
χ_{41}	−16.67	2.77	3.25	2.93	
χ_{42}	7.73	7.27	7.19	7.04	
χ_{43}	−19.32	−11.08	−10.98	−12.10	
χ_{44}	−0.40	−7.45	−7.50	−7.46	
g_{33}	10.85	10.84	10.85	10.89	
g_{43}	−1.94	−2.14	−2.07	−1.99	
g_{44}	4.16	4.15	4.07	4.03	
G_0		−0.79	−0.65	−0.53	
ZPVE	5704.0	5724.6	5724.5	5723.5	

[a] All spectroscopic constants are in units of cm^{-1}.

[b] The r_0 bond length and ν_3 are from Ref. 10, ν_2 and ν_4 are from Ref. 12, all are parameters are from gas-phase studies.

[c] r_e obtained by using experimental B_0, C_0 and computed vibrational-rotation interaction constants (α_v^B) and centrifugal distortion constants (complete basis set vaules, see Table 4.3).

lengthening of approximately 0.007 Å at all levels of theory. Using experimentally determined B_0 and C_0 rotational constants[10] for the $^{11}BH_3$ and $^{10}BH_3$ isotopomers and the CBS limit CCSD(T) vibration-rotation interaction constants (see Table 4.3), one is able to obtain an empirical r_e = 1.18716 via a least-squares fit of the data. This computed equilibrium bond length falls in the middle of the range bracketed by the cc-pCVQZ and CBS limit CCSD(T) results, but is still only 0.0007 Å longer than our extrapolated value. Computed r_0 structures show larger deviations, with bond length differences between 0.003 – 0.004 Å.

The harmonic frequencies are equally well resolved, with differences of less than 1 cm^{-1} between the cc-pCV5Z and extrapolated CBS limit CCSD(T) values. The *ab initio* fundamentals are in excellent agreement with the available gas-phase infrared results. The ν_2 and ν_4 modes, in converging to the CBS limit, appear to be converging to the experimental values as well. This gratifying result demonstrates the efficacy of the CCSD(T) quartic force field. The basis set trends for the ν_3 mode show convergence to a result that is 1.1 cm^{-1} larger than the experimental value, although it should be noted that all the of computed fundamentals are within the expected accuracy of 1 – 2 cm^{-1} that is associated with a second-order vibrational perturbation theory treatment.[15,16,32]

Anharmonic zero-point vibrational energies which include the oft-neglected G_0 term were computed using the resonance independent expression (4.4):

$$\mathrm{ZPVE} = \frac{1}{2}\sum_i \omega_i - \frac{1}{32}\sum_{ijk}\frac{\phi_{iik}\phi_{kjj}}{\omega_k} - \frac{1}{48}\sum_{ijk}\frac{\phi_{ijk}^2}{\omega_i+\omega_j+\omega_k} + \frac{1}{32}\sum_{ij}\phi_{iijj} + Z_{kinetic}\,. \qquad (4.4)$$

In the above expression, the indices i, j, and k run unrestricted over all modes, including both components of a degenerate manifold, ϕ_{ijk} are cubic force constants (see Table C.1)[33] in normal

TABLE 4.3: CCSD(T) computed vibration-rotation parameters for BH_3.[a]

	Ref. 7	cc-pCVQZ	cc-pCV5Z	CBS	Exp.[b]
B_e	7.8762	7.9089	7.9160	7.9221	7.90664[c]
C_e	3.9381	3.9544	3.9580	3.9611	3.95745[c]
B_0	7.8415	7.8741	7.8812	7.8872	7.87411(14)
C_0	3.8615	3.8777	3.8811	3.8839	3.8788
$\alpha_{\upsilon 1}^{B}$	0.0677	0.0672	0.0673	0.0675	
$\alpha_{\upsilon 2}^{B}$	0.0718	1.9026 (0.0716)	1.9061 (0.0717)	1.9110 (0.0718)	0.0151(37)
$\alpha_{\upsilon 3}^{B}$	0.0735	0.0733	0.0734	0.0736	0.07336
$\alpha_{\upsilon 4}^{B}$	−0.1065	−1.0234(−0.1079)	−1.0253(−0.1081)	−1.0279 (−0.1083)	−0.1176(61)
$\alpha_{\upsilon 1}^{C}$	0.0339	0.0336	0.0336	0.0337	
$\alpha_{\upsilon 2}^{C}$	−0.0194	−0.0198	−0.0198	−0.0198	−0.0154(24)
$\alpha_{\upsilon 3}^{C}$	0.0308	0.0308	0.0309	0.0310	0.02907(10)
$\alpha_{\upsilon 4}^{C}$	0.0392	0.0391	0.0392	0.0392	0.031(21)
$\zeta_{3,5}^{z}$		0.0857	0.0856	0.0854	0.09258(25)
$10^3\ D_J$	0.5638	0.5702	0.5721	0.5738	0.5975(34)
$10^3\ D_{JK}$	−0.9790	−0.9913	−0.9946	−0.9978	−1.104(13)
$10^3\ D_K$	0.4524	0.4584	0.4599	0.4614	0.5293
$10^6\ H_J$	0.1140	0.1166	0.1172	0.1179	0.060(24)
$10^6\ H_{JK}$	−0.4143	−0.4230	−0.4252	−0.4277	−1.01(15)
$10^6\ H_{KJ}$	0.4889	0.4984	0.5014	0.5042	2.34(29)
$10^6\ H_K$	−0.1882	−0.1917	−0.1928	−0.1939	−1.307

[a] All parameters given in cm^{-1}, values in parentheses have had (ν_2, ν_4) Coriolis resonance removed.
[b] All experimental results are from gas-phase infrared study in Ref. 12.
[c] Obtained via a fit of isotopic data from Ref. 10, employing vibration-rotation constants and centrifugal distortion constants computed in this study.

coordinates, and $Z_{kinetic}$ is the kinetic energy term arising from coupling of the vibrational angular momentum about the rotational axes and is given by (5):

$$Z_{kinetic} = -\frac{1}{4}\sum_{\alpha} B_{\alpha}^{\circ}\left[1+\sum_{i>j}\left(\zeta_{ij}^{\alpha}\right)^2 \frac{\left[B_{\alpha}^{\circ}\left(\omega_i+\omega_j\right)-\left(\omega_i-\omega_j\right)^2\right]}{\omega_i\omega_j}\right]. \tag{4.5}$$

In (4.5), ζ_{rs}^{α} and B_{α}° are the Coriolis constants and equilibrium rotational constants, respectively. The anharmonic ZPVE displays little basis set dependence, with the cc-pCVQZ CCSD(T) result only 1.1 cm^{-1} larger than the final recommended value of 5723.5 cm^{-1}.

Lastly, a host of rotational parameters were also computed and are summarized in Table 4.3. The agreement between the experimental and *ab initio* B_e, C_e, and B_0, C_0, is good, with observed deviations of 0.01 – 0.02 cm^{-1}. The Coriolis resonance that arises between ν_2 and ν_4, and its effect on the $\alpha_{\upsilon_2}^{B}$ and $\alpha_{\upsilon_4}^{B}$ vibration-rotation interaction constants, has been documented in previous *ab initio*[11] and experimental studies.[10,12] Both the deperturbed (in parentheses) and resonance-included terms are shown in Table 4.3. Due to the high symmetry of BH_3, there is but a single unique Coriolis coupling constant. The other non-zero constants may be determined by the symmetry relations:[12,34,35]

$$\zeta_{3,5}^{z} = -\zeta_{4,6}^{z} = \left(\zeta_{2,3}^{y}\right)^2 - \left(\zeta_{2,4}^{y}\right)^2 = \left(-\zeta_{2,5}^{x}\right)^2 - \left(-\zeta_{2,6}^{x}\right)^2, \tag{4.6}$$

$$\left(\zeta_{2,3}^{y}\right)^2 + \left(\zeta_{2,4}^{y}\right)^2 = 1, \text{ and} \tag{4.7}$$

$$\left(\zeta_{3,6}^{z}\right)^2 + \left(\zeta_{3,5}^{z}\right)^2 = 1, \tag{4.8}$$

where the *z* axis is perpendicular to the molecular plane.

In general, the agreement between the computed α_{υ}^{B} and quartic centrifugal distortion constants ($D_{J/K}$) constants and the experimental results is excellent. However, the computed sextic centrifugal distortion constants ($H_{J/K}$) deviate substantially from the spectroscopically

determined values, particularly for *ab initio* H_{KJ} and H_K terms which are 4 – 6 times smaller than those observed experimentally.

4.5 Summary

The *ab initio* quartic force field of BH_3 has been determined to VPT2 limit accuracy employing correlation-consistent basis sets and coupled-cluster electronic structure methods. While all the levels of theory employed here have yielded excellent results, the use of basis set extrapolation techniques to obtain both reference geometries and quartic force fields have performed particularly well. This method produced computed fundamental frequencies which display a mean absolute error of only 0.5 cm^{-1} in comparison to gas-phase spectroscopic results. Of the computed fundamentals, ν_1 = 2502.5 cm^{-1}, ν_2 = 1147.4 cm^{-1}, ν_3 = 2602.7 cm^{-1}, and ν_4 = 1196.3 cm^{-1}, ν_2 displayed an absolute error of 1.1 cm^{-1}, the largest deviation of the CBS limit fundamentals with experiment. In this investigation, the CBS limit CCSD(T) force field and spectroscopic parameters were used primarily to gauge the convergence in our computed results. However, one may envisage such techniques being invaluable for attaining qualitatively correct results when applied to systems displaying a more remarkable basis set dependence.

4.6 Acknowledgements

The research presented here was supported by the U. S. Department of Energy, Office of Basic Energy Sciences, Combustion Program (Grant No. DE-FG02-00ER14748) and Chemical Sciences, Geosciences and Biosciences Division (Grant No. DE-FG02-01ER15226).

REFERENCES

[1] H. C. Brown and B. C. S. Rao, J. Am. Chem. Soc. **78**, 5694 (1956).

[2] W. N. Lipscomb, *Boron Hydrides*. (W A Benjamin, New York, 1963).

[3] H. C. Brown, *Boranes in Organic Chemistry*. (Cornell University Press, Ithaca, 1972).

[4] E. L. Muetterties, *Boron Hydride Chemistry*. (Academic Press, New York, 1975).

[5] A. Kaldor and R. F. Porter, J. Am. Chem. Soc. **93**, 2140 (1971).

[6] K. Kawaguchi and E. Hirota, J. Chem. Phys. **87**, 6838 (1987).

[7] P. Botschwina, in *Ion and cluster spectroscopy and structure*, edited by J. P. Maier (Elsevier, Amsterdam, 1989), pp. 59.

[8] J. F. Stanton, R. J. Bartlett, and W. N. Lipscomb, Chem. Phys. Lett. **138**, 525 (1987).

[9] J. M. Galbraith, G. Vacek, and H. F. Schaefer, J. Mol. Struct. **300**, 281 (1993).

[10] K. Kawaguchi, J. Chem. Phys. **96**, 3411 (1992).

[11] J. M. L. Martin and T. J. Lee, Chem. Phys. Lett. **200**, 502 (1992).

[12] K. Kawaguchi, Can. J. Phys. **72**, 925 (1994).

[13] D. W. Schwenke, J. Phys. Chem. **100**, 2867 (1996).

[14] H. H. Nielsen, Rev. Mod. Phys. **23**, 90 (1951).

[15] J. K. G. Watson, in *Vibrational Spectra and Structure*, edited by J. R. Durig (Elsevier, Amsterdam, 1977), Vol. 6, pp. 1.

[16] D. Papoušek and M. R. Aliev, *Molecular Vibrational-Rotational Spectra*. (Elsevier, Amsterdam, 1982).

[17] L. Henry and G. Amat, J. Mol. Spectrosc. **5**, 319 (1960).

[18] L. Henry and G. Amat, J. Mol. Spectrosc. **15**, 168 (1965).

[19] *Mathematica* (Wolfram Research, Inc., Champaign, Illinois, 2003).

[20] INTDIF2004 is an abstract program written by Wesley D. Allen for *Mathematica* (Wolfram Research, Inc., Champaign, Illinois) to perform general numerical differentiations to high orders of electronic structure data.

[21] INTDER is a general program written by W. D. Allen which performs sundry vibrational analyses and higher-order nonlinear transformations among force field representations.

[22] W. D. Allen and A. G. Császár, J. Chem. Phys. **98**, 2983 (1993).

[23] W. D. Allen, A. G. Császár, V. Szalay, and I. M. Mills, Mol. Phys. **89**, 1213 (1996).

[24] see program descriptions in K. Sarka and J. Demaison, in *Computational Molecular Spectroscopy*, edited by P. Jensen and P. R. Bunker (Wiley, Chichester, 2000), pp. 255

[25] MOLPRO, a package of *ab initio* programs designed by H.-J. Werner and P. J. Knowles, version 2002.1, R. D. Amos, A. Bernhardsson, A. Berning, P. Celani, D. L. Cooper, M. J. O. Deegan, A. J. Dobbyn, F. Eckert, C. Hampel, G. Hetzer, P. J. Knowles, T. Korona, R. Lindh, A. W. Lloyd, S. J. McNicholas, F. R. Manby, W. Meyer, M. E. Mura, A. Nicklass, P. Palmieri, R. Pitzer, G. Rauhut, M. Schütz, U. Schumann, H. Stoll, A. J. Stone, R. Tarroni, T. Thorsteinsson, and H.-J. Werner.

[26] D. E. Woon and T. H. Dunning, Jr., J. Chem. Phys. **103**, 4572 (1995).

[27] Basis sets were obtained from the Extensible Computational Chemistry Environment Basis Set Database, Version 2/12/03, as developed and distributed by the Molecular Science Computing Facility, Environmental and Molecular Sciences Laboratory which is part of the Pacific Northwest Laboratory, P.O. Box 999, Richland, Washington 99352, USA, and funded by the U.S. Department of Energy. The Pacific Northwest Laboratory is a multi-program laboratory operated by Battelle Memorial Institue for the U.S. Department of Energy under contract DE-AC06-76RLO 1830. Contact David Feller or Karen Schuchardt for further information.

[28] K. Raghavachari, G. W. Trucks, J. A. Pople, and M. Head-Gordon, Chem. Phys. Lett. **157**, 479 (1989).

[29] G. E. Scuseria and T. J. Lee, J. Chem. Phys. **93**, 5851 (1990).

[30] D. Feller, J. Chem. Phys. **98**, 7059 (1993).

[31] T. Helgaker, W. Klopper, H. Koch, and J. Noga, J. Chem. Phys. **106**, 9639 (1997).

[32] I. M. Mills, in *Molecular Spectroscopy: Modern Research*, edited by K. N. Rao and C. W. Mathews (Academic Press, New York, 1972), Vol. 1, pp. 115.

[33] See Appendix C for a tabulation of the BH_3 cubic and quartic force constants in normal coordinates.

[34] T. Oka, J. Mol. Spectrosc. **29**, 84 (1969).

[35] J. K. G. Watson, J. Mol. Spectrosc. **39**, 364 (1971).

CHAPTER 5

CONCLUDING REMARKS

The results presented in the preceding chapters document the ability of basis set extrapolation methods, in conjunction with a judicious treatment of electron correlation, to produce reaction energies and molecular properties with accuracy on par with the most reliable experimental values. In the realm of computational thermochemistry, focal point analysis has proven its utility by yielding reaction energies of subchemical precision. In fact, the largest contributions to the mean absolute error in the enthalpies of formation of HNCO and NCO derive from the experimental enthalpies of formation of the component species and the zero-point vibrational energy (ZPVE) corrections, not the treatment of the electronic structure.

Obtaining anharmonic ZPVE values of the highest accuracy from second-order vibrational perturbation theory (VPT2) required the derivation of formulas that explicitly incorporate the oft-neglected G_0 term. *Ab initio* quartic force fields computed at high levels of theory employed in concert with these expressions yield ZPVEs that are often within a few wavenumbers of more rigorous variational vibrational treatments. However, as discussed in Chapter 3, the application of ZPVE formulas derived from VPT2 is limited to molecules that display exclusively small amplitude vibrational motion. As for the uncertainties in the experimental $\Delta_f H_0^\circ$ values, the refinement of enthalpies of formation for small molecules of import to the combustion chemistry community is an ongoing process. While the reference enthalpies employed in this study will no doubt be revised in response to new computational and experimental results, the electronic structure treatment is expected to be definitive.

Initial investigations into gradient extrapolation techniques appear promising. The prodigious basis set dependence of the r_e structure of BH_5 was overcome using gradient formulas obtained via the differentiation of the standard Hartree-Fock and correlation energy extrapolation functions with respect to nuclear coordinates. The convergence of the extrapolated gradients is

well-defined, as evidenced by the geometry optimization of BH_3 in which CBS limit CCSD(T) gradients were converged to less than 10^{-9} hartree/bohr at the minimum energy structure. Further study of these methods is warranted, particularly concerning the dependence of the CBS limit gradient on the cardinality of the correlation-consistent basis sets used in the extrapolation. Regardless, our results demonstrate that extrapolated gradient techniques are effective for obtaining qualitatively correct molecular structures for systems displaying exceptional basis set dependence, as well as highly accurate r_e structures for non-pathological cases.

Lastly, utilization of extrapolated electronic energies to numerically determine of quartic force fields yields vibrational frequencies via VPT2 that are in excellent agreement with known gas-phase fundamentals. These results encourage the investigation of CBS limit force fields as a route to highly accurate *ab initio* determinations of vibrational frequencies, anharmonic geometrical effects, and zero-point vibrational energies.

APPENDIX A

SUPPLEMENTARY MATERIALS FOR CHAPTER 2

TABLE A.1: Focal point analysis of core-correlation correction for NCO ($^2\Pi$) formation reactions[a]

	ΔE_e[MP2]	$+\delta$[CCSD]	$+\delta$[CCSD(T)]	$+\delta$[CCSDT]	$= \Delta E_e$[CCSDT]
Reaction 1: $N(^4S) + CO_2 \rightarrow O(^3P) + NCO(^2\Pi)$					
cc-pCVDZ	–0.00	–0.27	+0.26	+0.00	–0.01
cc-pCVTZ	+0.02	–0.06	–0.04	–0.00	+0.04
cc-pCVQZ	+0.02	+0.08	–0.05	[–0.00]	[+0.05]
cc-pCV5Z	+0.02	[+0.09]	[–0.05]	[–0.00]	[+0.05]
CBS limit	[+0.02]	[+0.10]	[–0.05]	[–0.00]	**[+0.05]**
Reaction 2: $NH(^3\Sigma^-) + CO_2 \rightarrow OH(^2\Pi) + NCO(^2\Pi)$					
cc-pCVDZ	–0.03	–0.24	+0.26	+0.01	–0.00
cc-pCVTZ	–0.05	+0.10	–0.04	–0.00	+0.01
cc-pCVQZ	–0.06	+0.12	–0.05	[–0.00]	[+0.02]
cc-pCV5Z	–0.06	[+0.13	[–0.05]	[–0.00]	[+0.02]
CBS limit	[–0.06]	[+0.13]	[–0.05]	[–0.00]	**[+0.02]**
Extrapolation scheme	$a+bX^{-3}$	$a+bX^{-3}$	$a+bX^{-3}$	add	
Points (X =)	4, 5	3, 4	3, 4	--	

[a] See footnote *a* of Table 2.3 for notations.

TABLE A.2: Focal point analysis of core-correlation correction for HNCO formation reactions[a]

	ΔE_e[MP2]	$+\delta$[CCSD]	$+\delta$[CCSD(T)]	$+\delta$[CCSDT]	$= \Delta E_e$[CCSDT]
Reaction 3: $NH_3 + CO_2 \rightarrow H_2O + HNCO$					
cc-pCVDZ	–0.06	+0.04	+0.01	+0.00	–0.01
cc-pCVTZ	–0.17	+0.06	+0.01	+0.00	–0.10
cc-pCVQZ	–0.18	+0.06	+0.00	[+0.00]	[–0.11]
cc-pCV5Z	–0.18	[+0.06]	[+0.00]	[+0.00]	[–0.11]
CBS limit	[–0.18]	[+0.07]	[+0.00]	[+0.00]	**[–0.11]**
Reaction 4: $NH(^3\Sigma^-) + CO_2 \rightarrow O(^3P) + HNCO$					
cc-pCVDZ	–0.11	–0.27	+0.29	+0.00	–0.09
cc-pCVTZ	–0.26	+0.03	+0.03	–0.00	–0.21
cc-pCVQZ	–0.28	+0.03	+0.03	[–0.00]	[–0.23]
cc-pCV5Z	–0.30	[+0.03]	[+0.03]	[–0.00]	[–0.24]
CBS limit	[–0.31]	[+0.04]	[+0.03]	[–0.00]	**[–0.25]**
Reaction 5: $H(^2S) + NCO(^2\Pi) \rightarrow HNCO$					
cc-pCVDZ	–0.26	–0.01	–0.01	–0.00	–0.25
cc-pCVTZ	–0.38	–0.06	+0.03	–0.00	–0.42
cc-pCVQZ	–0.39	–0.08	+0.03	[–0.00]	[–0.44]
cc-pCV5Z	–0.40	[–0.09]	[+0.03]	[–0.00]	[–0.45]
CBS limit	[–0.41]	[–0.09]	[+0.03]	[–0.00]	**[–0.46]**
Reaction 6: $H^+ + NCO^- \rightarrow HNCO$[b]					
aug-cc-pCVDZ	–0.19	–0.02	+0.00	+0.13	–0.08
aug-cc-pCVTZ	–0.19	–0.03	+0.01	[+0.13]	[–0.09]
aug-cc-pCVQZ	–0.18	[–0.03]	[+0.01]	[+0.13]	[–0.07]
aug-cc-pCV5Z	–0.18	[–0.03]	[+0.01]	[+0.13]	[–0.08]
CBS limit	[–0.19]	[–0.03]	[+0.01]	[+0.13]	**[–0.08]**
Extrapolation scheme	$a+bX^{-3}$	$a+bX^{-3}$	$a+bX^{-3}$	add	
Points (X=)	4, 5	3, 4	3, 4	--	

[a] See footnote *a* of Table 2.3 for notations.
[b] No extrapolation of the CCSD and CCSD(T) increments was performed; here additivity was assumed.

TABLE A.2: Focal point analysis of core-correlation correction for HNCO formation reactions (cont'd)[a]

	ΔE_e[MP2]	$+\delta$[CCSD]	$+\delta$[CCSD(T)]	$+\delta$[CCSDT]	$= \Delta E_e$[CCSDT]
Reaction 7: $NH(^3\Sigma^-) + NCO(^2\Pi) \rightarrow N(^4S) + HNCO$					
cc-pCVDZ	–0.11	–0.01	+0.03	–0.00	–0.09
cc-pCVTZ	–0.28	–0.04	+0.07	+0.00	–0.25
cc-pCVQZ	–0.30	–0.05	+0.08	[+0.00]	[–0.28]
cc-pCV5Z	–0.31	[–0.06]	[+0.08]	[+0.00]	[–0.29]
CBS limit	[–0.33]	[–0.06]	[+0.08]	[+0.00]	**[–0.30]**
Reaction 8: 1/3 $[NH_3 + 3NCO(^2\Pi) \rightarrow N(^4S) + 3HNCO]$					
cc-pCVDZ	–0.07	–0.02	+0.03	–0.00	–0.06
cc-pCVTZ	–0.18	–0.05	+0.05	+0.00	–0.18
cc-pCVQZ	–0.19	–0.07	+0.06	[+0.00]	[–0.19]
cc-pCV5Z	–0.19	[–0.07]	[+0.06]	[+0.00]	[–0.20]
CBS limit	[–0.20]	[–0.07]	[+0.07]	[+0.00]	**[–0.21]**
Reaction 9: 1/2 $[H_2O + 2NCO(^2\Pi) \rightarrow O(^3P) + 2HNCO]$					
cc-pCVDZ	–0.07	–0.04	+0.01	–0.00	–0.10
cc-pCVTZ	–0.17	–0.08	+0.06	+0.00	–0.19
cc-pCVQZ	–0.18	–0.10	+0.07	[+0.00]	[–0.21]
cc-pCV5Z	–0.19	[–0.10]	[+0.07]	[+0.00]	[–0.22]
CBS limit	[–0.20]	[–0.10]	[+0.07]	[+0.00]	**[–0.22]**
Extrapolation scheme	$a+bX^{-3}$	$a+bX^{-3}$	$a+bX^{-3}$	add	
Points (X=)	4, 5	3, 4	3, 4	--	

[a] See footnote *a* of Table 2.3 for notations.

TABLE A.3: Focal point analysis of core-correlation correction for HNCO isomerization reactions[a]

	ΔE_e[MP2]	$+\delta$[CCSD]	$+\delta$[CCSD(T)]	$+\delta$[CCSDT]	$= \Delta E_e$[CCSDT]
Reaction 10: HNCO $\rightarrow$ HOCN					
cc-pCVDZ	+0.08	+0.04	–0.01	+0.00	+0.10
cc-pCVTZ	+0.09	+0.06	–0.02	+0.00	+0.13
cc-pCVQZ	+0.07	+0.06	–0.03	[+0.00]	[+0.12]
cc-pCV5Z	+0.08	[+0.06]	[–0.03]	[+0.00]	[+0.11]
CBS limit	[0.08]	[+0.05]	[–0.03]	[+0.00]	**[+0.11]**
Reaction 11: HNCO $\rightarrow$ HCNO					
cc-pCVDZ	–0.04	+0.05	–0.04	–0.00	–0.03
cc-pCVTZ	–0.05	+0.07	–0.08	–0.01	–0.07
cc-pCVQZ	–0.08	+0.08	–0.09	[–0.01]	[–0.10]
cc-pCV5Z	–0.08	[+0.08]	[–0.10]	[–0.01]	[–0.11]
CBS limit	[–0.08]	[+0.07]	[–0.10]	[–0.01]	**[–0.12]**
Reaction 12: HNCO $\rightarrow$ HONC					
cc-pCVDZ	+0.16	+0.11	–0.02	+0.01	+0.26
cc-pCVTZ	+0.24	+0.19	–0.04	+0.01	+0.40
cc-pCVQZ	+0.33	+0.22	–0.04	[+0.01]	[+0.51]
cc-pCV5Z	+0.35	[+0.23]	[–0.04]	[+0.01]	[+0.55]
CBS limit	[+0.38]	[+0.24]	[–0.04]	[+0.01]	**[+0.59]**
Extrapolation scheme	$a+bX^{-3}$	$a+bX^{-3}$	$a+bX^{-3}$	add	
Points (X =)	4, 5	3, 4	3, 4	--	

[a] See footnote *a* of Table 2.3 for notations.

TABLE A.4: Summary of additive quadruples increments

Reaction	cc-pVTZ BD(TQ) increment	cc-pVTZ CCSDT+(QB) increment	cc-pVTZ CCSD(2) increment	cc-pVTZ CCSDT+(Q2) increment
(1)	–0.548	–1.095	+0.463	–0.329
(2)	–0.502	–0.987	+0.380	–0.168
(3)	–0.162	–0.138	+0.114	+0.111
(4)	–0.155	–0.087	+0.132	–0.028
(5)	+0.355	+0.877	–0.215	+0.339
(6)	+0.271[a]	–0.048[a]	+0.199[a]	–0.004[a]
(7)	+0.393	+1.008	–0.331	+0.301
(8)	+0.355	+0.865	–0.239	+0.292
(9)	+0.339	+0.819	–0.184	+0.218
(10)	–0.953	–0.808	–0.411	–0.256
(11)	–0.031	+0.220	–0.137	+0.237
(12)	–0.779	–0.753	–0.113	–0.096

[a] aug-cc-pVDZ result.

APPENDIX B

SUPPLEMENTARY MATERIAL FOR CHAPTER 3

Extrapolated Hartree-Fock Gradient Formula

The functional form adopted for extrapolation of the Hartree-Fock energy to the complete basis set limit is

$$E(X) = E_\infty + Ae^{-bX} \ , \tag{B.1}$$

where X is the cardinal number within the correlation-consistent basis set series. Suppose we have a series of n energies $\{E_1, E_2, \ldots, E_n\}$ computed with basis sets of cardinal numbers $\{X_1, X_2, \ldots, X_n\}$. For this data set, define the vector and scalar quantities:

$$\mathbf{y}_m = \left(X_1^m e^{-bX_1}, X_2^m e^{-bX_2}, ..., X_n^m e^{-bX_n}\right) \tag{B.2}$$

$$y_m = \sum_{k=1}^{n} X_k^m e^{-bX_k} \tag{B.3}$$

$$\mathbf{z}_m = \left(X_1^m e^{-2bX_1}, X_2^m e^{-2bX_2}, ..., X_n^m e^{-2bX_n}\right) \tag{B.4}$$

$$z_m = \sum_{k=1}^{n} X_k^m e^{-2bX_k} \tag{B.5}$$

$$\boldsymbol{\varepsilon}_m = \left(X_1^m E_1, X_2^m E_2, ..., X_n^m E_n\right) \tag{B.6}$$

$$\varepsilon_m = \sum_{k=1}^{n} X_k^m E_k \tag{B.7}$$

The least-squares-fit stationary conditions for the parameters $\{E_\infty, A, b\}$ can be written as

$$\varepsilon_0 = n E_\infty + A y_0 \ , \tag{B.8}$$

$$\boldsymbol{\varepsilon}_0 \cdot \mathbf{y}_0 = E_\infty y_0 + A z_0 \ , \tag{B.9}$$

and

$$\boldsymbol{\varepsilon}_1 \cdot \mathbf{y}_0 = E_\infty y_1 + A z_1 \ . \tag{B.10}$$

The solutions for E_∞ and A are given by

$$E_\infty = \frac{y_0\left(\boldsymbol{\varepsilon}_0 \cdot \mathbf{y}_0\right) - z_0 \varepsilon_0}{y_0^2 - n z_0} \tag{B.11}$$

and

$$A = \frac{y_0 \varepsilon_0 - n(\boldsymbol{\varepsilon}_0 \cdot \mathbf{y}_0)}{y_0^2 - n z_0}, \tag{B.12}$$

whereas b satisfies the nonlinear equation

$$\varepsilon_0 (y_1 z_0 - y_0 z_1) + (\boldsymbol{\varepsilon}_0 \cdot \mathbf{y}_0)(n z_1 - y_0 y_1) + (\boldsymbol{\varepsilon}_1 \cdot \mathbf{y}_0)(y_0^2 - n z_0) = 0 \ . \tag{B.13}$$

Because the energies $\{E_1, E_2, \ldots, E_n\}$ and the parameters $\{E_\infty, A, b\}$ depend on the nuclear positions (**q**), all quantities defined by Eqs. (B.2)-(B.7) have geometric dependence. By differentiating Eq. (B.11), and employing the derivative relations $\frac{d\mathbf{y}_0}{db} = -\mathbf{y}_1$ and $\frac{d\mathbf{z}_0}{db} = -2\mathbf{z}_1$, one finds that nuclear-coordinate gradients on the extrapolated surface can be evaluated via

$$\frac{\partial E_\infty}{\partial q} = \frac{\left(\frac{db}{dq}\right)\left[2E_\infty (y_0 y_1 - n z_2) + 2\varepsilon_0 z_2 - y_0 (\boldsymbol{\varepsilon}_0 \cdot \mathbf{y}_1) - y_1 (\boldsymbol{\varepsilon}_0 \cdot \mathbf{y}_0)\right] + y_0 \, \mathbf{y}_0 \cdot \left(\frac{d\boldsymbol{\varepsilon}_0}{dq}\right) - z_0 \left(\frac{d\varepsilon_0}{dq}\right)}{y_0^2 - n z_0} \tag{B.14}$$

where from Eq. (B.13)

$$\left(\frac{db}{dq}\right) = \frac{(y_1 z_0 - y_0 z_1)\left(\frac{d\varepsilon_0}{dq}\right) + (n z_2 - y_0 y_1)\mathbf{y}_0 \cdot \left(\frac{d\boldsymbol{\varepsilon}_0}{dq}\right) + (y_0^2 - n z_0)\mathbf{y}_0 \cdot \left(\frac{d\boldsymbol{\varepsilon}_1}{dq}\right)}{\left\{\begin{array}{r} \varepsilon_0 (y_1 z_1 + z_0 y_2 - 2 y_0 z_2) + (\boldsymbol{\varepsilon}_0 \cdot \mathbf{y}_1)(n z_2 - y_0 y_1) + (\boldsymbol{\varepsilon}_0 \cdot \mathbf{y}_1)(y_0^2 - n z_0) \\ - (\boldsymbol{\varepsilon}_0 \cdot \mathbf{y}_0)(y_1^2 + y_0 y_2 - 2 n z_2) - 2(\boldsymbol{\varepsilon}_1 \cdot \mathbf{y}_0)(n z_2 - y_0 y_1) \end{array}\right\}} . \tag{B.15}$$

TABLE B.1: Symmetrized internal quadratic force constants of BH_5 [C_s(I)][a]

i	*j*	F_{ij}	*i*	*j*	F_{ij}	*i*	*j*	F_{ij}
1	1	3.794	6	2	−0.068	8	5	0.393
2	1	−0.008	6	3	−0.018	8	6	0.130
2	2	0.115	6	4	0.039	8	7	0.226
3	1	−0.072	6	5	−0.276	8	8	3.817
3	2	−0.007	6	6	1.315	9	9	3.754
3	3	3.648	7	1	0.027	10	9	−0.048
4	1	−0.001	7	2	−0.071	10	10	0.448
4	2	0.000	7	3	−0.013	11	9	0.104
4	3	−0.115	7	4	0.019	11	10	0.174
4	4	0.349	7	5	0.040	11	11	0.517
5	1	0.031	7	6	−0.586	12	9	−0.048
5	2	−0.006	7	7	1.158	12	10	−0.087
5	3	0.188	8	1	−0.059	12	11	−0.134
5	4	0.010	8	2	0.034	12	12	0.045
5	5	0.569	8	3	0.036			
6	1	0.013	8	4	−0.079			

[a] Units are consistent with energy in aJ, distances in Å, and angles in degrees, with respect to internal coordinates defined in the text.

TABLE B.2: Symmetrized internal cubic force constants for BH_5 [C_s(I)][a]

i	j	k	F_{ijk}	i	j	k	F_{ijk}	i	j	k	F_{ijk}	i	J	k	F_{ijk}
1	1	1	−10.598	6	6	1	0.120	8	6	2	−0.007	11	9	7	−0.164
2	1	1	0.006	6	6	2	0.000	8	6	3	−0.135	11	9	8	0.137
2	2	1	−0.037	6	6	3	0.220	8	6	4	0.065	11	10	1	−0.072
2	2	2	−0.041	6	6	4	0.033	8	6	5	−0.418	11	10	2	0.047
3	1	1	0.234	6	6	5	−0.077	8	6	6	−0.251	11	10	3	0.032
3	2	1	0.003	6	6	6	−6.659	8	7	1	−0.022	11	10	4	0.007
3	2	2	−0.002	7	1	1	0.056	8	7	2	0.013	11	10	5	−0.188
3	3	1	−10.695	7	2	1	0.045	8	7	3	−0.189	11	10	6	−0.141
3	3	2	0.038	7	2	2	0.003	8	7	4	0.065	11	10	7	−0.045
3	3	3	−7.391	7	3	1	−0.011	8	7	5	−0.126	11	10	8	0.089
4	1	1	−0.004	7	3	2	0.008	8	7	6	0.731	11	11	1	−0.150
4	2	1	0.001	7	3	3	−0.017	8	7	7	−0.627	11	11	2	0.261
4	2	2	−0.002	7	4	1	−0.019	8	8	1	−0.056	11	11	3	0.153
4	3	1	0.027	7	4	2	−0.010	8	8	2	0.020	11	11	4	−0.083
4	3	2	0.017	7	4	3	0.008	8	8	3	0.061	11	11	5	0.174
4	3	3	−0.107	7	4	4	0.041	8	8	4	−0.078	11	11	6	−0.341
4	4	1	−0.162	7	5	1	−0.064	8	8	5	−0.117	11	11	7	−0.228
4	4	2	−0.057	7	5	2	−0.003	8	8	6	−0.035	11	11	8	0.139
4	4	3	0.017	7	5	3	−0.247	8	8	7	0.297	12	9	1	−0.009
4	4	4	−0.126	7	5	4	−0.022	8	8	8	−25.565	12	9	2	−0.026
5	1	1	−0.007	7	5	5	−0.117	9	9	1	−11.022	12	9	3	−0.015
5	2	1	0.008	7	6	1	0.003	9	9	2	0.033	12	9	4	0.024
5	2	2	−0.003	7	6	2	0.022	9	9	3	7.877	12	9	5	−0.087
5	3	1	0.034	7	6	3	0.162	9	9	4	0.133	12	9	6	0.074
5	3	2	0.069	7	6	4	−0.065	9	9	5	−0.019	12	9	7	0.076
5	3	3	−0.016	7	6	5	0.535	9	9	6	0.035	12	9	8	−0.156
5	4	1	0.035	7	6	6	0.173	9	9	7	0.005	12	10	1	0.059
5	4	2	−0.026	7	7	1	0.073	9	9	8	−0.027	12	10	2	−0.002
5	4	3	0.089	7	7	2	−0.014	10	9	1	0.033	12	10	3	−0.006
5	4	4	−0.025	7	7	3	−0.069	10	9	2	0.042	12	10	4	−0.066
5	5	1	−0.283	7	7	4	0.032	10	9	3	0.127	12	10	5	0.168
5	5	2	0.198	7	7	5	−0.396	10	9	4	−0.051	12	10	6	0.117
5	5	3	−0.331	7	7	6	0.629	10	9	5	0.016	12	10	7	0.007
5	5	4	0.249	7	7	7	−6.222	10	9	6	−0.083	12	10	8	−0.122
5	5	5	−0.698	8	1	1	−0.042	10	9	7	−0.130	12	11	1	0.068
6	1	1	0.045	8	2	1	−0.012	10	9	8	0.130	12	11	2	−0.067
6	2	1	0.043	8	2	2	−0.039	10	10	1	−0.204	12	11	3	−0.083
6	2	2	0.002	8	3	1	0.042	10	10	2	−0.070	12	11	4	−0.012
6	3	1	−0.029	8	3	2	0.018	10	10	3	−0.040	12	11	5	−0.019
6	3	2	−0.012	8	3	3	0.053	10	10	4	0.140	12	11	6	0.245
6	3	3	−0.079	8	4	1	0.034	10	10	5	−0.187	12	11	7	−0.059
6	4	1	−0.013	8	4	2	0.000	10	10	6	−0.029	12	11	8	−0.114
6	4	2	0.003	8	4	3	−0.006	10	10	7	0.006	12	12	1	−0.039
6	4	3	−0.062	8	4	4	−0.093	10	10	8	0.039	12	12	2	0.017
6	4	4	0.040	8	5	1	−0.062	11	9	1	0.046	12	12	3	0.013
6	5	1	0.069	8	5	2	0.120	11	9	2	0.062	12	12	4	0.093
6	5	2	−0.054	8	5	3	0.104	11	9	3	−0.007	12	12	5	−0.352
6	5	3	−0.138	8	5	4	0.208	11	9	4	−0.032	12	12	6	−0.052
6	5	4	−0.088	8	5	5	−0.693	11	9	5	0.131	12	12	7	0.090
6	5	5	0.095	8	6	1	−0.005	11	9	6	−0.207	12	12	8	−0.124

[a] Units are consistent with energy in aJ, distances in Å, and angles in degrees, with respect to internal coordinates defined in the text.

TABLE B.3: Symmetrized internal quartic force constants for BH_5 [C_s(I)].[a]

i	*j*	*l*	*k*	F_{ijkl}	*i*	*j*	*l*	*k*	F_{ijkl}	*i*	*j*	*l*	*k*	F_{ijkl}
1	1	1	1	26.725	5	4	3	3	−0.090	6	5	5	1	0.269
2	1	1	1	−0.055	5	4	4	1	0.042	6	5	5	2	−0.091
2	2	1	1	−0.019	5	4	4	2	−0.024	6	5	5	3	0.096
2	2	2	1	0.014	5	4	4	3	0.106	6	5	5	4	0.171
2	2	2	2	0.065	5	4	4	4	−0.074	6	5	5	5	−0.613
3	1	1	1	−0.609	5	5	1	1	−0.154	6	6	1	1	−0.268
3	2	1	1	0.007	5	5	2	1	−0.031	6	6	2	1	0.030
3	2	2	1	−0.003	5	5	2	2	0.059	6	6	2	2	0.003
3	2	2	2	−0.002	5	5	3	1	−0.143	6	6	3	1	−0.104
3	3	1	1	27.858	5	5	3	2	−0.034	6	6	3	2	0.097
3	3	2	1	0.022	5	5	3	3	−0.270	6	6	3	3	−0.146
3	3	2	2	−0.036	5	5	4	1	−0.194	6	6	4	1	0.024
3	3	3	1	19.518	5	5	4	2	0.003	6	6	4	2	0.004
3	3	3	2	0.029	5	5	4	3	−0.383	6	6	4	3	0.177
3	3	3	3	42.560	5	5	4	4	0.343	6	6	4	4	0.043
4	1	1	1	0.006	5	5	5	1	0.425	6	6	5	1	−0.428
4	2	1	1	0.004	5	5	5	2	−0.149	6	6	5	2	−0.029
4	2	2	1	0.000	5	5	5	3	0.818	6	6	5	3	−0.540
4	2	2	2	−0.007	5	5	5	4	−1.040	6	6	5	4	−0.179
4	3	1	1	0.142	5	5	5	5	3.139	6	6	5	5	0.029
4	3	2	1	0.007	6	1	1	1	−0.153	6	6	6	1	−0.531
4	3	2	2	−0.029	6	2	1	1	−0.013	6	6	6	2	0.109
4	3	3	1	0.066	6	2	2	1	0.002	6	6	6	3	−0.242
4	3	3	2	0.031	6	2	2	2	−0.012	6	6	6	4	−0.253
4	3	3	3	0.281	6	3	1	1	0.062	6	6	6	5	1.938
4	4	1	1	−0.009	6	3	2	1	−0.043	6	6	6	6	31.130
4	4	2	1	0.021	6	3	2	2	−0.004	7	1	1	1	−0.171
4	4	2	2	0.089	6	3	3	1	−0.068	7	2	1	1	−0.003
4	4	3	1	−0.003	6	3	3	2	−0.060	7	2	2	1	0.003
4	4	3	2	0.006	6	3	3	3	0.091	7	2	2	2	−0.012
4	4	3	3	−0.050	6	4	1	1	−0.022	7	3	1	1	−0.005
4	4	4	1	0.032	6	4	2	1	0.001	7	3	2	1	0.005
4	4	4	2	0.019	6	4	2	2	0.008	7	3	2	2	0.001
4	4	4	3	−0.141	6	4	3	1	0.020	7	3	3	1	−0.110
4	4	4	4	0.146	6	4	3	2	0.000	7	3	3	2	−0.019
5	1	1	1	−0.029	6	4	3	3	−0.100	7	3	3	3	−0.068
5	2	1	1	0.007	6	4	4	1	0.003	7	4	1	1	0.043
5	2	2	1	0.002	6	4	4	2	−0.007	7	4	2	1	−0.004
5	2	2	2	−0.002	6	4	4	3	−0.044	7	4	2	2	0.015
5	3	1	1	−0.262	6	4	4	4	−0.086	7	4	3	1	0.000
5	3	2	1	0.056	6	5	1	1	0.115	7	4	3	2	0.008
5	3	2	2	0.004	6	5	2	1	−0.001	7	4	3	3	−0.088
5	3	3	1	−0.241	6	5	2	2	−0.005	7	4	4	1	0.022
5	3	3	2	0.046	6	5	3	1	0.179	7	4	4	2	−0.015
5	3	3	3	−0.531	6	5	3	2	−0.087	7	4	4	3	0.019
5	4	1	1	−0.017	6	5	3	3	0.393	7	4	4	4	0.013
5	4	2	1	0.011	6	5	4	1	0.012	7	5	1	1	0.007
5	4	2	2	0.004	6	5	4	2	0.027	7	5	2	1	−0.009
5	4	3	1	−0.005	6	5	4	3	0.062	7	5	2	2	−0.004
5	4	3	2	0.002	6	5	4	4	−0.039	7	5	3	1	0.057

[a] Units are consistent with energy in aJ, distances in Å, and angles in degrees, with respect to internal coordinates defined in the text.

TABLE B.3: Symmetrized internal quartic force constants for BH_5 [C_s(I)] (cont'd).[a]

i	*j*	*l*	*k*	F_{ijkl}	*i*	*j*	*l*	*k*	F_{ijkl}	*i*	*j*	*l*	*k*	F_{ijkl}
7	5	3	2	−0.079	7	7	6	4	-0.078	8	6	3	3	-0.005
7	5	3	3	0.053	7	7	6	5	0.120	8	6	4	1	−0.071
7	5	4	1	−0.110	7	7	6	6	1.415	8	6	4	2	0.007
7	5	4	2	0.005	7	7	7	1	−0.513	8	6	4	3	−0.075
7	5	4	3	−0.079	7	7	7	2	0.147	8	6	4	4	0.054
7	5	4	4	−0.011	7	7	7	3	0.710	8	6	5	1	0.381
7	5	5	1	0.428	7	7	7	4	−0.048	8	6	5	2	−0.147
7	5	5	2	−0.078	7	7	7	5	0.193	8	6	5	3	0.311
7	5	5	3	0.412	7	7	7	6	−1.718	8	6	5	4	−0.150
7	5	5	4	0.020	7	7	7	7	30.722	8	6	5	5	0.896
7	5	5	5	−0.131	8	1	1	1	0.058	8	6	6	1	0.027
7	6	1	1	0.030	8	2	1	1	0.018	8	6	6	2	−0.009
7	6	2	1	−0.066	8	2	2	1	0.006	8	6	6	3	0.325
7	6	2	2	0.000	8	2	2	2	−0.001	8	6	6	4	−0.038
7	6	3	1	0.062	8	3	1	1	−0.088	8	6	6	5	0.311
7	6	3	2	0.050	8	3	2	1	0.058	8	6	6	6	0.226
7	6	3	3	0.164	8	3	2	2	0.000	8	7	1	1	0.089
7	6	4	1	0.070	8	3	3	1	−0.028	8	7	2	1	−0.011
7	6	4	2	−0.010	8	3	3	2	0.047	8	7	2	2	0.032
7	6	4	3	0.038	8	3	3	3	−0.135	8	7	3	1	−0.010
7	6	4	4	−0.069	8	4	1	1	−0.011	8	7	3	2	−0.029
7	6	5	1	−0.191	8	4	2	1	0.005	8	7	3	3	−0.060
7	6	5	2	0.177	8	4	2	2	−0.027	8	7	4	1	−0.087
7	6	5	3	0.010	8	4	3	1	0.016	8	7	4	2	−0.020
7	6	5	4	0.198	8	4	3	2	−0.012	8	7	4	3	0.020
7	6	5	5	−0.908	8	4	3	3	0.088	8	7	4	4	0.079
7	6	6	1	−0.046	8	4	4	1	−0.013	8	7	5	1	0.122
7	6	6	2	−0.020	8	4	4	2	0.015	8	7	5	2	−0.039
7	6	6	3	−0.404	8	4	4	3	0.016	8	7	5	3	0.150
7	6	6	4	0.075	8	4	4	4	−0.081	8	7	5	4	−0.155
7	6	6	5	−0.442	8	5	1	1	−0.141	8	7	5	5	0.977
7	6	6	6	−0.473	8	5	2	1	0.005	8	7	6	1	0.147
7	7	1	1	−0.240	8	5	2	2	0.037	8	7	6	2	0.077
7	7	2	1	0.010	8	5	3	1	−0.134	8	7	6	3	0.252
7	7	2	2	−0.005	8	5	3	2	0.022	8	7	6	4	0.106
7	7	3	1	−0.022	8	5	3	3	−0.319	8	7	6	5	−0.967
7	7	3	2	−0.049	8	5	4	1	0.056	8	7	6	6	−1.441
7	7	3	3	−0.027	8	5	4	2	0.012	8	7	7	1	0.231
7	7	4	1	−0.026	8	5	4	3	−0.035	8	7	7	2	−0.131
7	7	4	2	0.025	8	5	4	4	0.223	8	7	7	3	0.163
7	7	4	3	0.026	8	5	5	1	−0.153	8	7	7	4	−0.033
7	7	4	4	0.014	8	5	5	2	−0.142	8	7	7	5	0.281
7	7	5	1	0.263	8	5	5	3	−0.070	8	7	7	6	−0.773
7	7	5	2	−0.119	8	5	5	4	−0.688	8	7	7	7	0.355
7	7	5	3	0.068	8	5	5	5	2.150	8	8	1	1	−0.077
7	7	5	4	−0.009	8	6	1	1	0.107	8	8	2	1	0.028
7	7	5	5	−0.400	8	6	2	1	−0.024	8	8	2	2	−0.046
7	7	6	1	−0.198	8	6	2	2	0.032	8	8	3	1	−0.017
7	7	6	2	0.096	8	6	3	1	0.034	8	8	3	2	0.013
7	7	6	3	−0.342	8	6	3	2	−0.076	8	8	3	3	−0.069

[a] Units are consistent with energy in aJ, distances in Å, and angles in degrees, with respect to internal coordinates defined in the text.

TABLE B.3: Symmetrized internal quartic force constants for BH_5 [C_s(I)] (cont'd).[a]

i	*j*	*l*	*k*	F_{ijkl}	*i*	*j*	*l*	*k*	F_{ijkl}	*i*	*j*	*l*	*k*	F_{ijkl}
8	8	4	1	0.099	9	9	6	6	−0.037	10	9	8	6	−0.105
8	8	4	2	0.041	9	9	7	1	−0.151	10	9	8	7	−0.191
8	8	4	3	−0.071	9	9	7	2	−0.023	10	9	8	8	0.198
8	8	4	4	−0.060	9	9	7	3	0.086	10	9	9	9	0.138
8	8	5	1	−0.116	9	9	7	4	0.063	10	10	1	1	−0.018
8	8	5	2	−0.037	9	9	7	5	−0.099	10	10	2	1	0.024
8	8	5	3	−0.010	9	9	7	6	0.037	10	10	2	2	0.141
8	8	5	4	0.035	9	9	7	7	0.008	10	10	3	1	−0.004
8	8	5	5	−0.421	9	9	8	1	0.122	10	10	3	2	−0.007
8	8	6	1	0.134	9	9	8	2	−0.010	10	10	3	3	−0.364
8	8	6	2	−0.144	9	9	8	3	−0.109	10	10	4	1	−0.040
8	8	6	3	0.084	9	9	8	4	−0.024	10	10	4	2	0.024
8	8	6	4	−0.085	9	9	8	5	−0.024	10	10	4	3	−0.022
8	8	6	5	1.133	9	9	8	6	0.026	10	10	4	4	0.056
8	8	6	6	0.413	9	9	8	7	−0.051	10	10	5	1	0.062
8	8	7	1	−0.012	9	9	8	8	0.005	10	10	5	2	0.001
8	8	7	2	−0.033	9	9	9	9	44.444	10	10	5	3	−0.010
8	8	7	3	−0.152	10	9	1	1	0.069	10	10	5	4	−0.103
8	8	7	4	−0.035	10	9	2	1	0.016	10	10	5	5	0.493
8	8	7	5	0.765	10	9	2	2	−0.020	10	10	6	1	0.042
8	8	7	6	−0.904	10	9	3	1	−0.007	10	10	6	2	−0.025
8	8	7	7	−0.199	10	9	3	2	−0.038	10	10	6	3	−0.022
8	8	8	1	−0.102	10	9	3	3	0.043	10	10	6	4	0.027
8	8	8	2	0.108	10	9	4	1	−0.010	10	10	6	5	0.074
8	8	8	3	0.030	10	9	4	2	0.001	10	10	6	6	−0.045
8	8	8	4	0.186	10	9	4	3	0.092	10	10	7	1	0.059
8	8	8	5	−1.474	10	9	4	4	−0.036	10	10	7	2	−0.010
8	8	8	6	0.255	10	9	5	1	0.011	10	10	7	3	0.000
8	8	8	7	0.022	10	9	5	2	−0.002	10	10	7	4	0.023
8	8	8	8	153.811	10	9	5	3	−0.007	10	10	7	5	0.152
9	9	1	1	28.763	10	9	5	4	−0.038	10	10	7	6	0.057
9	9	2	1	−0.007	10	9	5	5	0.057	10	10	7	7	−0.205
9	9	2	2	−0.036	10	9	6	1	−0.003	10	10	8	1	−0.072
9	9	3	1	−20.789	10	9	6	2	−0.031	10	10	8	2	0.031
9	9	3	2	0.006	10	9	6	3	0.084	10	10	8	3	0.061
9	9	3	3	14.805	10	9	6	4	0.032	10	10	8	4	−0.002
9	9	4	1	−0.058	10	9	6	5	−0.046	10	10	8	5	−0.130
9	9	4	2	−0.030	10	9	6	6	0.024	10	10	8	6	−0.024
9	9	4	3	0.103	10	9	7	1	0.055	10	10	8	7	0.078
9	9	4	4	−0.270	10	9	7	2	−0.034	10	10	8	8	−0.088
9	9	5	1	0.143	10	9	7	3	0.031	10	10	9	9	−0.156
9	9	5	2	−0.031	10	9	7	4	−0.004	10	10	10	9	−0.188
9	9	5	3	−0.123	10	9	7	5	−0.034	10	10	10	10	0.276
9	9	5	4	−0.067	10	9	7	6	0.213	11	9	1	1	−0.139
9	9	5	5	−0.045	10	9	7	7	−0.054	11	9	2	1	0.049
9	9	6	1	−0.143	10	9	8	1	0.029	11	9	2	2	0.012
9	9	6	2	0.002	10	9	8	2	0.033	11	9	3	1	0.118
9	9	6	3	0.116	10	9	8	3	−0.067	11	9	3	2	−0.029
9	9	6	4	0.031	10	9	8	4	−0.050	11	9	3	3	−0.089
9	9	6	5	−0.004	10	9	8	5	0.093	11	9	4	1	−0.007

[a] Units are consistent with energy in aJ, distances in Å, and angles in degrees, with respect to internal coordinates defined in the text.

TABLE B.3: Symmetrized internal quartic force constants for BH_5 [C_s(I)] (cont'd).[a]

i	*j*	*l*	*k*	F_{ijkl}	*i*	*j*	*l*	*k*	F_{ijkl}	*i*	*j*	*l*	*k*	F_{ijkl}
11	9	4	2	−0.014	11	10	6	6	−0.135	11	11	8	4	−0.028
11	9	4	3	0.009	11	10	7	1	0.112	11	11	8	5	−0.152
11	9	4	4	0.046	11	10	7	2	−0.018	11	11	8	6	0.096
11	9	5	1	0.091	11	10	7	3	−0.069	11	11	8	7	0.292
11	9	5	2	0.031	11	10	7	4	−0.063	11	11	8	8	−0.326
11	9	5	3	−0.093	11	10	7	5	0.212	11	11	9	9	−0.239
11	9	5	4	−0.068	11	10	7	6	0.137	11	11	10	9	−0.050
11	9	5	5	0.025	11	10	7	7	−0.367	11	11	10	10	0.037
11	9	6	1	−0.027	11	10	8	1	−0.047	11	11	11	9	0.226
11	9	6	2	−0.090	11	10	8	2	0.091	11	11	11	10	−0.048
11	9	6	3	−0.001	11	10	8	3	0.081	11	11	11	11	1.503
11	9	6	4	0.009	11	10	8	4	−0.052	12	9	1	1	0.058
11	9	6	5	−0.159	11	10	8	5	−0.168	12	9	2	1	−0.004
11	9	6	6	0.155	11	10	8	6	−0.009	12	9	2	2	−0.002
11	9	7	1	0.020	11	10	8	7	0.163	12	9	3	1	−0.025
11	9	7	2	−0.094	11	10	8	8	−0.241	12	9	3	2	0.010
11	9	7	3	−0.066	11	10	9	9	−0.120	12	9	3	3	0.032
11	9	7	4	0.043	11	10	10	9	−0.042	12	9	4	1	−0.027
11	9	7	5	−0.113	11	10	10	10	0.092	12	9	4	2	0.007
11	9	7	6	0.280	11	11	1	1	−0.145	12	9	4	3	−0.015
11	9	7	7	−0.140	11	11	2	1	−0.057	12	9	4	4	0.012
11	9	8	1	0.087	11	11	2	2	0.109	12	9	5	1	−0.007
11	9	8	2	0.042	11	11	3	1	0.100	12	9	5	2	−0.021
11	9	8	3	−0.036	11	11	3	2	0.059	12	9	5	3	0.025
11	9	8	4	−0.051	11	11	3	3	−0.058	12	9	5	4	0.031
11	9	8	5	0.005	11	11	4	1	0.075	12	9	5	5	−0.074
11	9	8	6	−0.102	11	11	4	2	−0.056	12	9	6	1	0.015
11	9	8	7	−0.033	11	11	4	3	−0.022	12	9	6	2	0.046
11	9	8	8	−0.076	11	11	4	4	0.326	12	9	6	3	0.019
11	9	9	9	−0.248	11	11	5	1	−0.029	12	9	6	4	−0.035
11	10	1	1	−0.048	11	11	5	2	0.060	12	9	6	5	0.141
11	10	2	1	−0.010	11	11	5	3	−0.019	12	9	6	6	−0.065
11	10	2	2	0.037	11	11	5	4	−0.342	12	9	7	1	−0.009
11	10	3	1	0.025	11	11	5	5	0.615	12	9	7	2	0.036
11	10	3	2	0.015	11	11	6	1	0.261	12	9	7	3	0.086
11	10	3	3	−0.094	11	11	6	2	−0.242	12	9	7	4	0.002
11	10	4	1	0.033	11	11	6	3	−0.165	12	9	7	5	0.067
11	10	4	2	0.038	11	11	6	4	0.069	12	9	7	6	−0.214
11	10	4	3	−0.014	11	11	6	5	0.042	12	9	7	7	0.276
11	10	4	4	0.072	11	11	6	6	−0.535	12	9	8	1	−0.013
11	10	5	1	0.065	11	11	7	1	0.235	12	9	8	2	−0.048
11	10	5	2	−0.035	11	11	7	2	−0.119	12	9	8	3	−0.020
11	10	5	3	−0.047	11	11	7	3	−0.186	12	9	8	4	0.095
11	10	5	4	−0.200	11	11	7	4	−0.031	12	9	8	5	−0.218
11	10	5	5	0.339	11	11	7	5	−0.011	12	9	8	6	0.174
11	10	6	1	0.059	11	11	7	6	0.227	12	9	8	7	0.172
11	10	6	2	−0.080	11	11	7	7	−0.559	12	9	8	8	−0.352
11	10	6	3	−0.032	11	11	8	1	−0.044	12	9	9	9	0.093
11	10	6	4	0.059	11	11	8	2	0.094	12	10	1	1	−0.002
11	10	6	5	0.063	11	11	8	3	0.035	12	10	2	1	0.006

[a] Units are consistent with energy in aJ, distances in Å, and angles in degrees, with respect to internal coordinates defined in the text.

TABLE B.3: Symmetrized internal quartic force constants for BH_5 [C_s(I)] (cont'd).[a]

i	*j*	*l*	*k*	F_{ijkl}	*i*	*j*	*l*	*k*	F_{ijkl}	*i*	*j*	*l*	*k*	F_{ijkl}
12	10	2	2	−0.027	12	11	3	3	−0.001	12	12	3	3	−0.043
12	10	3	1	0.012	12	11	4	1	−0.046	12	12	4	1	−0.016
12	10	3	2	−0.002	12	11	4	2	−0.010	12	12	4	2	0.002
12	10	3	3	0.096	12	11	4	3	0.007	12	12	4	3	0.024
12	10	4	1	0.014	12	11	4	4	−0.038	12	12	4	4	−0.007
12	10	4	2	−0.006	12	11	5	1	0.061	12	12	5	1	−0.013
12	10	4	3	−0.018	12	11	5	2	0.000	12	12	5	2	−0.070
12	10	4	4	−0.018	12	11	5	3	−0.022	12	12	5	3	0.034
12	10	5	1	−0.019	12	11	5	4	0.080	12	12	5	4	−0.046
12	10	5	2	0.025	12	11	5	5	−0.369	12	12	5	5	0.253
12	10	5	3	0.020	12	11	6	1	−0.161	12	12	6	1	0.103
12	10	5	4	0.038	12	11	6	2	0.117	12	12	6	2	−0.023
12	10	5	5	−0.142	12	11	6	3	0.114	12	12	6	3	0.046
12	10	6	1	−0.108	12	11	6	4	−0.020	12	12	6	4	−0.123
12	10	6	2	0.003	12	11	6	5	0.012	12	12	6	5	0.424
12	10	6	3	−0.039	12	11	6	6	0.080	12	12	6	6	0.002
12	10	6	4	0.075	12	11	7	1	−0.064	12	12	7	1	0.039
12	10	6	5	−0.200	12	11	7	2	0.014	12	12	7	2	0.003
12	10	6	6	0.054	12	11	7	3	0.104	12	12	7	3	0.076
12	10	7	1	−0.064	12	11	7	4	0.093	12	12	7	4	−0.132
12	10	7	2	−0.003	12	11	7	5	−0.196	12	12	7	5	0.368
12	10	7	3	0.014	12	11	7	6	−0.238	12	12	7	6	−0.235
12	10	7	4	0.103	12	11	7	7	0.527	12	12	7	7	−0.174
12	10	7	5	−0.182	12	11	8	1	0.145	12	12	8	1	−0.120
12	10	7	6	−0.090	12	11	8	2	−0.061	12	12	8	2	−0.015
12	10	7	7	0.254	12	11	8	3	−0.171	12	12	8	3	0.127
12	10	8	1	0.153	12	11	8	4	−0.030	12	12	8	4	0.301
12	10	8	2	0.014	12	11	8	5	0.136	12	12	8	5	−0.691
12	10	8	3	−0.046	12	11	8	6	0.157	12	12	8	6	0.278
12	10	8	4	−0.193	12	11	8	7	−0.322	12	12	8	7	0.542
12	10	8	5	0.357	12	11	8	8	0.361	12	12	8	8	−0.917
12	10	8	6	0.095	12	11	9	9	0.053	12	12	9	9	0.031
12	10	8	7	−0.143	12	11	10	9	−0.023	12	12	10	9	−0.043
12	10	8	8	0.162	12	11	10	10	0.010	12	12	10	10	−0.012
12	10	9	9	0.034	12	11	11	9	−0.130	12	12	11	9	0.089
12	10	10	9	0.063	12	11	11	10	0.046	12	12	11	10	−0.034
12	10	10	10	−0.066	12	11	11	11	−0.445	12	12	11	11	−0.107
12	11	1	1	0.035	12	12	1	1	−0.009	12	12	12	9	0.055
12	11	2	1	0.028	12	12	2	1	−0.012	12	12	12	10	−0.030
12	11	2	2	−0.028	12	12	2	2	0.010	12	12	12	11	0.167
12	11	3	1	−0.013	12	12	3	1	−0.046	12	12	12	12	0.424
12	11	3	2	−0.026	12	12	3	2	0.009					

[a] Units are consistent with energy in aJ, distances in Å, and angles in degrees, with respect to internal coordinates defined in the text.

TABLE B.4: Core-correlation correction focal point extrapolations (kcal mol^{-1}).

	ΔE_e[MP2]	$+\delta$[CCSD]	$+\delta$[CCSD(T)]	$+\delta$[CCSDT]	$= \Delta E_e$[CCSDT]
BH_5 [C_s(I)] $\rightarrow$ $BH_3 + H_2$					
cc-pCVDZ	0.260	−0.008	0.006	0.000	0.258
cc-pCVTZ	0.309	−0.012	0.010	0.001	0.308
cc-pCVQZ	0.336	−0.010	0.013	[0.001]	[0.341]
cc-pCV5Z	0.341	[−0.004]	[0.014]	[0.001]	[0.352]
CBS limit	[0.346]	[0.002]	[0.015]	[0.001]	**[0.365]**
BH_5 [C_s(I)] $\rightarrow$ BH_5 [C_s(II)]					
cc-pCVDZ	0.003	0.000	0.000	0.000	0.003
cc-pCVTZ	0.004	0.000	0.000	0.000	0.004
cc-pCVQZ	0.005	0.000	0.000	[0.000]	[0.005]
cc-pCV5Z	0.005	[0.000]	[0.000]	[0.000]	[0.005]
CBS limit	[0.005]	[0.000]	[0.000]	[0.000]	**[0.005]**
BH_5 [C_s(I)] $\rightarrow$ BH_5 [C_{2v}]					
cc-pCVDZ	−0.147	0.017	−0.004	0.001	−0.132
cc-pCVTZ	−0.217	0.027	−0.006	0.001	−0.195
cc-pCVQZ	−0.258	0.028	−0.008	[0.001]	[−0.237]
cc-pCV5Z	−0.268	[0.023]	[−0.008]	[0.001]	[−0.252]
CBS limit	[−0.278]	[0.019]	[−0.009]	[0.001]	**[−0.267]**
$BH_3 \rightarrow B + 3H$					
cc-pCVDZ	0.234	0.227	−0.038	0.000	0.423
cc-pCVTZ	0.480	0.352	−0.066	0.001	0.766
cc-pCVQZ	0.703	0.412	−0.082	[0.001]	[1.034]
cc-pCV5Z	0.760	[0.456]	[−0.087]	[0.001]	[1.130]
CBS limit	[0.820]	[0.502]	[−0.093]	[0.001]	**[1.230]**
Extrapolation scheme	$a + bX^{-3}$	$a + bX^{-3}$	$a + bX^{-3}$	add	
Points, X=	(3,4,5)	(3,4)	(3,4)	--	

APPENDIX C

SUPPLEMENTARY MATERIAL FOR CHAPTER 4

TABLE C.1: CCSD(T) computed cubic and quartic force constants in normal coordinates.[a]

	cc-pCVQZ	cc-pCV5Z	CBS
ϕ_{111}	−822.73	−823.27	−824.21
ϕ_{221}	232.49	232.50	232.49
$\phi_{3a3a1} = \phi_{3b3b1}$	−904.16	−904.38	−904.97
$\phi_{3a3a3a} = -\phi_{3b3b3a}$	685.67	685.75	686.05
$\phi_{4a3a1} = \phi_{4b3b1}$	1.48	1.34	1.20
$\phi_{4a3a3a} = -\phi_{3b3b4a} = -\phi_{4b3b3a}$	78.21	78.32	78.48
$\phi_{4a4a1} = \phi_{4b4b1}$	144.62	144.44	144.30
$\phi_{4a4a3a} = -\phi_{4b3b4a} = -\phi_{4b4b3a}$	134.15	134.29	134.48
$\phi_{4a4a4a} = -\phi_{4b4b4a}$	102.91	102.00	101.13
ϕ_{1111}	233.88	234.49	234.60
ϕ_{2211}	−145.93	−146.32	−146.89
ϕ_{2222}	75.43	76.40	78.39
$\phi_{3a3a11} = \phi_{3b3b11}$	268.65	268.73	268.32
$\phi_{3a3a22} = \phi_{3b3b22}$	−176.61	−177.16	−177.77
$\phi_{3a3a3a1} = -\phi_{3b3b3a1}$	−204.73	−204.67	−204.23
$\phi_{3a3a3a3a} = 3\phi_{3b3b3a3a} = \phi_{3b3b3b3b}$	448.82	448.47	447.31
$\phi_{4a3a11} = \phi_{4b3b11}$	0.08	0.25	0.43
$\phi_{4a3a22} = \phi_{4b3b22}$	−5.32	−5.68	−6.04
$\phi_{4a3a3a1} = -\phi_{3b3b4a1} = -\phi_{4b3b3a1}$	−22.79	−22.81	−22.88
$\phi_{4a3a3a3a} = 3\phi_{3b3b4a3a} = 3\phi_{4b3b3a3a} = \phi_{4b3b3b3b}$	−2.05	−1.78	−1.73
$\phi_{4a4a11} = \phi_{4b4b11}$	−110.10	−109.95	−109.93
$\phi_{4a4a22} = \phi_{4b4b22}$	13.91	12.95	11.90
$\phi_{4a4a3a1} = -\phi_{4b3b4a1} = -\phi_{4b4b3a1}$	−87.37	−87.33	−87.50
$\phi_{4a4a3a3a} = \phi_{4b4b3b3b}$	−69.69	−68.72	−70.24
$\phi_{4a4a4a1} = -\phi_{4b4b4a1}$	−29.67	−29.13	−28.53
$\phi_{4a4a4a3a} = -3\phi_{3b3b4a3a} = -3\phi_{4b3b3a3a} = \phi_{4b3b3b3b}$	−13.39	−13.12	−12.43
$\phi_{4a4a4a4a} = 3\phi_{4b4b4a4a} = \phi_{4b4b4b4b}$	41.48	41.24	39.13
$\phi_{3b3b4a4a} = \phi_{4b4b3a3a}$	−222.94	−223.40	−223.57
$\phi_{4b3b4a3a}$	76.55	76.56	76.82

[a] All force constants are in units of cm^{-1}.